The Identification and Characterization of six novel ATG genes

Von der Fakultät Chemie der Universität Stuttgart

zur Erlangung der Würde eines

Doktors der Naturwissenschaften (Dr. rer. nat.)

genehmigte Abhandlung

vorgelegt von

Khuyen M. Meiling-Wesse

aus Portland, Oregon/USA

Hauptberichter: Prof. Dr. Michael Thumm

Mitberichter: Prof. Dr. Dieter H. Wolf

Tag der mündlichen Prüfung:

April 3, 2009

Institut für Biochemie der Universität Stuttgart

2009

Kurzfassung

Autophagozytose ist ein zellulärer Prozeß den man in Lebewesen von der Hefe bis zum Menschen findet. Sie ist eine Antwort auf Stressfaktoren wie z.B. Stickstoffmangel und wird benötigt für die Zelldifferenzierung. Der Autophagozytose-Prozess produziert doppelmembranlagige Vesikel, genannt Autophagosomen. Diese Vesikel hüllen zytoplasmische Proteine und ganze Organellen ein und transportieren diese zur Vakuole/ zum Lysosom. Im Lysosom werden diese Bestandteile abgebaut und wiederverwendet.

Autophagozytose ist außerdem für den Transport von Proteinen zur Vakuole verantwortlich. In der Hefe *Saccharomyces cerevisiae* gibt es zwei parallele Abläufe, die gezielt Kargoproteine, wie Aminopeptidase I, transportieren. Aminopeptidase I wird während des vegetativen Wachstums durch einen biosynthetischen Weg namens Zytosol-zur-Vakuole Transportweg (Cvt Weg) befördert. Autophagozytose hingegen wird hungerinduziert, und Aminopeptidase I, eingehüllte Proteine und Organellen werden zur Vacuole gebracht und aktiviert, bzw. abgebaut. Die meisten Autophagie-Proteine spielen sowohl in der Autophagozytose als auch im Cvt-Weg eine Rolle. Es gibt aber Proteine, die selektiv für den einen oder der anderen Weg gebraucht werden.

Über die Jahre ist die Studie der Autophagozytose wichtiger geworden, nachdem mehr und mehr Verbindungen zwischen autophagischen Defekten und Krankheiten nachgewiesen wurden. Die Autophagozytose wurde eingangs als recycelnder Mechanismus für Aminosäuren und andere Komponenten bezeichnet. Inzwischen wissen wir, daß Krankheiten wie Brust- oder Eierstockkrebs häufiger vorkommen, wenn autophagische Gene Defekte aufweisen. Die Autophagozytose spielt auch eine Rolle im Alterungsprozeß und beim programmierten nicht-apoptotischen Zelltod. Bakterien und Viren haben Methoden entwickelt, um dieses System zum eigenen Vorteil zu nutzen. Angesichts der Rolle, die Autophagozytose bei Krankheiten und u.a. genannten Themen spielt, ist es jetzt wichtig möglichst viel Wissen über die Autophagozytose und ihre verwandten Mechanismen zu erlangen.

Ziel der vorliegenden Arbeit war es neue Gene/Proteine, die an der Autophagozytose beteiligt sind, zu finden und zu charakterisieren. Dabei wurde der eukaryotische

Modellorganismus *Saccharomyces cerevisiae*, die Bäckerhefe, verwendet. Wir nutzten eine reverses genetisches Auswahlverfahren basierend auf autophagozytotischen Phänotypen. Der zuerste eingesetze Phänotyp war die reduzierte Überlebensrate von Autophagozytose Deletionsmutanten auf stickstoffarmen Agarplatten. Die eingangs rund 5,000 Deletionsstämmen wurden mit diesem Kriterium auf ca. 1,300 Stämme reduziert. Diese 1,300 wurden weiter bis auf ca. 30 Stämme reduziert, durch eine Überprüfung der Stämme auf ihre Unfähigkeit vakuoläre Hydrolase Aminopeptidase I zu reifen. Daraus konnten sechs Gene im Rahmen dieser Arbeit der Autophagozytose oder dem Cvt Weg zugeordnet werden.

In Folge konzentriert sich diese Arbeit auf die Charakterisierung der sechs Autophagozytose-Gene und deren Proteine. Die ersten zwei Gene *ATG18* und *ATG21* sind zueinander homolog. Trotz Homologie ist *ATG18* in der Autophagozytose und im Cvt Weg involviert, wohingegen *ATG21* nur dem Cvt Weg zugeordnet werden kann. Die Charakterisierung von genau solchen Genen ist notwendig, um die unterschiedlichen Mechanismen der zwei verwandten Wege beschreiben zu können. Die nächsten zwei Gene, *CCZ1* und *MON1*, sind beide an der Fusion von Autophagosomen bzw. Cvt-Vesikeln mit der Vakuole beteiligt. Analoge Effekte sind in vielen myopathischen und neurodegenerativen Krankheiten zu beobachten, wo eine Anhäufung von autophagischen Vakuolen (Säuger Autophagosomen) in muskulären oder neuralen Zellen auftritt. Die zwei Gene, *ATG23* und *TRS85/GSG1*, haben nur eine Funktion im Cvt Weg. Im Rahmen der Arbeit wurden weitere relevante Gene identifiziert deren genaue Zuordnung zu Autophagozytose und/oder dem Cvt Weg über weitere Experimente geklärt werden muss.

Dieses Studie hat zu den folgenden Publikationen geführt:

1. Barth, H., Meiling-Wesse, K., Epple, U. D., and Thumm, M. (2001). Autophagy and the cytoplasm to vacuole targeting pathway both require Aut10p. FEBS Lett *508*, 23-28.

2. Barth, H., Meiling-Wesse, K., Epple, U. D., and Thumm, M. (2002). Mai1p.is essential for maturation of proaminopeptidase I but not for autophagy. FEBS Lett *512*, 173-179.

3. Meiling-Wesse, K., Barth, H., and Thumm, M. (2002a). Ccz1p/Aut11p/Cvt16p is essential for autophagy and the cvt pathway. FEBS Lett *526*, 71-76.

4. Meiling-Wesse, K., Barth, H., Voss, C., Barmark, G., Muren, E., Ronne, H., and Thumm, M. (2002b). Mon1p/Aut12p functions in vacuolar fusion of autophagosomes and cvt-vesicles. FEBS Lett *530*, 174-180.

5. Meiling-Wesse, K., Barth, H., Voss, C., Eskelinen, E. L., Epple, U. D., and Thumm, M. (2004a). Atg21 is required for the effective recruitment of Atg8 to the preautophagosomal structure during the Cvt pathway. J Biol Chem *279*, 37741-37750.

6. Meiling-Wesse, K., Bratsika, F., and Thumm, M. (2004b) ATG23, a novel gene required for the maturation of proaminopeptidase I, but not for autophagy. FEMS Yeast Res *4*, 459-465.

7. Meiling-Wesse, K., Epple, U. D., Krick, R., Barth, H., Appelles, A., Voss, C., Eskelinen, E. L., and Thumm, M. (2005) Trs85 (Gsg1), a component of the TRAPP complexes, is required for the organization of the preautophagosomal structure during selective autophagy via the Cvt pathway. J Biol Chem *280*, 33669-33678.

Schlagwörter: Autophagocytose, Zytosol-zur-Vakuole Transport Weg, ATG

Abstract

Autophagy is a pathway common to creatures ranging from yeast to humans. It is a cellular response to stress factors such as nutrient depletion and also functions during cell differentiation. During autophagy double-membrane vesicles are formed. These are known as autophagosomes. These vesicles engulf proteins and whole organelles, transferring them to the vacuole/lysosome, where they are broken down into elementary components.

Autophagy is also responsible for transporting certain cargo proteins to the vacuole. In yeast there are two parallel pathways that selectively transport cargo proteins, *e.g.* proaminopeptidase I. It is known that during times of vegetative growth aminopeptidase I is transported by a related pathway, the cytoplasm-to-vacuole targeting pathway (Cvt-pathway). Autophagy, on the other hand, is a starvation-induced process. During starvation, autophagy is "switched on" and aminopeptidase I, engulfed proteins and organelles are transported to the vacuole to be processed or digested. Though most of the genes needed for autophagy are also used by the mechanisms of the Cvt-pathway, in each pathway there are also genes that are selectively used by one or the other.

The study of autophagy has become increasingly important as more and more links between autophagic defects and disease become prevalent. Autophagy was once just thought of as a recycling mechanism for amino acids and other components. Now it is known that diseases such as breast and ovarian cancer or Danon's disease, a form of muscular degeneration, are more likely to occur due to defects in genes involved in autophagy. Autophagy is also thought to play a role in aging and in non-apoptotic programmed cell death. Bacteria and viruses have also developed methods of controlling this system and utilizing it for their own intracellular replication. Because the role of autophagy has become so intertwined with many different diseases and topics, it is imperative to gain as much knowledge as possible about the mechanisms of autophagy.

The goal of this study was to identify novel genes/proteins and to characterize their function during autophagy by studying the organism *Saccharomyces cerevisiae*, the common baker's yeast. This was accomplished by developing a reverse genetic screen

based on certain autophagic phenotypes. The first phenotype utilized was the inability of autophagy-related deletion strains to survive on amino acid depleted agar plates. This process reduced the number of strains from ~5000 to about 1,300. These ~1,300 strains were further narrowed down to about 30 strains by checking their ability to mature the vacuolar enzyme aminopeptidase I. This effort resulted in identification of six novel genes with a function during autophagy or the Cvt pathway.

This study concentrated on characterizing six deletion strains and their corresponding proteins. The first two genes, *ATG18* and *ATG21*, are homologues of one another. Though similar, *ATG18* was found to be important for both autophagy and the Cvt-pathway, whereas *ATG21* was found to affect only the Cvt-pathway. Characterizations of such genes are important for investigating the mechanistic differences in the two related pathways. The next two genes, *CCZ1* and *MON1*, were both found to be involved in the fusion of autophagosomes and Cvt-vesicles with the vacuole. In many myopathic and neurodegenerative diseases an accumulation of autophagic vacuoles (mammalian autophagosomes) has been observed in muscular or neural cells. The last two genes, *ATG23* and *TRS85*/*GSG1*, have also been found to function within the Cvt-pathway. Additional genes were also been identified within this study, though many more experiments need to be made to determine exactly if and where they obstruct autophagy and/or the Cvt-pathway.

This study lead to the following publications:

1. Barth, H., Meiling-Wesse, K., Epple, U. D., and Thumm, M. (2001). Autophagy and the cytoplasm to vacuole targeting pathway both require Aut10p. FEBS Lett *508*, 23-28.

2. Barth, H., Meiling-Wesse, K., Epple, U. D., and Thumm, M. (2002). Mai1p.is essential for maturation of proaminopeptidase I but not for autophagy. FEBS Lett *512*, 173-179.

3. Meiling-Wesse, K., Barth, H., and Thumm, M. (2002a). Ccz1p/Aut11p/Cvt16p is essential for autophagy and the cvt pathway. FEBS Lett *526*, 71-76.

4. Meiling-Wesse, K., Barth, H., Voss, C., Barmark, G., Muren, E., Ronne, H., and Thumm, M. (2002b). Mon1p/Aut12p functions in vacuolar fusion of autophagosomes and cvt-vesicles. FEBS Lett *530*, 174-180.

5. Meiling-Wesse, K., Barth, H., Voss, C., Eskelinen, E. L., Epple, U. D., and Thumm, M. (2004a). Atg21 is required for the effective recruitment of Atg8 to the preautophagosomal structure during the Cvt pathway. J Biol Chem *279*, 37741-37750.

6. Meiling-Wesse, K., Bratsika, F., and Thumm, M. (2004b) ATG23, a novel gene required for the maturation of proaminopeptidase I, but not for autophagy. FEMS Yeast Res *4*, 459-465.

7. Meiling-Wesse, K., Epple, U. D., Krick, R., Barth, H., Appelles, A., Voss, C., Eskelinen, E. L., and Thumm, M. (2005) Trs85 (Gsg1), a component of the TRAPP complexes, is required for the organization of the preautophagosomal structure during selective autophagy via the Cvt pathway. J Biol Chem *280*, 33669-33678.

Keywords: Autophagy, Cvt pathway, ATG

Table of Contents

List of Figures

List of Tables

Abbreviations

Ade	adenine
ALP	alkaline phosphatase
(m)A	(milli-)ampere
Amp	ampicillin
API	aminopeptidase I
ApeI	aminopeptidase I
APS	ammonium persulfate
ATG	autophagy related gene
(k)bp	(kilo-)base pair
C. elegans	*Caenorhabditis elegans*
CPY	carboxypeptidase Y
Cvt	cytoplasm to vacuole targeting
d	days
(k)Da	(kilo-)dalton
ddH$_2$O	Millipore™ water or double distilled water
DMSO	dimethyl sulfoxide
DNA	deoxyribonucleic acid
dNTP	deoxynucleic acid
E.coli	*Eschericia coli*
EtBr	ethidium bromide
EDTA	ethylene diaminetetra-acetic acid
ER	endoplasmic reticulum
GEF	guanine nucleotide exchange factors
Glc	glucose
(p, n, μ, m)g	(pico-, nano-, micro-, milli-)gram
h	hour(s)
H. polymorpha	*Hansenula polymorpha*
HEPES	*N*-[2-hydroxyethyl]-piperazine-*N'*-[2-ethanesulfoic acid]
His	histidine
HOPS	homotypic fusion and vacuole protein sorting
KAc	potassium acetate
Leu	leucine
(μ, m)l	(micro-, milli-)liter(s)
Lys	lysine
MgCl$_2$	magnesium chloride
min	minute(s)
β-ME	β-mercaptoethanol
MOPS	3-morpholino-propanesulfonic acid
NEB	New England Biolabs
NSF	*N*-ethylmaleimide-sensitive factor
nm	nanometer
OD$_{600}$	optical density at 600 nm
ORF	open reading frame
pApe1	precursor aminopeptidase I
PAS	pre-autophagosomal structure
PBS	phosphate buffered saline
PBS-T	phosphate buffered saline with tween 20
PCR	polymer chain reaction
PE	phosphatidylethanolamine
P. gingivalis	*Porphyromonas gingivivalis*
P. pastoris	*Pichia pastoris*
PGK	3-phosphoglycerate kinase
PIPES	piperazine-N-N'-bis [2-ethanesulfonic acid]
PMSF	phenylmethylsulfonyl fluoride
PrB	proteinase B
PtdIns	phosphatidylinositol
PtdIns(3)P	phosphatidylinositol 3-phosphate
PVDF	polyvinylidene difluoride
RT	room temperature
s	seconds
S. cerevisiae	*Saccharomyces cerevisiae*

SDS	sodium dodecyl sulfate
SNAP	soluble *N*-ethylmaleimide-sensitive factor attachment protein
SNARE	soluble *N*-ethylmaleimide-sensitive factor attachment protein receptor
TBS	tris buffered saline
TBS-T	tris buffered saline with tween 20
TEMED	N,N,N',N'-tetramethylethylendiamine
TRAPP	transport protein particle
Tris	tris-(hydroxymethyl)-aminomethane
Trp	tryptone
Trs	TRAPP subunit
Tween 20	polyoxyethylene sorbitan monolaurate
Ura	uracil
Vps	vacuolar protein sorting
xg	RCF
(m)V	(milli-)volt

Acknowledgment

I would like to thank Prof. Dr. Michael Thumm for introducing me to and advising me in the interesting field of autophagy.

Additionally, I would like to thank his research group for helping me with difficult methods and providing me with many amusing afternoons.

Christiane Voß, my roommate and friend, I really am glad that I met you. Thank you for the hours of laughter and fun.

My parents, Gregory and Huong Meiling, I would especially like to thank for supporting me throughout my studies. Without them none of this would have been possible.

My parents-in-Law, Siegfried and Sigrid Wesse, I would like to express my appreciation for their support over the years.

Most of all I would like to thank my husband, Thorsten Wesse, for his ever-giving love and encouragement that have motivated me to accomplish this work.

1   Introduction

1.1   What is autophagy?

The word autophagy comes from the Greek meaning to eat oneself, and that is exactly what seems to happen. All eukaryotes from yeast to humans carry out a form of self-digestion during times of stress or nutrient depletion. When autophagy is induced double-membrane transport vesicles are formed, unspecifically carrying bulk cytosolic proteins and whole organelles to the vacuole. There they are degraded releasing important building blocks for the cell's homeostasis and survival during periods of stress.

Autophagy embraces the functions of specific and non-specific autophagy. Autophagy is divided into macroautophagy, microautophagy, micro and macropexophagy, and the cytoplasm-to-vacuole targeting pathway (Cvt pathway). Macroautophagy is the most studied form of autophagy. In general when the term autophagy is mentioned macroautophagy is meant. Macroautophagy, hereafter autophagy, is the non-specific collection and digestion of cytosolic matter and organelles. Microautophagy involves the direct uptake of cytosolic proteins through invagination of the vacuolar membrane, though not much is known about its mechanism or constituents.

Pexophagy is a selective process using the machinery of autophagy to sequester and degrade peroxisomes when they are no longer needed. The formation of peroxisomes is induced when methanol is the only available carbon source. During carbon catabolite inactivation these peroxisomes are degraded in the vacuole. Micropexophagy involves the selective degradation of peroxisomes through direct invagination of the vacuolar membrane, somewhat like the unspecific microautophagy.

Autophagy is inducible through nutrient starvation or by adding the TOR inhibitor rapamycin to the selected growth medium. In yeast, when autophagy is not induced a parallel process occurs called the cytoplasm-to-vacuole-transport (Cvt) pathway. The Cvt pathway is a biosynthetic pathway used to transport the vacuolar hydrolases aminopeptidase I and α-mannosidase to the vacuole. This pathway uses much of the same genetic machinery that the autophagic pathway uses, though there are a few proteins that are specific to one pathway or the other. It was the goal of this study to identify and characterize genes that are a part of autophagy or the Cvt pathway.

Autophagy was first described over forty years ago by Clark (1) "as an unusual presence of cytoplasmic organelles (mitochondria, in that instance) in the lumen of degradative vacuoles of developing kidneys" (from Abeliovich *et al.* (2)). Originally described as a cellular response to starvation it was only characterized phenomenally through electron microscopy. Its study first started to develop in the 1990's after Y. Ohsumi and his colleagues discovered the evidence of autophagy in yeast cells (3). The study of autophagy really blossomed in the late 90's, with the help of modern genetics and biochemistry, and the collecting evidence that autophagy is connected to many common diseases.

1.2   Autophagy and disease

Over the years the importance of autophagy has increased tremendously as defects in this machinery have been associated to diseases such as Huntington's, cancer and cardiomyopathy. Diseases such as breast and ovarian cancer or Danon's disease, a form of muscular degeneration, are also more likely to occur due to defects in genes involved in autophagy. Through the advances in molecular and biochemistry it is now possible to investigate the role of specific genes through fluorescence microscopy, knock out strains (*e.g.* in yeast and mice) and through RNA interference (*e.g.* in *C. elegans*). However, autophagy has not only been linked to positive effectors in disease, it seems that inadvertently disease and pathogens can also use the autophagic process for its own uses (4).

1.2.1 Links to cancer

Autophagy has been linked to cancer through Beclin1, the human homolog to the yeast Vps30/Atg6. In a high percentage of human breast, ovarian, and prostate cancers Beclin1 is monoallelically deleted (5). Beclin1 appears to be a tumor suppressor; its absence increases the tumorigenesis of cancer cells. Another positive factor of autophagy is its unspecific "clean-up" of cytosolic material. Damaged organelles and free radicals can be taken up and degraded by autophagosomes, protecting the cell by reducing their ability to introduce further damage. However, the ability of autophagy to provide cells with energy under nutrient limitations can also feed tumor cells, and cause them to evade certain cancer treatments, such as radiation (6,7).

1.2.2 Links to neurodegenerative disorders

In pathological studies autophagy has been linked to neurodegenerative disorders. In the neurons of Alzheimer patients electron microscopic studies show an increased accumulation of autophagosomes and immature autophagic vacuoles (8). During Huntington's disease characteristically there is an accumulation of insoluble Huntingtin aggregates in neurons caused by a mutation in the N-terminal polyglutamine domain (9). This mutant Huntingtin induces the accumulation of autophagic vesicles (10). During these diseases autophagy may play a protective role in removing accumulating aggregates. On the other hand, it is not known if autophagy induces a form of cell death in neurons where these aggregates accumulate. This induced cell death seems to add to the pathological condition of these diseases.

1.2.3 Pathogens and autophagy

Autophagy is known to be of use in the fight against pathogens. The herpes simplex-1 virus has been shown to induce autophagy after entering into the cell (11). It was also found that autophagy could effectively eliminate group A streptococcus in nonphagocytic cells (12). Both pathogens evade the endocytic pathway and release themselves into the cellular cytoplasm to multiply. Autophagy then sequesters these escaped pathogens into autophagosomes eliminating them in the lysosome/vacuole. This innate mechanism is useful in protecting the cells from invaders.

Nonetheless, some pathogens such as *Porphyromonas gingivivalis*, a gram negative bacterium, evades phagocytosis by sequestering itself into autophagosomes (13). *P. gingivivalis* causes adult peridontitis and is also located in coronary artery endothelial cells. After entering the autophagic pathway the bacterium somehow halts the acquisition of vacuolar hydrolases to late autophagosomes. These autophagosomes are then unable to digest the bacteria allowing the parasite to reproduce unimpededly. Studies indicate that when autophagy is inhibited through addition of wortmannin the uptake of *P. gingivivalis* in autophagosomes is blocked and the bacteria enter the endocytic pathway where they are lysed. Two other bacterial pathogens *Brucella abortus* and *Legionella pneuophila* utilize similar tactics to evade endocytosis (14,15). These bacteria use the autophagic pathway, where they can multiply undisturbed in immature autophagosomes making the most of this isolated cytosolic environment.

Viruses such as the coronavirus mouse hepatitis virus (MHV) also need autophagic factors to efficiently replicate (16). MHV is a positive sense RNA virus like the poliovirus and the equine arthritis virus. These viruses have replication complexes that form double membrane vesicles in the cytoplasm similar to autophagosomes. They

perform RNA replication on these double membrane vesicles. A viral study in wild type and ATG5-/- (*atg5Δ*) mouse cells indicated that the formation of double membrane vesicles is needed for the efficient replication of MHV but is not essential for viral growth. MHV was shown to induce autophagy and autophagic markers such as LC3, a mammalian Atg8 homolog, co-localized with replication complexes. This is a good indicator that these viruses exploit autophagy to multiply.

Autophagy is useful in sequestering and eliminating invading pathogens, but through evolutionary development some pathogens have found ways to elude the autophagic system, expanding their mechanisms to even utilize autophagy for their own benefit.

1.2.4 Autophagy in mammals

Eukaryote cells induce autophagy in response to starvation. Still it has been questioned if mammals, compared to other organisms like worms and yeast, really have periods of extreme starvation that would make autophagy necessary for them. Quite recently (17), it has been shown that in neonatal mice elevated levels of autophagy occurs in cells of heart muscles, diaphragm, lung alveoli and in the skin immediately after birth. Autophagy reaches its peak 3-6 hours after birth then is regulated to normal levels after nursing begins. Mice lacking the autophagy gene *ATG5* die within the first day of life, but force-feeding them can extend their survival. This is an interesting study that suggests that autophagy is needed for the survival of neonatal mammals after their separation from the placenta. Autophagic products are needed to immediately supplement the nutrients lacking during their "starvation" before being first fed.

Autophagy is a cellular mechanism that responds to stress, whether through starvation, pathogenic invasion or cellular disease. Its molecular mechanism has yet to be fully elucidated. Through more insight into this interesting pathway, it may be possible to find ways to further protect us and other organisms against invading pathogens and disease.

1.2.5 The Yeast model organism: *Saccharomyces cerevisiae*

The study of Autophagy began to flourish after its discovery in the yeast *Saccharomyces cerevisiae* (3). *S. cerevisiae* also known as the common baker's yeast has many advantages over other eukaryotic species. Compared to many cell lines, yeast does not require much care. It will grow in growth medium or on agar plates at moderate temperatures and a complete sterile environment is not needed. Yeast grows relatively quickly, with a duplication time of two to four hours. It can be stored in the

freezer and is easily revived in growth medium. Yeast will grow in a test tube or flask and does not require large cages.

Yeast has the advantage of being a simple single celled eukaryote. It contains most of the cellular pathways and organelles that more complex organisms have but has a manageable amount of genes (approx. 6000) and gene products. The complete genome of *S. cerevisiae* has been deciphered and many proteins found in yeast are conserved in higher eukaryotes. Yeast exists in a haploid and in a diploid form, with two sexes termed **a** and **α**. The separate haploid forms can be mated, which assists in the manipulation and insertion of altered genetic information into the genome. Through homolog recombination and yeast's rapid propagation, the formation of knockout strains is easily performed and they are quickly generated. The availability of a commercial knockout collection has also helped in the development of genomic screens and the discovery of new protein connections and interactions within cellular pathways.

In regards to autophagy the yeast *S. cerevisiae* also has a unique interacting pathway of its own, the Cvt pathway. This biosynthetic pathway, which delivers the vacuolar hydrolyses aminopeptidase I and α-mannosidase to the vacuole, is only found in *S. cerevisiae*. It is an interesting pathway that shares many of the proteins needed for autophagy. As its mechanisms and those of autophagy are further deciphered we will gain greater insights into the influence and abilities of this interesting process.

1.3   The phases of autophagy and the Cvt pathway in the yeast *Saccharomyces cerevisiae*
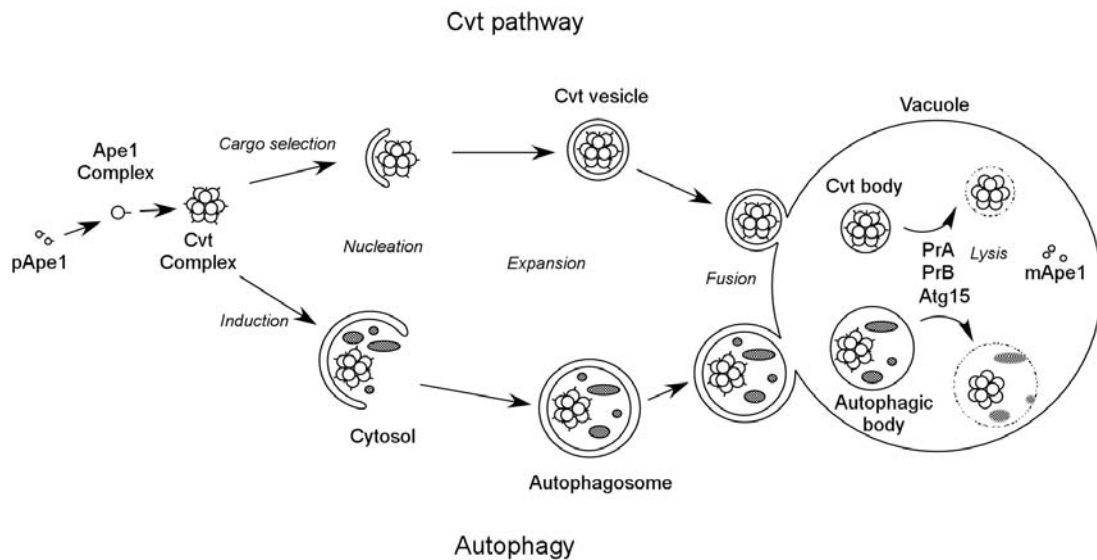
Figure 1-1 Schematic of the Cvt pathway and autophagy[1]

1.3.1   Induction and regulation of autophagy

1.3.1.1   Tor signaling and the Atg1/Atg13 system

The induction and regulation of autophagy is a largely unknown process. Many components and its exact mechanism have yet to be discovered. What is known is that it involves the protein Tor (Target of Rapamycin). Tor is a phosphatidylinositol kinase-related serine/threonine protein kinase (20). It is involved in nutrient sensing and cell growth and coordinates a number of aspects of cell physiology (21). The nutrient sensing function of Tor regulates autophagy. When Tor is inhibited either by nutrient depletion or treatment with rapamycin autophagy is induced (22). The kinase activity of Tor hyperphosphorylates directly or indirectly the protein Atg13. Atg13 is part of the Atg1 complex. Atg1 and Atg13 are phosphoproteins that are needed for regulating between autophagy and the Cvt pathway. When Tor is active Atg13 is hyperphosphorylated. This hyperphosphorylation prevents Atg13 from undergoing a interaction with Atg1. Though when Tor is inhibited, Atg13 is partially dephosphorylated. Hypophosphorylated Atg13 then has a higher affinity to Atg1, which activates autophagy and the formation of larger transport vesicles, autophagosomes. The Atg1 complex involves components that are specific to either the autophagy or the Cvt

---

[1] Figure modified from Thumm 2000 (18) and Klionsky 2005 (19).

pathway; only Atg1 is involved in both. Therefore Atg1 is considered the activating switch between both pathways.
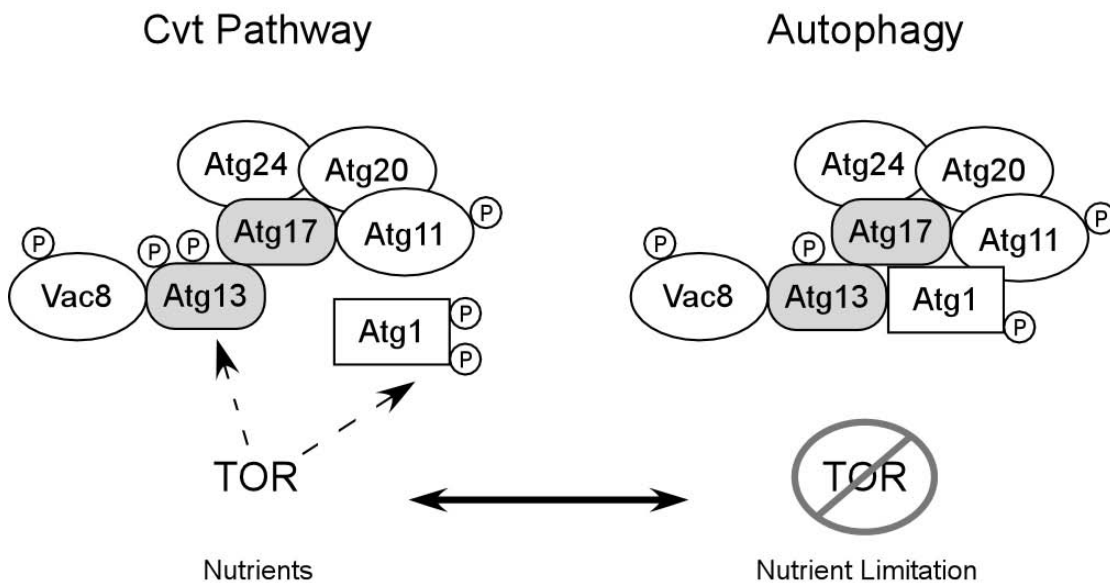
Figure 1-2 Nutrient sensing and induction of autophagy by the TOR kinase[2]

Atg1, like Tor, is a serine/threonine protein kinase. Previously, the dephosphorylation and binding of Atg13 to Atg1 was shown to stimulate this kinase activity *in vitro* (23). Recently though, using in vivo studies, it was suggested that the kinase activity of Atg1 is only needed for the Cvt pathway and not for the induction of autophagy. Atg1 could possible carry out a structural role in the induction of autophagy and the switch could be mediated by a structural change in Atg1 (24).

The other components of the Atg1 complex are Vac8, Atg11, Atg20 and Atg24 which are Cvt specific and Atg13 and Atg17 whose mutation affects the maturation of aminopeptidase I during autophagy. A possible schematic interaction is shown in *Figure 1-2*. Vac8 is located at the vacuolar membrane and is required for vacuolar inheritance, vacuolar fusion, and the Cvt pathway. Atg11 is another protein that is required for the Cvt pathway. In a recent article (25) Atg11 was investigated and four coiled-coil domains were identified and protein-protein interactions were assigned to different domains. Atg11 interacts with Atg1, Atg17, Atg19, Atg20 and itself. It is thought that Atg11 assists in bringing the cargo (the Cvt complex, including Atg19) to the vesicle-forming machinery. Atg20 and Atg24 (both Cvt specific) interact with Atg17 (necessary for autophagy) (26). They are both proteins that contain a PX or phosphatidylinositol 3-phosphate (PtdIns(3)P) binding domain. The function of both PX domains is necessary for the Cvt pathway. Their membrane association is dependent on

the interaction/binding of PtdIns(3)P, and Vps34, the only phosphatidylinositol 3-kinase in *S. cerevisiae*. Thus connecting the Atg1 complex mechanism with the phosphatidylinositol 3-kinase complex.

1.3.1.2   The PtdIns 3-kinase complex

Vps34, the phosphatidylinositol 3-kinase of *S. cerevisiae* is involved in two distinct complexes (I/II) that function in autophagy and in CPY sorting (27), see *Figure 1-3*. Vps34 interacts with Vps15, a membrane associated serine/threonine kinase that regulates the kinase activity of Vps34. In yeast the lack of either one of these proteins has a number adverse effects such as growth defects and the inadequate maturation of vacuolar hydrolases (28,29). Vps30/Atg6 is also part of both complexes. Complex II, necessary for the sorting of CPY is located at the endosomal membrane and consists of Vps15, Vps34, Vps30 and Vps38. This complex is more abundant than the second Vps34 complex, complex I, needed for autophagy (27). In complex I Vps30 joins Atg14 to form a connection to Vps34-Vps15. This complex is found to be located at the vacuolar membrane where a number of other autophagic proteins localize to the pre-autophagosomal structure. Without Atg14 only autophagy is disrupted; the CPY pathway retains its function. Both complexes, though at different locations, convert PtdIns to PtdIns(3)P, perhaps directing the kinase activity of Vps34 to specific membranes.

---

[2] Figure modified from Klionsky 2005 (19)

Complex I

Autophagy

Complex II

CPY Sorting
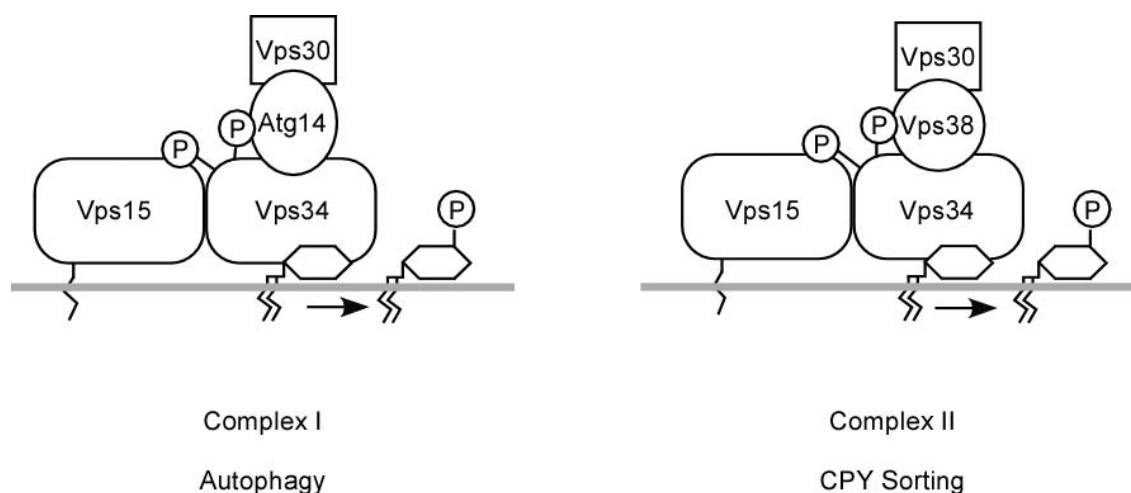
Figure 1-3 Schematic drawing of the two Vps34 complexes in yeast[3]. Vps34 containing complexes phosphorylate phosphatidylinositols along different membranes.

Phosphorylated phosphatidylinositols, called phosphoinositides, are lipid second messengers that are produced on the cytosolic side of membranes where they recruit and/or activate effector proteins (30,31). Phosphoinositides are required for cell growth, apoptosis and membrane trafficking. In human cell lines, when the production of PtdIns(3)P is inhibited by wortmannin autophagy is also inhibited, on the other hand over production of PtdIns(3)P promotes autophagy (32). This indicates a direct role of phosphoinositides in autophagy. A number of autophagic proteins bind with PtdIns(3)P by way of FYVE, PX or other amino acid domains. Atg18, Atg21 discussed in this study also have such domains and are shown to bind to PtdIns(3)P and PtdIns(3,5)P_2 (33). Another protein Atg27/Etf1 was shown to have a PtdIns(3)P binding domain. It functions as a downstream effector of Vps34 that is specific to the Cvt pathway (31). It will be interesting to see if there is a downstream effector specific for the autophagy. The PtdIns 3-kinase complex I is thought to be involved in the nucleation of autophagosomes and Cvt vesicles. Nucleation is the process where all proteins responsible for the generation of transport vesicles collect and initiate their development.

1.3.2 Nucleation and formation of transport vesicles

There are two ubiquitin-like conjugating cascades needed for the formation of autophagosomes and Cvt vesicles. One is thought to be a form of scaffolding for the

---

[3] Figure modified from Kihara *et al.* 2001 (27)

developing transport vesicle; the other is thought to be part of the membrane recruitment. Most single membrane vesicles are formed by the pinching off of membranes from the ER (ALP and CPY pathways) or the plasma membrane (endocytosis). The exact origin of the membrane used to form the double membrane autophagosomes and Cvt vesicles is not known. The vesicles are thought to form *de novo* in a nucleation-assembly-elongation process. Where nucleation and assembly are necessary for both the Cvt vesicles and autophagosomes, but elongation is needed only for the larger autophagosomes.

1.3.2.1   The pre-autophagosomal structure

During the formation of autophagic and Cvt transport vesicles many of the proteins needed collect at a novel organelle called the pre-autophagosomal structure (PAS) (34). This organelle is found at the vacuolar membrane but it does not co-sediment or co-fractionate with the vacuolar membrane, ER, Golgi or late-endosomal markers (35). Through fluorescence microscopy many proteins needed for autophagy and the Cvt pathway are shown to co-localize at this perivacuolar structure i.e.: Atg2, Atg5, Atg8, Atg9, Atg19 and Ape1.

1.3.2.2   The Atg12-Atg5 complex

It has been shown that a 350 kDa complex, comprising of a multimer of Atg12, Atg5 and Atg16, is needed for the formation of autophagosomes and Cvt-vesicles (36). The conjugation of Atg12 to Atg5 proceeds in an ubiquitin like process as illustrated in *Figure 1-4*. First cytosolic Atg12 is activated by Atg7, its E1 activator. Second the activated Atg12 is covalently conjugated to Atg5 by its E2 conjugating protein Atg10. Atg5 is found to localized to the PAS in wild type cells as observed using the Atg5-YFP fluorescent protein (34). Another protein Atg16 multimerizes through a coiled coil domain to itself and then rapidly links over Atg5 to the Atg12-Atg5 conjugate. This forms a tetramer of Atg12-Atg5·Atg16 (36). This multimeric complex is created before the induction of autophagy during nutrient rich conditions. It is not known how this complex is needed for the formation of transport vesicles but it might function as a transient coat (19), since proteins from this complex are not found to mark completed autophagosomes or Cvt vesicles. This complex has also been shown to be necessary for the lipidation of Atg8 (37), the second ubiquitin like conjugating cascade.
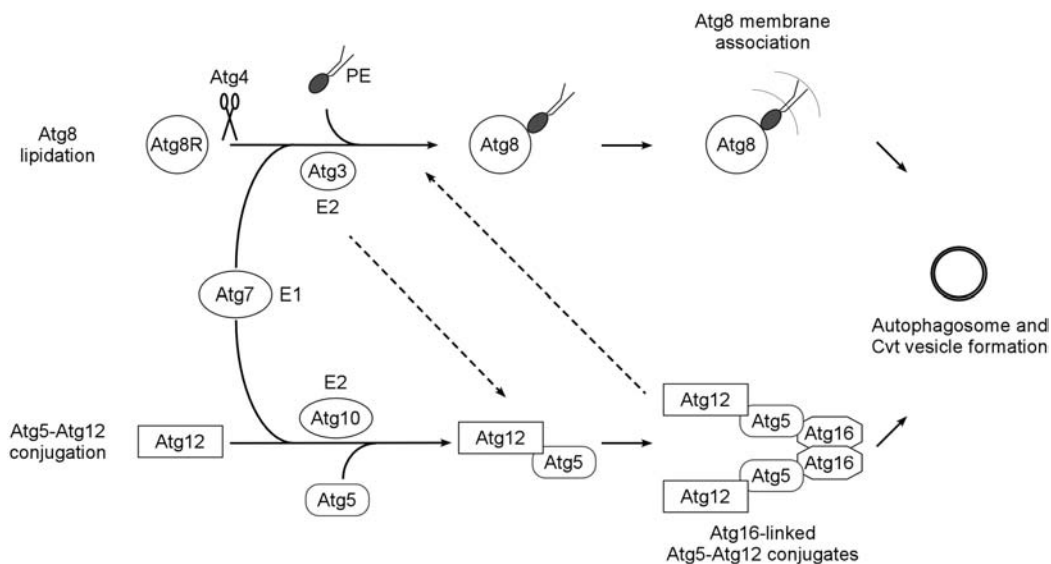
Figure 1-4 Schematic drawing of the two ubiquitin-like cascades involved in the formation of autophagosomes and Cvt vesicles.[4]

1.3.2.3   Atg8-lipidation

Atg8 was discovered as a low copy suppressor of Atg4 (39) and was found to be essential for the maturation of Ape1 not only during autophagy but also during the Cvt pathway (40). Atg8 was also identified as the first starvation induced protein of autophagy and a vesicle labelling protein (41).

The cytosolic Atg8, processed by Atg4, is schematically diagrammed in *Figure 1-4*. The protease Atg4 cleaves the C-terminal arginine residue revealing a glycine residue (40). This modification is necessary for the membrane association of Atg8. In GFP-Atg8 studies, Atg8 is found to be located as a cytosolic pool and at a point on the vacuolar membrane, the PAS (34). After starvation induction Atg8 was found within the vacuolar lumen (42),(34). In the absence of Atg4, Atg8 does not localized to the PAS.

As in the case of Atg12, Atg7 is also the E1 activator of Atg8 (43). The then modified Atg8 is covalently conjugated to phosphatidylethanol-amine (PE) by Atg3, its conjugating E2 enzyme. This step is dependent on the 350 kDa complex, although it is not known how. Lipidated Atg8, Atg8-PE, is then integrated into the double lipid bilayer of the forming autophagosome or Cvt vesicle. After the transport vesicle is completed, Atg8 is found attached inside and outside of the membrane. Atg4 then cleaves Atg8 from the outer surface allowing it to be recycled, while the Atg8 attached to the inner membrane is trapped within the vesicle and is transported to the vacuole where it is degraded with the cargo. This transfer of Atg8 to the vacuole can be used for

---

[4] Figure modified from Khalfan and Klionsky 2002 (38)

observing how autophagosomes travel to the vacuole. Using GFP-Atg8, the transport, degradation and release of free-GFP can be utilized in determining the ability and rate of autophagy in mutant strains.

1.3.2.4   The cargo proteins

The Cvt and autophagy pathways specifically transport the vacuolar hydrolases aminopeptidase I (Ape1) and α-mannosidase (Ams1) to the vacuole, where they are matured. In addition, other proteins/organelles seem to be transported to the vacuole through a specific autophagy, i.e. Ald6 (44) and peroxisomes (45), (46). Screening for a block in the maturation of aminopeptidase I in *S. cerevisiae* (47-50) lead to the discovery of several Cvt and autophagy mutants, in addition to those found in this study. Several autophagy related genes have also been identified in *H. polymorpha* and *P. pastoris* due to defects in the degradation of peroxisomes ref (51).
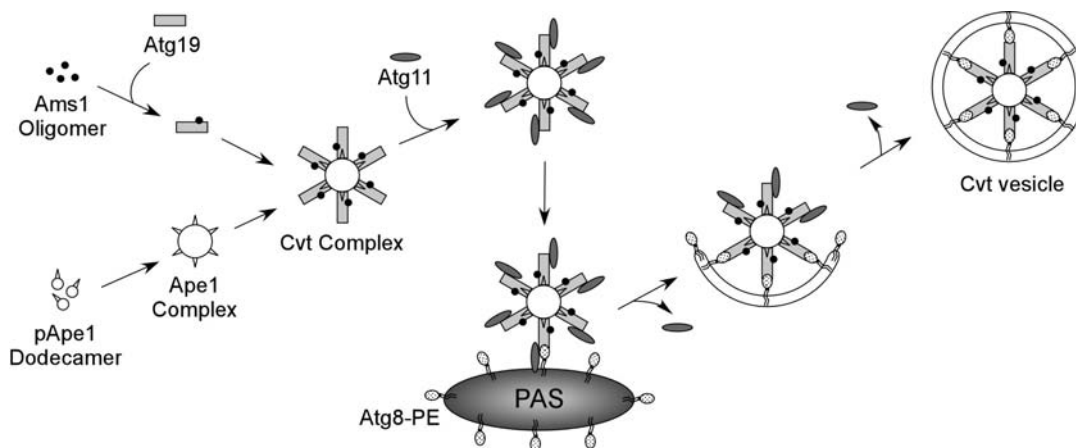
Figure 1-5 Schematic drawing of the selective packaging of Ape1 and Ams1 during Cvt vesicle formation.[5]

Precursor aminopeptidase I (pApe1) is synthesized on free ribosomes in the cytosol and oligomerizes rapidly to a dodecamer (54). As indicated in *Figure 1-5*, several dodecamers join together to form what is called the Ape1 complex (52). Atg19 the receptor protein of pApe1 attaches itself to the propeptide domain of Ape1 (55) and α-mannosidase is also bound to the Atg19 receptor (56) completing the Cvt complex. Atg11 then connects to Atg19 and somehow brings the Cvt complex to the PAS where it is bound to Atg8-PE (52). How this is done is not understood, but once the Cvt complex has reached the PAS, Atg11 disengages and is recycled.

---

[5] Figure modified from Shintani *et al.* 2002 and Thumm 2002 (52,53)

Once the other necessary proteins have accumulated at the PAS, the Cvt complex is packed within the transport vesicles. These vesicles then move to the vacuole to be ingested.

1.3.3 Fusion with the vacuole

After the autophagosome or Cvt vesicle is complete it travels and fuses with the vacuole. The fusion of autophagosomes and Cvt vesicles is a unique cellular process. Unlike other transport vesicles, such as those formed by endocytosis, these vesicles are made of a double lipid-bilayer. As the outer membrane fuses with the vacuole the inner membrane is released into the vacuolar lumen as an intact single membrane bound vesicle. This vesicle, called either an autophagic body or a Cvt body, is set free and degraded in the vacuolar lumen. The cell is therefore challenged; it must take up the outer membrane layer and release and degrade the inner membrane though both membranes originated from the same source. It is yet unknown how this is accomplished without compromising the integrity of the vacuole.

The fusion of vesicles with the vacuole is a selective process. The fusion is facilitated by the pairing of four soluble *N*-ethylmaleimide-sensitive factor attachment protein receptor (SNARE) proteins: Vma3, Vma7, Vti1, Ykt6 and/or Nyv1. The fusion of the outer membrane layer of autophagosomes and Cvt vesicles is not unlike that of other single membrane vesicles found in endocytosis, the CPY pathway or in that of homotypic vacuolar fusion.

As with the fusion of single membrane transport vesicles, this process is broken down into 1) priming; 2) docking: a) tethering and b) trans-SNARE pairing; and 3) fusion (57). During priming the target SNARE Vma3 is prepared for docking by the binding of the Class C-Vps protein/HOPS complex. The Class C-Vps complex consists of Vps11, 16, 18 and 33 proteins. Mon1 and Ccz1 (found in this study) have also been found to interact with the C-Vps complex during fusion (58,59). This connection is facilitated by ATP and homologs Sec17 and Sec18, the *N*-ethylmaleimide-sensitive factor (NSF) and the soluble *N*-ethylmaleimide-sensitive factor attachment protein (SNAP). Once the vacuole is primed, the cargo vesicle, e.g. our autophagosome, with its attached vesicle SNARE Vti1 is docked. This occurs in two steps. First, Vti1 is tethered to Vma3 with the help of Ypt7, Vps39 and Vps41. Ypt7 is a Rab GTPase that is needed for the fusion of vesicular intermediates with the vacuole (60). Second, Vam7, another vacuolar target SNARE, binds Vti1 and Vma3 together forming a trans-SNARE complex. This formation of the trans-SNARE complex initiates the fusion process. Many of these proteins are also needed for the homotypic fusion of vacuoles. Thus when genes such as *YPT7* are deleted fractionated vacuoles are seen.

1.3.4 Lysis of transport vesicles

After the single membrane bound autophagic body (or Cvt body) is released into the vacuolar lumen, it is lysed releasing its cargo. The cargo is then degraded into building blocks for the cell's survival. This degradation must be strongly regulated to maintain the integrity of the vacuolar membrane itself, since the outer lipid-bilayer has now fused and become part of the vacuolar membrane itself. Apart from the cytosolic proteasome, the vacuole is the main site of intercellular protein degradation (61). The degradation of these proteins and organelles is important for the homeostasis of the cell. Autophagy transports and recycles nearly half of all cellular proteins within 24 hours; under nutrient depletion about 85% of cellular proteins are turned over (62).

The lysis of these vesicular bodies depends on the proteinases A and B (3), an acidic vacuolar pH (63) and the proteins Atg15 (64,65) and Atg22 (66). When one of the above listed proteins is missing, deleted or inactivated, vesicles accumulate and are visible, moving rapidly within the vacuole.

Proteinase B (Prb1) is activated by proteinase A (Pep4). It is inhibited by the chemical phenylmethylsulfonyl fluoride (PMSF), which causes an accumulation of autophagic bodies in the vacuolar lumen. Prb1 is needed for the activation of several other vacuolar proenzymes, therefore its affect on lysis could be indirect (67).

The protein Atg15 is a putative serine lipase (65), whose exact functional mechanism has not be determined. Atg15 is inserted in the ER and is transported to the vacuole via the multi-vesicular body (MVB) pathway in 50 nm vesicles. In the vacuole it is involved in the lysis of Cvt bodies, autophagic bodies and MVB vesicles. It is also involved in the breakdown of peroxisome containing autophagic bodies (68).

Another protein that influences the lysis of autophagic bodies is Atg22 (66). Interestingly, in *atg22Δ* cells Ape1 is matured normally, indicating that Atg22 is not responsible for the lysis of all autophagic bodies. Atg22 is an integral membrane protein located on the vacuolar membrane. It shows homologies with drug transporters and is considered a putative permease that may be involved in the lysis of microautophagic bodies.

The lysis of Cvt and autophagic bodies is the last step in the processing of intracellular proteins; yet it is not less important than any other of the steps involved in the autophagic machinery.

2   Goals of this thesis

The goal of this study was to identify and characterize novel genes/proteins that are a part of autophagy or the Cvt pathway in the organism *Saccharomyces cerevisiae*, the common baker's yeast.

Six novel genes were identified utilizing a reverse genetic screen based on the autophagic phenotypes of reduced survival on amino acid depleted agar plates and the inability to mature the vacuolar hydrolase aminopeptidase I.

3   Materials and methods

3.1   Materials

3.1.1   Media

Standard media were used according to Ausubel *et al.* (69). Agar Plates were made by adding 4 % Bacto Agar to the selected medium resulting in a 2 % mixture.

3.1.1.1 Yeast media

<u>Complete Medium (YPD), pH 5.5</u>
1%   Yeast extract
2%   Peptone
2%   D-Glucose

<u>Synthetic Complete Medium (CM), pH 5.6</u>

0.67 %   Yeast nitrogen base w/o amino acids
2 %   D-Glucose
0.0117 %   L-Alanine, L-Arginine, L-Asparagine, L-Aspartic acid, L-Cysteine,
           L-Glutamine, L-Glutamic acid, L-Glycine, L-Isoleucine, L-Methionine,
           L-Phenylalanine, L-Proline, L-Serine, L-Threonine, L-Tyrosine, L-Valine,
           myo-Inositol
0.00117 % p-Aminobenzoic acid

The following supplements were added as needed:
0.3 mM   L-Histidine
1.7 mM   L-Leucine
1.0 mM   L-Lysine
0.4 mM   L-Tryptophane
0.3 mM   Adenine
0.2 mM   Uracil

<u>Synthetic Minimal Medium MV, pH 5.5</u>

0.67 %   Yeast nitrogen base w/o amino acids
2 %   D-Glucose
+ needed supplements

<u>Starvation Media</u>

For yeast cells, starvation was induced by shifting them to 1% potassium acetate, SD(-N) or growth medium containing 1 µl/ml rapamycin.

SD(-N)

0.17 %	Yeast nitrogen base w/o amino acids and ammonium sulfate
2 %	D-Glucose

Media for Direct Fluorescence Microscopy (SD+CA)

0.17 %	Yeast nitrogen base w/o amino acids and ammonium sulfate
0.5 %	Ammonium sulfate
0.5 %	Casamino acids
2 %	D-Glucose
+ needed supplements	

Media for Inducing Sporulation

Yeast cells were sporulated in either:

1 % potassium acetate or

1 %	Potassium acetate
0.1 %	Yeast Extract
0.05 %	Dextrose

3.1.1.2 Media for *E.coli*

Luria Brutani Broth for *E.coli* (LB), pH 7.5

10 %	Bacto-Trypton
5 %	Yeast Extract
5 %	NaCl

SOC Medium, pH 7.4

20 %	Bacto-Trypton
0.5 %	Yeast Extract
0.4 %	D-Glucose
0.4 %	2,5 M NaCl
0.25 %	1 M KCl
10 %	1 M $MgCl_2$
10 %	1 M $MgSO_4$

3.1.2 Antibodies

Cy3-conjugated goat α-mouse Fab fragment (Jackson ImmunoResearch, Suffolk, UK)

Mouse α-HA: hemaglutanin clone 16B12 (BAbCo, Richmond NC, USA)

Mouse α-GFP: monoclonal green fluorescent protein (Molecular Probes, Leiden, NL)

Mouse α-PGK: 3-phosphoglycerate kinase (Molecular Probes, Leiden, NL)

Mouse α-CPY: carboxypeptidase Y (Molecular Probes, Leiden, NL)

Mouse α-Dpm1: dolichol phosphate mannose synthase (Molecular Probes, Leiden, NL)

Mouse α-vATPase: vacuolar ATPase 100 kDa subunit (Molecular Probes, Leiden, NL)

Mouse α-Pep12   (Molecular Probes, Leiden, NL)

Horseradish peroxidase (HRPO)-conjugated goat α-rabbit   (Medac, Hamburg)

Horseradish peroxidase (HRPO)-conjugated goat α-mouse   (Dianova, Hamburg)

Rabbit α-API: pro-aminopeptidase I (49)

Rabbit α-Vps33   (W.Wickner, USA)

Rabbit α-Vac8   (D.S. Goldfarb, USA (70))

Rabbit α-FAS: fatty acid synthase (62)

Rabbit α-Atg8:   Atg8 (71)

Rabbit α-GFP: polyclonal green fluorescent protein   (Molecular Probes, Leiden, NL)

Rabbit α-PrB: polyclonal proteinase B (D. Wolf, Stuttgart)

3.1.3 Plasmids

pECFP: enhanced CFP fluorescent protein (BD Clontech, Heidelberg)

pEYFP: enhanced YFP fluorescent protein (BD Clontech, Heidelberg)

Yeast centromeric vectors: (New England Biolabs, Frankfurt)

   pRS313 (HIS3), pRS314 (TRP1), pRS315 (LEU2), pRS316 (URA3)

Yeast high-copy vectors: (New England Biolabs, Frankfurt)

   pRS423 (HIS3), pRS424 (TRP1), pRS425 (LEU2), pRS426 (URA3)

pKMW1:   pRS313-YFP (this study)

   The ECFP or EYPF-fluorescent protein was excised from pECFP or pEYFP with XmaI and EcoRI
   and inserted into the pRS313 vector at the same sites.

pKMW2:   pRS313-CFP (this study)

   The ECFP or EYPF-fluorescent protein was excised from pECFP or pEYFP with XmaI and EcoRI
   and inserted into the pRS313 vector at the same sites.

pKMW5:   pRS316-YFP (this study)

   The EYFP-fluorescent protein was excised from pEYFP with XmaI and EcoRI and inserted into the
   pRS316 vector at the same sites.

pKMW13:   Ape1-YFP (this study)

   The vector pKMW1 was cut with KspI and XmaI, and a PCR fragment, containing *APE1* with its
   native promoter and the added KspI and XmaI incision sites, was inserted yielding the plasmid
   pKMW13. The PCR Fragment was constructed with the primer KSPI-APEI (AGGGCCGCGGCTAC
   TTTAGGGTATAGGTTG) and XMAI-APEI (AGGGCCCGGGACAACTCGCCGAATTCATCG)
   and the plasmid pRN1.

pKMW16:   Atg21-YFP (this study)

   This vector pKMW5 was cut with KspI and AgeI, and a PCR fragment, containing *ATG21* with its
   native promoter and the added KspI and AgeI incision sites, was inserted yielding the plasmid
   pKMW16. The PCR fragment was constructed with the primer KSPI-MAI1
   (AGGGccgcggGTTCAATTTATGGGAAATATAC) and AGEI-MAI1 (agggAccggtgATGTAAATT
   TATTATTTTTAGtcag) and the plasmid cen-ATG21-HA.

pKMW17:   Ape1-CFP (this study)

   The vector pKMW2 was cut with KspI and XmaI, and a PCR fragment, containing *APE1* with its
   native promoter and the added KspI and XmaI incision sites, was inserted yielding the plasmid
   pKMW17. The PCR Fragment was constructed with the primer KSPI-APEI (AGGGCCGCGGCTAC
   TTTAGGGTATAGGTTG) and XMAI-APEI (AGGGCCCGGGACAACTCGCCGAATTCATCG)
   and the plasmid pRN1.

pRN1:   centromeric *APEI* (47)

pRS316 GFP-AUT7:   centromeric GFP-ATG8 (34)

pMet25::GFP-AUT9:   GFP-ATG9 controlled by a Met promoter (72)

pGFP-YOL082:   GFP-ATG19 (73)

pRS426-AUT7:   high copy plasmid containing ATG8 (39)

p_{CUP1}::Nvj1-CFP: NVJ1-CFP controlled by a *CUP1* (copper) promoter (70)

2μ-ATG18-HA: high-copy plasmid containing ATG18-HA (71)

cen-ATG21-HA: centromeric plasmid containing ATG21-HA (71)

2μ-ATG21-HA: high-copy plasmid containing ATG21-HA (71)

pUG6:   deletion plasmid conferring kanamycin resistance (74)

pGF10:   pho8Δ::LEU2 deletion plasmid (75)

pCC5:   Pho8Δ60 expression plasmid (76)

3.1.4 Yeast Strains

Table 3-1 Yeast Strains

Name	Genotype	Yeast Strain	Mating Type	Reference
WCG4a	*his3-11,15 leu2-3,112 ura3*		(α)	(77)
WCG4a	*his3-11,15 leu2-3,112 ura3*		(a/α)	(77)
YKMW1	*trs85::KAN^R*	WCG4a	(α)	(78)
YKMW2	*mon1::KAN^R*	WCG4a	(α)	(79)
YKMW3	*ccz1::KAN^R ypt7::HIS3*	WCG4a	(α)	this study
YKMW6	*trs85::KAN^R*	WCG4a	(a)	this study
YKMW7	*ccz1::KAN^R*	WCG4a	(α)	(80)
YKMW10	*ypt7::HIS3*	WCG4a	(a)	(80)
YKMW11	*mon1::KAN^R*	WCG4a	(a)	this study
YKMW12	*ccz1::KAN^R*	WCG4a	(a)	(80)
YKMW15	*ccz1::KAN^R ypt7::HIS3*	WCG4a	(a)	this study
YKMW16	*atg3::ADE2 ypt7::HIS3*	WCG4a	(a)	(71)
YKMW17	*mon1::KAN^R ypt7::HIS3*	WCG4a	(α)	this study
YKMW18	*trs85::KAN^R ypt7::HIS3*	WCG4a	(α)	(78)
YKMW19	*mai1::KAN^R ypt7::HIS3*	WCG4a	(α)	(71)
YKMW20	*ccz1::KAN^R pho8::LEU2*	WCG4a	(α)	(79)
YKMW21	*trs85::KAN^R pho8::LEU2*	WCG4a	(α)	(78)
YKMW22	*mon1::KAN^R pho8::LEU2*	WCG4a	(α)	(79)
YKMW23	*pho8::LEU2*	WCG4a	(α)	this study
YKMW24	*mai1::KAN^R GFPAPE1*	WCG4a	(a)	this study
YKMW27	*ypt7::KAN^R*	WCG4a	(a)	this study
YKMW28	*trs85::KAN^R*	SEY6211	(a)	(78)

YKMW29	*mai1::KAN^R*	SEY6211	(**a**)	this study
YKMW30	APE1-RFP-KAN^R	WCG4a	(**α**)	this study
YKMW31	APE1-RFP-KAN^R	WCG4a	(**a**)	this study
YKMW32	*vps34::KAN^R*	WCG4a	(**a**)	this study
YKMW33	*vps34::KAN^R*	WCG4a	(**α**)	this study
YKMW36	*ape1::KAN^R*	WCG4a	(**α**)	(78)
YFB1	*atg23::KAN^R*	WCG4a	(**α**)	(81)
YHB1	*atg18::KAN^R*	WCG4a	(**α**)	(50)
YHB4	*atg21::KAN^R*	WCG4a	(**α**)	(71)
YHB5	MAI1HA-HIS5	WCG4a	(**α**)	(82)
YHB7	*ypt7::KAN^R*	WCG4a	(**α**)	(71)
YHB8	*atg21::KAN^R pho8::LEU2*	WCG4a	(**α**)	(71)
YIS4	*atg15::KAN^R*	WCG4a	(**α**)	(65)
YMS6	*atg3::ADE2*	WCG4a	(**a**)	(83)
YMS30	*atg1::KAN^R*	WCG4a	(**a**)	(84)
YMTA	*pep4::HIS3*	WCG4a	(**a**)	(77)
YUE47	*atg19::KAN^R*	WCG4a	(**α**)	(79)
YUE63	*atg15::KAN^R pho8::LEU2*	WCG4a	(**α**)	(79)
YUE66	*pho8::LEU2*	WCG4a	(**α**)	(79)
SEY6210	*leu2-3,112 ura3-52 his3-Δ200 trp1Δ901 lys2-801 suc2Δ9*		(**α**)	(85)
SEY6211	*leu2-3,112 ura3-52 his3-Δ200 trp1Δ901 ade2-101 suc2Δ9*		(**a**)	(85)
AHY41	*cvt13-1*	SEY6210	(**α**)	(48)
AHY377	*cvt14-1*	SEY6210	(**α**)	(48)
AHY1468	*cvt10-4 (atg1-1)*	SEY6211	(**a**)	(48)
AHY1915	*cvt11-1*	SEY6210	(**α**)	(48)
AHY2215	*cvt16-1 (ccz1-1)*	SEY6210	(**α**)	(48)
DYY101	*ape1::LEU2*	SEY6210	(**α**)	(86)
THY119	*cvt3-1*	SEY6211	(**a**)	(47)
THY144	*cvt6-1*	SEY6211	(**a**)	(47)
THY193	*cvt2-1 (atg7-1)*	SEY6211	(**a**)	(47)
THY313	*cvt5-1 (atg8-1)*	SEY6211	(**a**)	(47)
BY4741	*his3-Δ1 leu2-Δ0 met15-Δ0 ura3-Δ0*	Y00000	(**a**)	Euroscarf
BY4742	*his3Δ1 leu2-Δ0 lys2-Δ0 ura3-Δ0*	Y10000	(**α**)	Euroscarf
BY4743	*his3-Δ1/his3Δ1 leu2-Δ0/ leu2-Δ0 met15-Δ0/MET15 LYS2/lys2-Δ0 ura3-Δ0/ura3-Δ0*	Y20000	(**a/α**)	Euroscarf
Y30575	*ypt7::KAN^R/ypt7::KAN^R*	BY4743	(**a/α**)	Euroscarf
Y32152	*atg21::KAN^R/atg21::KAN^R*	BY4743	(**a/α**)	Euroscarf
Y32098	*pep4::KAN^R/pep4::KAN^R*	BY4743	(**a/α**)	Euroscarf

Y32371	*trs33::KAN^R/trs33::KAN^R*	BY4743	(**a**/α)	Euroscarf
Y33357	*atg12::KAN^R/atg12::KAN^R*	BY4743	(**a**/α)	Euroscarf
Y33883	*vma1::KAN^R/vma1::KAN^R*	BY4743	(**a**/α)	Euroscarf
Y34491	*mon1::KAN^R/mon1::KAN^R*	BY4743	(**a**/α)	Euroscarf
Y34042	*trs85::KAN^R/trs85::KAN^R*	BY4743	(**a**/α)	Euroscarf
Y34796	*trs36::KAN^R/trs36::KAN^R*	BY4743	(**a**/α)	Euroscarf
Y34953	*ape1::KAN^R/ape1::KAN^R*	BY4743	(**a**/α)	Euroscarf
Y35700	*atg18::KAN^R/atg18::KAN^R*	BY4743	(**a**/α)	Euroscarf
Y37164	*ccz1::KAN^R/ccz1::KAN^R*	BY4743	(**a**/α)	Euroscarf

3.1.5 Oligonucleotides

s-GSG1
CTTTATTCAGTCGGCTTTACAGATACTGAGGTAACTTATAcagctgaagcttcgtacgc

as-GSG1
TACGTATAATTTATACTCAAAACATGAATTTTCCATAAAGgcataggccactagtggatctg

s-CCZ1
CTAAATCGTACAACTATTAAATTGATATATGAAAGACGGATcagctgaagcttcgtacgc

as-CCZ1
TATGTTATCAAATGCTAAACGTTACATTTTTAAATTTCCCgcataggccactagtggatctg

s-MON1
TCTATCAAAGTACACAAACGTAGAATCAGTACATCGGAACTcagctgaagcttcgtacgc

as-MON1
AATAACCTCCCTGTCACAAGTTAAAACACGGCCCCATCACgcataggccactagtggatctg

S-vps34-kan
CATAGTCCTTCATTCGGTATATGCAGATCCGGCATCAAACAcagctgaagcttcgtacgc

AS-vps34-kan mit stop
GAAGCACCAATTATCAATCAGGTCCGCCAGTATTGTGCgcataggccactagtggatctg

S-APE1-kan
GTGAGGAATATGAATTAGTCAGCTTCTACTTTAGGGTATAGcagctgaagcttcgtacgc

AS-APE1-kan mit Stop
GTGGCAAAATCACAACTCGCCGAATTCATCGTAGACTGgcataggccactagtggatctg

S-APG13-kan
GGGAACACACGTGAAAGTGAAGGACAGCACCAACCAAGGGGcagctgaagcttcgtacgc

AS-APG13-kan
CCTTCTTTAGAAAGGTTCATATCACTCATGAAAAATACgcataggccactagtggatctg

S-APG7-kan
GGAAGAACAAGCCACCACATGTTGAAAACTAGATAGGCAAGcagctgaagcttcgtacgc

AS-APG7-kan

CTTAATTACGGAAAGTGGCACCACAATATGTACCAATGgcataggccactagtggatctg

S-APG5-kan
GCTAGTAGAGGATGGGGGGGAATCCTACAGCGTAGGTACCGGcagctgaagcttcgtacgc

AS-APG5-kan im Gen
GTATATAACAGCTCTTAGAGCTCAGAGGAAGCTTTATCgcataggccactagtggatctg

KSPI-APEI
AGGGCCGCGGCTACTTTAGGGTATAGGTTG

XMAI-APEI
AGGGCCCGGGACAACTCGCCGAATTCATCG

KSPI-MAI1
AGGGccgcggGTTCAATTTATGGGAAATATAC

AGEI-MAI1
agggAccggtgATGTAAATTTATTATTTTTAGtcag

F-431-KAN
GTTGTTCTATAAGGTAACAAAATAAAGTGAAGAAGTAAATCAGCTGAAGCTTCGTACGC

R-431-KAN
AATTTACATTATCCTCATGGCTACTCTAGCTATTTGCATTGCATAGGCCACTAGTGGATCTG

3.1.6 Enzymes

All enzymes were obtained from Roche Diagnostics (Mannheim) or New England Biolabs (Frankfurt).

3.1.7 Chemicals

Chemicals not specifically mentioned were obtained from Roth (Karlsruhe) or Sigma (Deisenhofen) in analytical grade; all others are listed below.

Optiprep™ (Axis Shield, Oslo, Norway); Bacto Agar, Bacto Peptone, Bacto Tryptone, Bacto Yeast Nitrogen Base w/o AA, Casamino acids, Yeast Extract, Yeast Nitrogen Base w/o AA AS (BD Bioscience, Heidelberg); Ammonium persulfate (Bio-Rad, Munich); ProtoGel™ (Biozym Scientific GmbH, Hessisch Oldendorf); Antipain, Benzamidin, Chymostatin, Leupeptin, Pepstatin, G418 (Calbiochem, San Diego CA, USA); Citifluor (Citifluor Ltd., London, UK); Complete® protease inhibitor mix (Roche Diagnostics, Mannheim); Oxalyticase (Enzogenetics, Corvallis OR, USA); Zymolyase 100T (Seikagaku Kyogo, Tokyo, Japan); Copper (II)-sulfate pentahydrate (Serva, Heidelberg).

3.1.8 Kits

ECL™ Western blotting detection kit (Amersham, Braunschweig)

QIAprep® Spin Miniprep Kit (Qiagen, Hilden)

QIAquick® Gel Extraction Kit (Qiagen, Hilden)

QIAquick® PCR Purification Kit (Qiagen, Hilden)

Gene Images™ CDP-Star™ Detection Module Kit (Amersham, Braunschweig)

3.1.9 Equipment

Electroporator 2510 (Eppendorf, Hamburg)

Mastercycler® gradient (Eppendorf, Hamburg)

Robocycler® gradient 40 (Stratagene, La Jolla CA, USA)

Centrifuge 5804R (Eppendorf, Hamburg)

Centrifuge 5415C (Eppendorf, Hamburg)

Ultracentrifuge TL-100, (Beckman Coulter, Krefeld)

    Rotors: TLA-100.2, TLA-100.3, TLS-55 rotor

Ultracentrifuge Centrion T-1065 (Kontron Lab Instruments)

Ultracentrifuge L-80, SW41Ti rotor (Beckman Coulter, Krefeld)

Wide Mini-Sub Cell GT (Bio-Rad, Munich)

Mini-Sub Cell GT (Bio-Rad, Munich)

Mini-PROTEAN 3 Cell (Bio-Rad, Munich)

Vortexer Genie 2, Scientific Industries, Inc. (Bohemia, NY USA)

Water bath

Centrifuge Biofuge pico (Heraeus Instruments, Hanau)

Shaker KS10 (Edmund Buehler, Tuebingen)

Multi-vortexer IKAMAG® REO (IKA Labortechnik, Staufen)

Water Milli-Q (Millipore, Eschborn)

X-Ray Film Processor Optimax (Protec Medizintechnik, Oberstenfeld)

3.2   Long term storage methods

3.2.1 Storage culture for *E.coli*

E.coli strains were conserved in a 30 % glycerol solution. A 60 % glycerol solution was prepared and 500 µl was sterilized in a 2 ml cyro tube. The desired strain was inoculated in 2 ml LB-Amp and grown for 8-16 h at 37 °C. 500 µl culture was added to the glycerol solution and the cyro tube was stored at -80 °C.

3.2.2 Storage culture for yeast

S. cerevisiae yeast strains were conserved in a 15 % glycerol solution. The 15 % glycerol solution was prepared and 1 ml was sterilized in 2 ml cyro tubes. The desired strain was either inoculated in the necessary medium or streaked out on to the necessary agar plate and grown overnight at 30 °C. A pea-sized cell pellet was resuspended in the 15 % glycerol solution. The pellet was obtained either through centrifugation at 500 xg from a liquid culture or scraped from an agar plate with a sterilized toothpick. The cyro tube was stored at -80 °C.

3.3   Molecular biological methods

3.3.1   DNA isolation

3.3.1.1 Isolation of plasmid DNA from *E. coli* "Mini-Prep"

3.3.1.1.1 Mini-prep via alkaline lysis

2 ml LB-Amp was inoculated with the desired bacterial colony and incubated overnight at 37 °C with vigorous shaking. 1.5 ml of the overnight culture was inserted into a microfuge tube and centrifuged at 13,000 xg for 30 s. The supernatant was removed by aspiration and the remaining bacterial pellet was completely resuspended in 100 µl ice-cold solution I by vortexing. On ice, 200 µl solution II was added and the reaction was mixed immediately by inverting 4-6 times. 150 µl Solution III was the added and the reaction was vortexed gently. The suspension was incubated on ice for 3-5 min and the precipitate was pelleted at 13,000 xg for 6 min. The supernatant was transferred to a fresh microfuge tube and the DNA was precipitated with two volumes of ethanol at room temperature. The microfuge tube was then centrifuged at 13,000 xg for 10 min and the supernatant removed. The DNA pellet was washed with 70 % ethanol and then resuspended in 50 µl H_2O containing 0.2 µg/µl RNase A. The plasmid solution was stored at –20 °C.

Solution I, pH 8,0
50 mM Glucose
25 mM Tris
10 mM EDTA
sterilized and stored at 4 °C

Solution II
0.2 N NaOH
1 % SDS
Made fresh from 20 µl 10 N NaOH, 10 µl 10 % SDS and 970 µl H_2O.

Solution III, pH 5.2
60 ml 5 M potassium acetate
11.5 ml glacial acetic acid
ad 100 ml H_2O
sterilized and stored at 4 °C

3.3.1.1.2 Mini-prep via the QIAprep® Spin Miniprep Kit

2 ml LB-Amp was inoculated with the desired bacterial colony and incubated overnight at 37 °C with vigorous shaking. 1.5 ml overnight culture was centrifuged in a microfuge tube at 13,000 xg for 1 min. The pellet was resuspended in 250 µl cold P1 buffer containing RNase. 250 µl P2 buffer was added and the tube was inverted 4-6x. 350 µl N3 buffer was then added and the tube a mixed by inversion. The microfuge tube was then centrifuged for 10 min at 13,000 xg and the resulting supernatant was given to the QIAprep spin column. The column was centrifuged at 13,000 xg for 30 s and the flow-through was discarded. The column was washed with 750 µl PB buffer and centrifuged for 30 s at 13,000 xg. The flow-through was discarded and the column dried by centrifuging for 1 min at 13,000 xg. The QIAprep spin column was inserted into a fresh microfuge tube, 30-50 µl ddH$_2$O was pipetted directly onto the membrane and incubate for 1 min. The microfuge tube and spin column were centrifuge for 1 min at 13,000 xg and the eluated DNA plasmid was stored at -20 °C.

3.3.1.2 Isolation of plasmid DNA from yeast "Plasmid-Rescue"

In a microfuge tube a pea-sized amount of yeast cells was resuspended in 400 µl H$_2$O. 200 µl breaking buffer, 200 µl glass beads and 200 µl of a 1:1 phenol/chloroform mixture were added and the reaction was rapidly shaken for 15 min at 4 °C. Afterwards, the microfuge tube was centrifuged at 13,000 xg for 10 min. The supernatant was then removed and precipitated with one-tenth the volume of 3 M sodium acetate and twice the volume of ethanol. This was incubated for 30 min at –20 °C. The plasmid DNA was then pelleted at 13,000 xg for 10 min and the resulting pellet was washed with 70 % ethanol, dried and then taken up in 30 µl H$_2$O.

Breaking-Buffer, pH 8,0
10 mM   Tris/HCl
100 mM   NaCl
1 mM   EDTA
1 % (w/v) SDS
2 % (v/v) Triton X-100

3.3.1.3 Isolation of yeast chromosomal DNA

The selected yeast strains were inoculated in 2 ml YPD or the corresponding selection medium and grown overnight at 25 °C or 30 °C. 1.5 ml of the overnight culture was pelleted in a microfuge tube at 13,000 xg for 1 min. The pellet was then washed with 500 µl H$_2$O and resuspended in 200 µl breaking buffer (see 3.3.1.2). 200 µl glass beads and 200 µl of a phenol-chloroform mixture (see 3.3.1.2) were added and the microfuge tube was vortexed four times for 1 min. After every vortexing procedure the reaction was allowed to cool on ice. When finished, 200 µl H$_2$O was added and the microfuge

tube was centrifuged at 13,000 xg for 10 min. The upper phase was transferred to a new tube and 1 ml ethanol was added. After precipitating for 10 min at –20 °C. The chromosomal DNA was pelleted at 13,000 xg and 4 °C for 10 min and the resulting pellet was resuspended in 400 µl containing 3 µl RNase A (10 mg/ml). The RNA was digested at 37 °C for 5 min. Then the chromosomal DNA was again precipitated after adding 1 ml ethanol and 10 µl 5 M ammonium acetate. The DNA was then pelleted, dried and resuspended in 20-50 µl H_2O.

3.3.2 DNA modification

3.3.2.1 Digestion of DNA using restriction endonucleases

Plasmid or chromosomal DNA was cut with the help of restriction endonucleases. Endonucleases recognize symmetrical sequences in the DNA chain and cleave them specifically. Depending on the enzyme, a blunt or sticky-end cleavage was obtained. A standard digestion was carried out as followed:

2 µl plasmid DNA was combined with 2 µl 10x reaction buffer and 0.2-1 µl restriction enzyme, ddH2O was added until the total reaction volume was 20 µl. When indicated, BSA was added to the reaction mixture to obtain a final concentration of 0.1 mg/ml. The digestion was carried out at 37 °C or at one specified by the manufacturer.

If the digestion involved the cleavage with two enzymes that are compatible, reacting in the same buffer and at the same temperature, then the digestion was carried out simultaneously. If the reaction buffers differed, the digestion was carried out successively. The DNA was precipitated with ethanol between digestion steps.

3.3.2.2 Hydrolysis of 5'-phosphate groups

Calf intestine alkaline phosphatase (CIP) was used to hydrolyze 5'phosphate groups of vectors to prevent unwanted re-ligation of the backbone-plasmid. After digesting, 1 µl CIP was added to the vector DNA in a digestion buffer and allowed to incubate for 1 h at 37 °C. The DNA was then either precipitated with ethanol or isolated with a purification column from Qiagen.

3.3.2.3 Ligation of DNA fragments

The ligation of a plasmid vector with the insert was carried out with the DNA from the insert and the vector in approximate relationship of three to one. The digested DNA, in 1x ligation buffer and 1 µl T4 DNA ligase was combined in a microfuge tube and incubated either for 2 h at room temperature or overnight at 18 °C.

3.3.2.4 Polymer chain reaction "PCR"

The polymer chain reaction (PCR) is a useful tool to amplify DNA fragments. It is also a helpful tool to modify DNA sequences. Using selected primers, restriction sites can be inserted or bridging segments can be added to the resulting PCR fragment. This allows the fragment to be easily inserted into a vector or genomic modifications to be made.

DNA was amplified *in vitro* with PCR. Thermostable $Vent_R$® DNA Polymerase (NEB) was used in a 100 µl standard reaction.

Table 3-2 Standard PCR reaction

Reagent[6]	Concentration/Amount
Sense Primer	100 pmol (1 µl)
Anti-sense Primer	100 pmol (1 µl)
DNA Template (plasmid)	1 µl
10x ThermoPol Buffer	10 µl
100 mM $MgSO_4$	1 µl
DNTP-Mix[7]	1 µl
Thermostable Polymerase	1 µl
Total Volume	Ad 100 µl ddH_2O

1x ThermoPol Reaction Buffer, pH 8.8 (NEB)
10 mM   KCl
10 mM $(NH_4)_2SO_4$
20 mM   Tris-HCl
 2 mM $MgSO_4$
0.1 %   Triton X-100

The PCR reaction was performed in the Robocycler® gradient (Stratagene) or a Mastercycler® gradient (Eppendorf, Hamburg). Before adding the polymerase, the reaction was heated to 94 °C for 2 min, to denature the template. This procedure is called a "Hot-Start". The PCR program was selected according to the primer annealing temperature or a temperature gradient was selected. After the PCR was completed, a 5 µl sample was separated by gel electrophoresis and correct PCR products were purified using the *QIAquick® PCR Purification Kit*.

---

[6] Sometimes 10 µl DMSO was added to improve the PCR reaction.

[7] The desoxynucleotide (dNTP)-Mix consisted of equal amounts of dATP, dCTP, dGTP and dTTP.

Table 3-3 Standard PCR program

No. Cycles	Denaturation Temp. 95 °C	Annealing Temp.[8] 55 °C	Elongation Temp. 72 °C
1	5 min	40 s	3 min
25-30	40 s	40 s	3 min
1	40 s	40 s	6 min

3.3.3 Purification of DNA fragments

3.3.3.1 Agarose gel electrophoresis

To separate DNA fragments horizontal 0.8 % (w/v) agarose gels in 1 % TAE buffer were used. The negatively charged DNA fragments travel through the agarose gel and are separated according to size. Larger fragments are better separated by thinner gels and smaller by gels containing more agarose. DNA fragments were visualized by staining with ethidium bromide (EtBr). 1 µl of a 1 % EtBr solution per 10 ml gel was added. Ethidium bromide intercalates between the stacked bases in the DNA structure and emits fluorescent light when subjected to UV radiation. The cast gel was placed in the mini-sub cell apparatus from Bio-Rad. Loading buffer was added to the samples and they were pipetted into the wells. At least one well was reserved for the 5 µl DNA Marker (1 kb DNA Ladder, NEB). The separation was carried out at 120 V until the desired separation was achieved. The DNA bands were recorded with instant print film or captured with a digital camera.

50x TAE, pH 8.5
1 M   Tris/acetic acid
100 mM   EDTA

10x Loading Buffer, pH 8,0
1 M   Tris/HCl
50 % (v/v) Glycerol
0.1 % (w/v) Bromophenol blue

3.3.3.2 Isolation of DNA fragments in agarose gel

After separation with gel electrophoresis, distinct bands can be extracted from the gel for later use. This was done using the *QIAquick® Gel Extraction Kit*, Qiagen 2002. A microfuge tube was weighed and the weight noted. The selected band was excised out of the gel with a scalpel and inserted into a microfuge tube, the size of the gel was held at a minimum. The tube was again weighed and the weight of the gel deduced. For

---

[8] The annealing temperature was selected according to the primers or a temperature gradient was selected.

every 100 mg gel, 300 µl of QG buffer was added[9]. The microfuge tube was incubated for 10 min at 50 °C, vortexing every few minutes until the gel piece was dissolved. The mixture was given to the QIAquick spin column and centrifuged at 13,000 xg for 1 min. The flow-through was discarded and the column was washed with 700 µl PE buffer. The column was centrifuged for 30 s and the flow-through was discarded. After centrifuging the column for 1 min at 13,000 xg, it was inserted into a clean 1.5 ml microfuge tube. 30-50 µl ddH$_2$O was given directly to the membrane and incubated for 1 min at RT. The microfuge tube and the column were then centrifuge for 1 min at 13,000 xg and the eluated DNA fragment was stored at -20 °C.

3.3.3.3 Purification of PCR products

A simple method for purifying PCR products was using *QIAquick® PCR Purification Kit* as described by the manufacturer, Qiagen 2002. The PCR reaction was mixed with 500 µl buffer PB. The mixture was the transferred to the QIAquick spin column and centrifuged for 30 s at 13,000 xg. The flow-through was discarded. The column was washed with 750 µl PE buffer and centrifuged for 30 s at 13,000 xg. The flow-through was discarded and the spin column was centrifuged for 1 min to dry the column. The column was inserted into a clean 1.5 ml microfuge tube and 30-50 µl ddH$_2$O was given directly to the membrane and incubated for 1 min at RT. The microfuge tube and the column were then centrifuge for 1 min at 13,000 xg and the eluated DNA fragment was stored at -20 °C.

If more than one PCR product was obtained, the desired fragment was separated with in an agarose gel. The fragment was then excised and extracted with the *QIAquick® Gel Extraction Kit*.

3.3.4 Transformation of plasmid DNA

3.3.4.1 Plasmid transformation in *E.coli*

3.3.4.1.1 Preparation of electro-competent *E.coli*

The E.coli strain, DH5α, was inoculated in 10 ml LB medium and grown overnight at 37 °C. 600 ml LB medium was then combined with 6 ml of the overnight culture and allowed to grown until log phase ~0.5 OD$_{600}$ units. The culture was then cooled on ice for 30 min and then pelleted in two centrifuge bottles for 8 min at 5,000 xg and 4 °C (JA-10 rotor, Beckman). The pellets were each washed consecutively with 300 and 150 ice-cold 10 % Glycerol. The pellets were then resuspended in 5 ml ice-cold 10 %

---

[9] Depending on the length of the DNA fragment, the gel was dissolved in different solution mixtures. For fragments >4 kb two equivalents of ddH$_2$O were added.

Glycerol and transferred into two 15-ml falcon tubes and centrifuged for 8 min at 4,500 xg and 4 °C. The pellets were each resuspended in 0.5 ml ice-cold 10 % Glycerol. The cells were divided into 40 µl aliquots in ice-cooled microfuge tubes. The competent *E.coli*s were shock frozen in liquid nitrogen and stored at -80 °C.

3.3.4.1.2 Transformation through electroporation

For each needed plasmid or ligation one competent *E.coli* aliquot was thawed on ice. Accordingly per aliquot, one 2 mm electroporation cuvette was cooled on ice or by -20 °C. 1-2 µl of a plasmid or ligation was given to the *E.coli* aliquot and incubated on ice for a few minutes. The aliquot and DNA were pipetted into the cuvette and placed into the electroporator (Gene Pulser™ (Bio-Rad), or Electroporator 2510 (Eppendorf)). The electroporation was carried out at 2.3-2.5 kV, 400 Ω and 250 µF. Afterwards, the *E.coli*s were resuspended in 1 ml SOC medium, transferred to a microfuge tube and incubated for 1 h at 37 °C while shaken. The aliquots were then plated onto LB-Amp plates and incubated overnight at 37 °C.

3.3.4.2 Competent yeast transformation

In order to transfer a plasmid or PCR Fragment into a yeast strain the cells have to be made competent.

The selected strain was grown to an optical density (OD_{600}) of 0.3-0.5. 10 ml culture was pelleted at 1,600 xg for 3 min. The pellet was washed twice with 10 ml sterile ddH$_2$O and once with 2.5 ml of a lithium-sorbitol (Li-Sorb) solution. The pellet was then resuspended in 100 µl Li-Sorb and incubated for 30 min at 30 °C. After the incubation, the cell pellet was aliquoted into sterile microfuge tubes in 40 µl portions. 300 µl PEG-Mix was then added to the cell pellet. 5 µl single-stranded DNA[10] and 2 µl plasmid DNA were also added and the suspension mixed. The reaction was then incubated for 30 min at 30 °C and then "heat-shocked" exactly 15 min at 42 °C. The yeast cells were pelleted and plated onto selection media agar plates. The plates were then incubated for 2-3 d at 30 °C.

10x TE, pH 7.5 sterilized
100 mM   Tris/HCl
10 mM   EDTA

10x LiAcetate, pH7.5 sterilized
1 M   Lithium acetate/acetic acid

---

[10] Herring sperm was used for single-stranded DNA. Before use, the DNA was heated for 5min at 95 °C and then cooled on ice.

50 % PEG sterilized
50 % (w/v) Polyethylene glycol 4000 in ddH$_2$O

Li-Sorbitol sterilized
25 ml   10x LiAcetate
25 ml   10x TE
1 M   Sorbitol
ad 250 ml ddH$_2$O

PEG-Mix
4/5   50 % PEG
1/10   10x TE
1/10   10x LiAcetate

3.3.4.2.1 Rapid transformation

Often, for a plasmid transformation it was not necessary to use competent yeast cells. Yeast cells were scraped from an agar plate with a sterile toothpick. The cell pellet was resuspended directly in 300 µl PEG-Mix. 5 µl single-stranded DNA and 2 µl plasmid DNA were added and the suspension mixed. The reaction was then treated like the standard yeast transformation.

3.3.4.2.2 Transformation of DNA fragments into the yeast genome

DNA Fragments that integrate themselves through homologue recombination into the yeast genome are transferred using a modified transformation procedure. The yeast strain is treated like in the competent yeast transformation (3.3.4.2) up until the DNA fragments are added. Unlike for the plasmid transformation, more fragment DNA (e.g. PCR product) is required, because the chance of a homologue recombination is small. 10 µl fragment DNA and 5 µl single-stranded DNA were added to the cell pellet in PEG-Mix. The suspension was incubated for 30 min at 30 °C and then "heat shocked" for 15 min at 42 °C. The yeast cells were pelleted at 500 xg for 1 min and resuspended in 1-5 ml YPD medium. The cells were shaken at 220 rpm and 30 °C for 3-4 h and then pelleted and plated out onto selection medium plates, e.g. YPD + G418 (200 mg/l). The plates were incubated for 2-3 d at 30 °C. In the case of a kanamycin resistance selection marker the plates were then replica plated onto the same kind of selection plates, YPD + G418. The correct integration of gene fragments can be monitored with Southern blot analysis.

3.3.5 Southern blot analysis

Chromosomal DNA from the yeast strains being controlled were digested with multiple restriction enzymes that cut left and right of the inserted gene. The size of the DNA fragments containing the gene was noted. The digestion reactions and marker DNA were separated on a 1 % agarose electrophoresis gel. The gel was examined, cut to size[11] and photographed alongside a ruler. The gel was washed twice for 8 min (under gentle agitation) with acid nicking buffer, once for 15 min with denaturation buffer and once for 1 h with neutralizing buffer. A nylon membrane (Hybond-N, Amersham) was cut to size[11] and a 4 cm pile of GB 03 blotting paper was cut to fit. A 1 cm pile of blotting paper and the membrane was wet in 6x SSC buffer. A long strip of blotting paper was folded over the gel-casting tray and wet with 6x SSC buffer in a basin. The gel was placed on top and wet. The membrane was placed upon the gel, with the cut corners together; the wet blotting paper was placed on the membrane and the rest of the blotting paper on that. 4 cm of folded cellulose was placed on the blotting paper; a glass plate and a 1 kg weight topped off the tower. The tower was then supported and allowed to stand overnight.
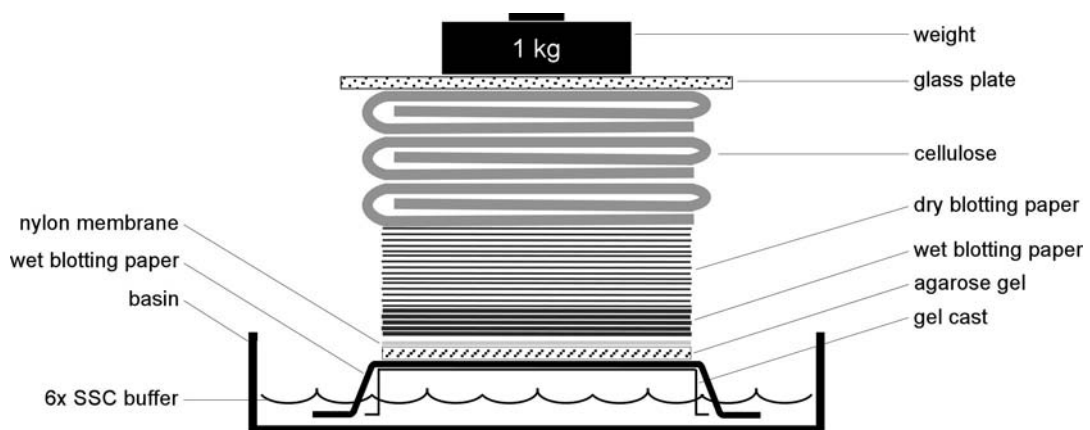
Figure 3-1 Southern blot setup

The next morning, the tower was dismantled. The DNA on the nylon membrane was fixated with 5 min of UV-irradiation. The membrane was placed in a pre-heated (60 °C) hybridization tube and pre-hybridized with hybridization buffer for 5 h at 60 °C in a hybridization oven. Afterwards, the hybridization buffer was removed and the probe was added and incubated overnight at 60 °C. The gene-probe was previously labeled with fluorescein using the *Gene Images™ random prime labeling module* (Amersham).

---

[11] For orientation the upper right corner was cut off.

The probe was removed the next morning and stored by -20 °C. The membrane was then washed for 15 min with 200 ml of 60 °C 1x SSC buffer containing 0.1 % SDS and then with 0.5x SSC buffer containing 0.1 % SDS. Afterwards, for 5 min at RT with sterile diluent buffer and then incubated for 1 h in 60 ml 10 % liquid block/diluent buffer. The membrane was then washed for 5 min with diluent buffer and then incubated for 1 h in 30 ml anti-fluorescein conjugate diluted (1 to 5,000) in diluent buffer containing 0.5 % BSA. Finally, the membrane was washed 3x for 10 min with diluent buffer containing 0.3 % Tween 20. The membrane was then dabbed onto cellulose and 2-3 ml detection reagent was distributed over the membrane and incubated for 4 min. The membrane was sealed in cellophane and developed with an ECL™ detection kit. Using photograph of the agarose gel and the size of the membrane on the film the size of the bands were determined.

Acid Nicking Buffer
250 mM Hydrochloric acid

Denaturation Buffer
1.5 M Sodium chloride
500 mM Sodium hydroxide

Neutralizing Buffer, pH 7.0
3 M Sodium chloride
500 mM Tris/HCl

20x SSC Buffer, pH 7.0
3 M Sodium chloride
300 mM Sodium citrate

Hybridization Buffer
5x SSC buffer
0.1 % (w/v) SDS
5 % (w/v) Dextran sulfate
5 % (v/v) Liquid Block

Diluent Buffer, pH 9.5
300 mM Sodium chloride
100 mM Tris/HCl
sterilized

3.4   Cell biological methods

3.4.1   Yeast specific procedures

3.4.1.1 Yeast conjugation

Yeast strains of opposite mating types, **a** and alpha (**α**), were mated on MV selection plates containing only the necessary supplements and glucose. The yeast strains to be crossed were streaked out freshly and grown overnight at 30 °C. A small amount of one strain was streaked in a downward motion; the second strain was streaked perpendicular to the other strain, forming a cross. On the correct selection medium, yeast colonies should only form on the downstream arm of the cross.

If no specific selection medium can be chosen, the different mating type strains can be transformed with each a plasmid of a different selection marker. Only strains containing both plasmids are diploid. Another possibility is to smear the two haploid strains together on an YPD plate. After 2-3 h, a sample of the cell mixture is examined under a microscope. The presence of so-called "schmoos", were two cells melt together looking like a three-legged star, indicates that diploids have been formed. These schmoos can be picked out with a micromanipulator.

3.4.1.2 Sporulation and tetrad dissection

The diploid strain was inoculated in 2 ml YPD and grown overnight at 30 °C. 1.5 ml cell culture was pelleted at 500 xg for 1 min and washed twice with ddH$_2$O. The pellet was then resuspended in 2 ml 1 % potassium acetate and shaken for 3-4 d at RT. The formation of tetrads was checked under the microscope. 300 µl Sporulated cells were washed 3x with 1 ml ddH$_2$O and resuspended in 200 µl ddH$_2$O. 3 µl Glusulase (DuPont de Nemours) was added and the asci-sack digested for 3 min at hand temperature. The reaction was stopped by adding 800 µl ddH$_2$O. The mixture was stored at 4 °C overnight. The mixture was diluted to one third and 16 µl was pipetted onto one point along the edge of an evenly poured YPD plate. The plate was then tipped so that the cell mixture ran down the center, dividing the plate in two. The plate was then dried for 30 min. The tetrads were found and transferred to a free position on the YPD plate using a micromanipulator (Lawrence Instruments). Using the dissection needle and gentle tapping the tetrad was dissected. The plate was incubated at 30 °C and completely dissected tetrads were examined for their mating type and auxotrophic markers.

3.4.1.3 Mating type test

Similar to mating two haploid strains, the yeast strains being examined and two control strains YR312 (Mat **a** *his1-123*) and YR320 (Mat **α** *his1-123*) were streaked out freshly and grown overnight at 30 °C. On a MV + Glc plate, the two control strains were streaked in a downward motion in two lines parallel to each other[12]. The strains to be tested were then streaked, one after the other, perpendicular across one control strain, and with a new toothpick across the second strain. The perpendicular streak should be performed in one fluid motion. Mat **a** strains should only grow after crossing with the Mat **α** control strain and Mat **α** only with the Mat **a** control strain. Diploid strains cannot conjugate with either of the control strains. The two control strains are defective in the *his1* gene; therefore they cannot grow on plates lacking histidine unless conjugated with a strain containing *HIS1*.

3.4.1.4 Mating type switch

Using a plasmid containing the homothallismus (HO) gene a haploid strain can be switched over to the opposite mating type. The desired yeast strain is transformed with the plasmid pGAL::HO and selected on CM(-Ura) plates. The strain containing the pGAL::HO plasmid is then inoculated in 2 ml YPGal overnight at 30 °C. The overnight culture was diluted (1 to 100), (1 to 1,000) and (1 to 10,000) in ddH$_2$O and 50 µl of each was plated onto an YPD plate. The plates were incubated 2-3 d at 30 °C, until single colonies were obtained. These plates were then replica-plated onto CM(-Ura) plates and grown overnight at 30 °C; it is important to keep the original YPD plates. Both replica and original were compared and those colonies which did not grown on CM(-Ura) were freshly streaked and further examined with the mating type test for a switch in the mating type.

3.4.2 Microscopy

3.4.2.1 "Vesicle Test"

Yeast cells were incubated by 30 °C in YPD or selection medium to a late logarithmic early stationary phase. 10 ml cell culture was pelleted at 500 xg for 3 min. The pellet was divided in half and each pellet was washed twice with sterile ddH$_2$O. One pellet was resuspended in 2 ml SD(-N)[13] medium and the other in 2 ml SD(-N) containing 1 mM PMSF. A PMSF stock solution was freshly prepared; PMSF was dissolved in ethanol at a concentration of 100 mM and then added to the medium. The culture was

---

[12] The tester strains need to be at least 3 cm apart from one another or on separate plates.

[13] Instead of SD(-N) medium, starvation induction was also carried out in 1 % potassium acetate.

incubated while shaken at 30 °C for 2-4 h and then visualized using Nomarski optics with a Zeiss Axioskop 2 microscope.

3.4.2.2 Sporulation test

The selected diploid strain was grown overnight in YPD medium at 30 °C. The cells were then pelleted, washed twice with ddH$_2$O and resuspended in sporulation medium. After 3-4 d at RT the first tetrad-spores should appear. These are visualized under a light microscope.

3.4.2.3 Fluorescence microscopy

For direct fluorescence microscopy the desired protein was visualized using a fluorescent protein tag. The most common fluorescent tagging protein is the green fluorescent protein or GFP from the jellyfish *Aequorea victoria* (87). Meanwhile, there are many variants of GFP[14] such as the cyan fluorescent protein (CFP) and the yellow fluorescent protein (YFP).

The yeast strain with the desired protein(s) and fluorescent tag(s) (either chromosomally integrated or carried on a plasmid) were grown overnight to the preferred growth phase in SD+CA medium at 30 °C, while rapidly shaken. It is important that the culture is circulated with enough oxygen; the GFP chromophore needs to be in an oxidized state to properly fluoresce. 2-3 µl culture was dropped onto a slide and covered with a cover glass. The GFP-protein was observed under a Zeiss Axioskop 2 microscope installed with the needed fluorescent filter

Table 3-4 Excitation and emission wavelengths of GFP and GFP variants

Fluorescent Protein	Color	Excitation wavelength (nm)	Emission wavelength (nm)
CFP	Cyan	433	475
GFP	Green	488	509
YFP	Yellow	488 (or 513)	527

3.4.2.4 Suspended cell fluorescent microscopy

For very weak fluorescent signals it was useful to visualize fluorescent proteins according to (88)

0.8 % Agarose in ddH$_2$O was boiled and poured between two glass plates of a SDS apparatus. After cooling, the agarose was cut into 5 x 5 mm pieces and incubated for 30

---

[14] GFP and its variants are available through BD Bioscience Living Colors® Fluorescent Proteins.

min at 30 °C in the medium used for cell cultivation. 2-3 µl cells containing fluorescent proteins were dropped onto a 60 x 40 mm cover glass. A piece of agarose was taken out of the medium and the excess medium was removed carefully with cellulose. The agarose piece was placed over the cells on the cover glass. The cover glass was then fixed with double-sided tape onto a special spacer (Figure 3-2) and the spacer was fixed onto a glass slide. The slide was the placed in a humid chamber for 30 min at 30 °C. The cells were placed under a fluorescence microscope (Figure 3-3) and observed.
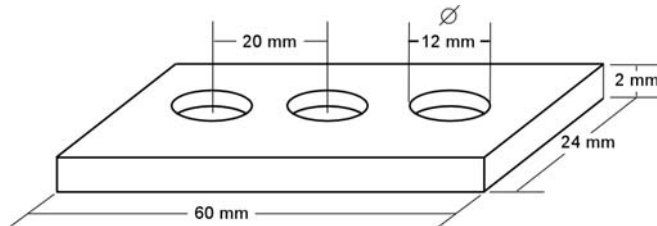
Figure 3-2 Spacer specifications
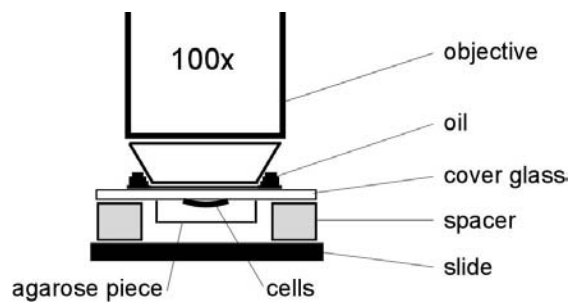
Figure 3-3 Complete setup for suspended cell microscopy

3.4.2.5 Quinacrine staining

An important requirement for many vacuolar proteases is an acidic environment. Quinacrine staining (89) was used to check if the pH in the vacuole is acidic.

The cells were pelleted and washed in 10 mM HEPES, pH 7.4 containing 2% glucose, and incubated in this buffer for 3-5 min with 200 mM quinacrine (89). Afterwards the cells were washed with buffer and 2-3 µl were dropped onto a glass slide. The cells were then viewed using a fluorescence microscope and a GFP filter.

3.4.2.6 FM4-64 vacuolar membrane staining

For use as a reference point the vacuolar membrane was sometimes stained with FM4-64. FM4-64 reaches the vacuolar membrane through endocytosis.

The yeast cells were grown to 0.5-0.8 OD_{600} units. 1.5 ml Cells were harvested through centrifugation at 500 xg for 1 min. The pellet was resuspended in 1 ml YPD containing

2 µl of a 16 mM FM4-64 Solution (1 mg/100 µl DMSO), and the suspension was incubated while shaken for 30min at 30°C. The cells were again pelleted and then either starved in SD(-N) or resuspended in 1 ml YPD. The fluorescence was observed with a fluorescence microscope using a CY3 red filter.

3.4.2.7 Hoechst 33342 staining (live cell nucleus staining)

10 µl 2 mM Hoechst 33324 was added to 1 ml cells in medium. After incubating for 15 min at 30 °C while shaken, the cells were observed under a fluorescence microscope using a DAPI filter.

3.4.2.8 Indirect immunofluorescence

1 ml cell culture (log, stationary or starved) was transferred into a microfuge tube. To fix the cells* 125 µl 37 % formaldehyde and 125 µl 1 M potassium phosphate, pH 6.5 were added and the suspension was rolled for at least 2 hours at RT. The cells were then pelleted at 2,000 rpm for 5 min and then washed 3x with 1 ml SP buffer. After washing, the cells were resuspended in 1 ml SP buffer containing 20 mM β-ME and 15 µl of a 3 mg/ml zymolyase T100 solution[15]. The cells were spheroplasted for 30 min at 30 °C. The spheroplasts were then pelleted at 2,000 rpm for 5 min, washed and resuspended in 1 ml buffer I. At this step the fixed spheroplasts were stored at 4 °C for up to 4 d.

The following day welled slides were prepared. One drop of poly-L-lysine was applied to each well and then each well was washed 3-5x with 20 µl ddH$_2$O and then allowed to dry. When the wells were dry, 30 µl of fixed spheroplasts were applied to the wells with a cut pipette tip. The cells were allowed to settle and adhere for at least 15 min. Afterwards they were rinsed 3x with 20 µl PBS, then covered with 20 µl PBT and incubated for 30 min. The spheroplasts were then covered with 15 µl primary antibody (e.g. mouse a HA) diluted in PBT and incubate for 2 hours in a humid chamber. After washing off unbound antibodies by rinsing 5x with PBT, the cells were then incubated for 1.5 h with 15 µl secondary antibody (e.g. goat α mouse cy[3]) diluted in PBT in a darkened humid chamber. Unbound secondary antibodies were also removed, by rinsing five times with PBS. Finally, the cells were cover cells with one drop of Citifluor containing DAPI and the cover glass was sealed to the slide with nail polish. The cells were viewed immediately with a fluorescence microscope or store at 4°C in a dark humid chamber.

---

[15] This solution was prepared by first dissolving 1.5 mg zymolyase T100 in 500 µl SP buffer and then agitating for 30 min at 37 °C. Note: 20 mM is 1.4 µl/ml β-ME.

*For viewing a green fluorescent protein alongside an indirect immunofluorescence it is important to avoid the use of methanol. Therefore, these cells are fixed with methanol-free 16 % formaldehyde. 1 ml Cell culture is then fixed with 350 µl formaldehyde and 150 µl 1 M potassium phosphate. It is also important to remember that most nail polishes contain methanol that could disturb the GFP fluorescence.

SP Buffer, pH 6.5
1.2 M   Sorbitol
0.1 M KH_2PO_4

PBS
53 mM Na_2HPO_4
13 mM NaH_2PO_4
75 mM   NaCl

PBT
50 ml   PBS
500 mg   BSA
25 µl   NP 40

Citifluor/DAPI Stock Solution
200µl   Citifluor
8µl   DAPI (1µg/ml)

3.4.2.9 Electron microscopy

For visualization with electron microscopy the cells were fixed with permanganate (90) and Epon embedded according to M. Bredschneider, (91) based on Luft (92). The cells to be examined, approx. 2.5 ml, were spun down at 3,000 rpm and washed twice with water. The cell pellet was resuspended in 1 ml 1.5 % potassium permanganate. Before use, the bright purple permanganate solution was filtered through a 0.2 µ sterile filter to remove large undissolved fragments. The resuspended pellet was rolled for 20 min at RT. The pellet was then repeatedly washed with water 3-5x until the supernatant became clear. The cells were then resuspended in 1.3 ml ddH_2O. The fixed samples were stored at 4 °C until shipment.

The Epon embedding and examination was performed by E.-L. Eskelinen (University of Kiel, Kiel, Germany) with a Zeiss EM 900 transmission electron microscope. The photographs were taken at 12,000x magnification.

3.5   Protein biochemical methods

3.5.1 Making protein extracts "Cell Lysis"

There are different methods for extracting proteins from cells: glass bead disruption, homogenization with a glass douncer, alkaline lysis and hypotonic lysis. Each method is selectively used for different experiments.

3.5.1.1 Native cell lysis

Protein structure and complexes are maintained when the cells are opened with the native cell lysis. Yeast cells were pelleted in a microfuge tube at 500 xg and 4 °C for 3 min. The pellet was resuspended in ice-cold 0.1 M potassium phosphate containing Complete® inhibitor mix and PMSF. A pellet-sized amount of glass beads was added and the reaction mixture was vortexed 4x for 1 min; the mixture was cooled for 30 s between vortexing steps. The microfuge tube was then pierced with a needle and placed in a clean microfuge tube. The lysis fluid was won after the two tubes were carefully centrifuged. Cell debris was removed by centrifuging at 13,000 xg for 10 min and the native extract transferred to a clean microfuge tube.

3.5.1.1.1 Glycerol gradient

50 OD unit cells were pelleted at 500 xg for 3 min at 4 °C and washed twice with cold ddH$_2$O. The pellet was then resuspended in 800 µl ice-cold 0.1 M KH$_2$PO$_4$, pH 7.0 containing 1 mM PMSF and Complete® inhibitor mix and transferred to a microfuge tube. A pellet-size amount of glass beads was added and the cells beaten for 30 °min at 4 °C in a multi-vortexer. The mixture was centrifuged for 15 min at 13,000 xg and 4 °C, and the supernatant was applied on top of the glycerol step gradient. The gradient consisted of 450 µl of 20, 30, 40 and 50 % glycerol in 20 mM PIPES, pH 6.8. The gradient was centrifuged for 4 h at 200,000 xg (55,000 rpm) and 4 °C in a Beckman ultracentrifuge TL-100 (TLS-55 rotor). Ten 200 µl fractions were collected and precipitated with TCA. The precipitate was pelleted at 13,000 xg for 10 min. The pellets were washed with acetone, dissolved in 50 µl Laemmli buffer and processed for immunodetection.

3.5.1.2 Homogenization: in the sucrose gradient

800 OD$_{600}$ unit cells were harvested at 1,600 xg and 4 °C. The cells were washed with 30 ml cold 10 mM sodium azide solution and pelleted for 5 min at 500 xg and 4 °C. The pellet was resuspended in 9 ml spheroplast buffer and kept cold on ice. 500 µl Zymolyase solution was added and the cells were gently shaken in a water bath for 30

min at 30 °C. The spheroplasts were pelleted for 10 min at 500 xg and 4 °C and then washed by adding, ml for ml, 10 ml cold SP buffer on ice. Each ml of SP buffer was carefully stirred in using a plastic inoculation rod. The cells were again pelleted for 10 min at 500 xg and 4 °C. The pellet was resuspended in 1 ml cold lysis buffer containing PMSF and Complete® Inhibitor mix and transferred into a cold douncer. The cells were homogenized on ice with 40 strokes of the douncer. The lysate was transferred into a 2 ml microfuge tube and centrifuged for 10 min at 2,500 xg and 4 °C. The supernatant was transferred into a clean microfuge tube and centrifuged for 15 min at 10,000 xg and 4 °C. The pellet was resuspended in 200 µl sucrose gradient buffer and layered on top of the sucrose gradient. The sucrose gradient consists of 1 ml each of a 54, 50, 46, 42, 38, 34, 30, 26, 22, and 18 % (w/v) sucrose in sucrose gradient buffer. The gradient was placed into the SW41Ti rotor (Beckman) and centrifuged for 3 h at 143,000 xg (34,000 rpm) and 4 °C. After the centrifugation 18 samples were taken, each 610 µl from the top of the gradient. 200 µl thereof was precipitated with TCA, washed with acetone and dissolved in 30 µl Laemmli buffer. The rest was stored at -20 °C for further use.

<u>Sodium Azide Solution</u>
10 mM Sodium Azide

<u>Spheroplast Buffer (SP), pH 7.5</u>
1.4 M Sorbitol
50 mM KH_2PO_4
10 mM Sodium azide
40 mM β-ME added fresh (28 µl/10 ml)

<u>Zymolyase Solution</u>
3 mg Zymolyase dissolved in 1 ml SP Buffer shaken for 30 min at 37 °C

<u>Lysis Buffer, pH 7.2</u>
0.8 M Sorbitol
10 mM MOPS
1 mM EDTA

<u>Inhibitors</u> see: *Hypotonic Lysis 3.5.1.4*

<u>Sucrose Gradient Buffer, pH 7.5</u>
10 mM HEPES
5 mM $MgCl_2$

3.5.1.3 Denaturation cell lysis "Alkaline Lysis"

For standard Western blot analysis, yeast strains were prepared by alkaline lysis. The optical density of the culture was measured and the desired amount of cells was pelleted in a microfuge tube, normally about 3 OD_{600} units, at 500 xg for 1 min. The supernatant was removed through aspiration and the pellet cooled on ice. The cells were

resuspended in 1 ml ice-cold ddH$_2$O and 150 µl lysis solution by vortexing and then incubated for 10 min on ice. 150 µl Trichloroacetic acid (TCA) was added, the reaction mixed and then incubated for another 10 min on ice. The protein precipitate was pelleted at 13,000 xg for 10 min and then washed twice with 500 µl acetone. The pellet was dried and then dissolved in 50 µl/OD Laemmli buffer containing 1 % β-mercaptoethanol.

<u>Lysis Solution</u>
For 1 ml: (made fresh)
925 µl 2 M NaOH
75 µl   β-Mercaptoethanol (β-ME)

<u>6x Laemmli Buffer</u>
35 ml 1 M Tris, pH 6.8
36 ml Glycerol
10.3 g SDS
ad 100 ml ddH2O
add Bromophenol blue until solution is a strong blue color

(1 % β-ME is added to the 1x Laemmli buffer before use.)

3.5.1.4 Cell fractionation through hypotonic lysis

A hypotonic lysis is a gentle method to break open cells. Hypotonic solutions have a lower electrolytic concentration than the cells being disrupted. This change in osmotic pressure causes water to enter the cells, causing them to mechanically burst. The first step is the reduction of disulfide bonds in the cell wall with dithiothreit. The second step is the perforation of the cell wall with oxalyticase, a spheroplasting preparation. The last step is the gentle resuspension of the cells in a buffered sorbitol solution. Sorbitol helps maintain the stability of some cell membranes, including the vacuole when properly performed. Magnesium was also added to stabilize peripheral membrane proteins and complexes. The hypotonic lysis was use for the experiments: membrane association, protease protection assay and the OptiPrep™ gradient.

<u>Buffer A</u>
100 mM Tris/H$_2$SO$_4$, pH 9.4
20 mM DTT

<u>Oxalyticase Buffer</u>, pH 7.4
1 M Sorbitol
50 mM NaPO$_4$

<u>PS200 + 5mM MgCl$_2$</u>, pH 6.8
200 mM Sorbitol
20 mM PIPES
5 mM MgCl$_2$

Roche Complete® Inhibitor Mix (25x)
One tablet dissolved in 2 ml ddH$_2$O

Inhibitor Mix (1000x)
1 mg/ml Antipain
1 mg/ml Chymostatin
1 mg/ml Leupeptin
1 mg/ml Pepstatin
dissolved in DMSO

PMSF
100 mM PMSF

3.5.1.4.1 Membrane association

Similar to other experiments the yeast cells were hypotonically lysed according to (55). Forty OD$_{600}$ units of early stationary cells were harvested, washed twice with ddH$_2$O and incubated in 4 ml buffer A containing 20 mM DTT while shaken for 20 min at 30 °C. The cells were pelleted and resuspended in 4 ml oxalyticase buffer containing 50 mg/ml oxalyticase. The mixture was gently shaken for 30 min at 30 °C in at water bath. The spheroplasts were harvested at 2,000 rpm for 5 min and then lysed by resuspending in 2 ml PS200 Buffer including the inhibitors: PMSF, Complete® Inhibitor Mix and 1000x inhibitor mix. The whole cells were removed by pre-clearing 3x for 5 min at 500 xg and 4 °C. The supernatant was isolated and 300 µl was each given to five ultracentrifuge tubes (Beckman) on ice. 300 µl of the following solutions (

Table 3-5) were added and mixed by pipetting once with cut tips. The ultracentrifuge tubes were placed into a TLA-100.3 rotor (Beckman) and centrifuged for 1 h at 100,000 xg and 4 °C. The supernatants were carefully removed, precipitated with 110 % TCA, washed with acetone and dissolved in 50 µl Laemmli buffer. The pellet fractions were directly dissolved in 50 µl Laemmli buffer.

For buffers see: *Hypotonic Lysis 3.5.1.4*.

Table 3-5 Membrane association reactions

Tube No.	Amount of Supernatant	Amount of added Solution	Added Solution	End Concentration
1	300 µl	300 µl	PS200	Control
2	300 µl	300 µl	2 M KAc	1 M Kac
3	300 µl	300 µl	0.2 M Na$_2$CO$_3$	0.1 M Na$_2$CO$_3$
4	300 µl	300 µl	5 M Urea	2.5 M Urea
5	300 µl	300 µl	2 % Triton X-100	1 % Triton X-100

3.5.1.4.2 Protease protection assay

The protease protection experiment was executed according to (55) with the following modifications. Forty OD_{600} units of early stationary or starved cells were harvested, washed twice with water and incubated for 20 min in 4 ml buffer A containing 20 mM dithiothreitol. The cells were then pelleted, resuspended in 4 ml oxalyticase buffer containing 50 µg/ml oxalyticase and spheroplasted for 30 min at 30 °C. The spheroplasts were harvested at 2,000 rpm for 5 min and hypotonically lysed by resuspending in 2 ml PS200. The lysis solution was repeatedly pre-cleared for 5 min at 500 xg and 4 °C, and the supernatant divided into three 300 µl aliquots. The aliquots were each mixed with 300 µl PS200, PS200 with 100 µg/ml proteinase K, and PS200 with 100 µg/ml proteinase K and 0.4 % Triton X-100, respectively. After 15 min on ice, the digestion was halted through trichloroacetic acid precipitation. The pellets were dissolved in 100 µl Laemmli buffer.

For buffers see: Hypotonic Lysis 3.5.1.4.

3.5.1.4.3 OptiPrep™ gradient

One hundred OD_{600} unit cells were pelleted and resuspended in 50 mM DTT dissolved in 10 ml buffer A. The suspension was shaken for 15 min at 30 °C then pelleted again at 500 xg for 5 min. The pellet was taken up in 10 ml oxalyticase buffer containing 50 µg/ml oxalyticase and rocked gently in a water bath for 30 min at 30 °C. The spheroplasts were won by centrifugation at 1,500 xg and 4 °C for 5 min. All steps hereafter were preformed on ice with cut pipette tips. The spheroplasts were hypotonically lysed by carefully resuspending them in 4 ml PS200 buffer containing 5 mM $MgCl_2$, 160 µl Complete® inhibitor mix, 10 µl inhibitor mix and 40 µl PMSF. The lysate was transferred into two 2 ml reaction cups and centrifuged for 5 min at 500 xg and 4 °C. This pre-clearing step was repeated three times to remove unlysed cells; the lysate was transferred to a fresh cup before every centrifugation.

2.4 ml lysate was then divided into two aliquots and centrifuged in a TL100 ultracentrifuge in the TLA 100.3 rotor for 1 h at 4 °C and 100,000 xg (49,000 rpm). 480 µl supernatant was removed and labeled (1S). The remaining supernatant was removed and the pellets combined in 500 µl PS200 buffer (plus all, see above) 100 µl was removed and labeled (1P). 100 µl buffer was added to the remaining pellet fraction. 400 µl pellet was pipetted onto the OptiPrep™ gradient. The OptiPrep™ gradient is a discontinuous gradient consisting of 7 layers: 0.5 ml 50 %, 1 ml 40 %, 1 ml 30 %, 1.5 ml 25 %, 2 ml 20 %, 2 ml 15 %, and 1.5 ml 10 % OptiPrep™ in PS200 + 5 mM $MgCl_2$ buffer. The gradient was centrifuged in a Beckman L-80 ultracentrifuge in the SW41Ti rotor for 16 h at 100,000 xg (36,000 rpm) and 4 °C. The remaining 100 µl pellet was

centrifuged again for 1 h at 100,000 xg and 4 °C in the TLA 100.3 rotor. The supernatant was removed and labeled (2S). The pellet was resuspended in 50 µl Laemmli buffer and labeled 2P. The proteins in 1S, 1P and 2S were precipitated with 110% TCA and the precipitate was dissolved in 50 µl Laemmli buffer and 1 % β-mercaptoethanol.

After the centrifugation, twelve 800 µl fractions were removed from the top of the gradient. The proteins in the twelve fractions were precipitated with TCA and dissolved in 50 µl Laemmli buffer and 1 % β-mercaptoethanol.

3.5.2 Sodium dodecyl sulfate – polyacrylamide gel electrophoresis "SDS-PAGE"

Sodium dodecyl sulfate (SDS) containing gels separate proteins according to their molecular weight. SDS binds to the nonpolar regions of proteins and has a large negative charge, which masks the native charge of the protein. β-Mercaptoethanol is usually added to lysis buffers to reduce disulfide bonds and disassociate protein subunits.

The SDS-PAGE was conducted according to Laemmli (93) in a mini-protean 3 electrophoresis chamber (Bio-Rad). The following recipes were used for mixing the gels.

For 2 Gels	Stacking Gel	Separating Gel				
Percent Acrylamide [%]	4	7	7.5	10	12	15
ProtoGel[1] [ml]	0.65	2.35	2.5	3.35	4	5
0.5 M Tris/HCl, pH 6.8 [ml]	1.25	-	-	-	-	-
1.5 M Tris/HCl, pH 8.8 [ml]	-	2.5	2.5	2.5	2.5	2.5
H_2O [ml]	3.05	5	4.85	4	3.35	2.35
10% (w/v) SDS [µl]	50	100	100	100	100	100
10% (w/v) APS [µl]	50	100	100	100	100	100
TEMED [µl]	5	10	10	10	10	10

[1] ProtoGel: 30% (w/v) acrylamide, 0.8% (w/v) bisacrylamide stock solution

After the gels were cast and put into place, the chamber was filled with SDS electrophoresis buffer and the samples (5-20 µl) were inserted into the wells. A protein

standard (Precision Plus Protein™ Standard, Bio-Rad) was also added to one of the wells. The gel was run at 150 V until the dye front (bromophenol blue) exited the gel or the desired standard band reached the glass edge.

10x Electrophoresis Buffer
  30.29 g/l = 0.25 M Tris
150.14 g/l = 2 M Glycine
     10 g/l = 10 % SDS

3.5.3 Western blot analysis

After being separated through electrophoresis the proteins were then transferred through Western blotting onto either a polyvinylidene difluoride (PVDF)- or a nitrocellulose-membrane using a semi-dry blotting apparatus.

Six blotting filters (GB002, 9.5 x 7.0 cm) were wetted with 1x blotting buffer. Three were placed upon the carbon electrode of the blotting apparatus; the protein gel was carefully released from the glass plates and slid onto the blotting filter. A PVDF membrane (9.0 x 6.5 cm) was wetted successively with methanol and blotting buffer and then placed upon the protein gel. The remaining three filters were then placed onto the membrane and the stack was carefully compressed by rolling a glass pipette over the surface to remove air pockets between the layers. A constant current was applied for 1.5 h so that the negatively charged proteins are transported to the membrane, one blot 70 mA, and two blots 150 mA.

5x Blotting Buffer
6.5 g/l = 54 mM Tris
7.2 g/l = 96 mM Glycine

1x Blotting Buffer
1/5 5x Blotting Buffer
1/5 MeOH
3/5 H_2O

3.5.4 Immunodetection of proteins

After blotting, the membranes were then coated in 10 % (w/v) skim milk powder in TBS-T (or PBS-T) for at least one hour, but usually overnight. Excess milk was removed by washing the membrane 3x 5 min with the above used buffer. After washing, the membrane was incubated at least one hour with the desired antibody against the protein to be examined. The primary antibody was generally generated in a rabbit or mouse host and diluted in the washing buffer at a tested concentration. Antibodies not bound to proteins on the membrane were removed by washing the membrane with buffer 3x 10 min. A secondary antibody against the former host was diluted in buffer (goat anti-rabbit 1:5,000 and goat anti-mouse 1:10,000) and incubated for not more than

one hour. After incubation the excess second antibody was also removed by washing with buffer 5x 5 min. The membrane is then ready to be developed.

The second antibody used in Western blotting was conjugated to the horseradish peroxidase (HRPO). Using ECL™ Western blotting detection reagents from Amersham, the HRPO oxidizes a peracid releasing a chemiluminescence signal that can be detected. The reagents in the ECL™ Kit are mixed 1:1 with approximately 1 ml mixture per membrane. The mixture is applied to the membrane and incubated for 1 min, making sure that the membrane is completely covered with the reagents. Excess reagents are then removed and the membrane was placed between two plastic sheets. Excess reagents are again removed by squeegeeing the plastic. The luminescence was then either detected using Hyperfilm ECL™ (Amersham) in a darkroom or using an ECL camera (Fuji LAS-3000). A developing time is selected empirically according to the needed strength of signal. The signal obtained corresponds to the location of the protein specific to the primary antibody (ideally there are very few cross-reactions).

10x Tris Buffered Saline + 1% Tween 20 (TBS-T)
pH 7.6
24.2 g/l = 0.2 M Tris/HCl
80.8 g/l = 1.4 M NaCl
10   g/l = 1 % Tween 20

10x Phosphate Buffered Saline +1% Tween 20 (PBS-T)
pH 7.5
22.7 g/l = 0.16 M Na_2HPO_4
5.52 g/l = 0.04 M $NaH_2PO_4 \cdot H_2O$
58.4 g/l = 1   M NaCl
10   g/l = 1% Tween 20

3.5.4.1 Carboxypeptidase Y (CPY) secretion screen

The strains to be tested were streaked in small patches onto an YPD plate and grown overnight at 30 °C. The following day, a round nitrocellulose membrane was placed on the face of a new YPD plate, avoiding bubbles under the membrane. The patched plate was replica-plated onto the nitrocellulose membrane and incubated for 2 d at 30 °C. The membrane was then removed from the plate and the yeast cells were carefully washed with distilled water from the membrane surface. The membrane was then washed with PBS-T and coated with 10 % milk powder in PBS-T for 1 h. The membrane was washed 3x with PBS-T and then incubated for 1 h with mouse α CPY (1 to 1,000) in PBS-T. The membrane was washed again 3x with PBS-T and the second antibody, goat α mouse HRPO-conjugate (1 to 10,000) in PBS-T, was then applied for 1 h. The membrane was finally washed 5x with PBS-T and then developed with the ECL™ detection kit.

3.5.5   Alkaline phosphatase assay (ALP Assay)

In the strains to be tested the *PHO8* gene was chromosomally deleted using the deletion plasmid pGF10 (75). Before transforming into the desired strains, the plasmid was digested with the enzymes Stu1 and BamH1 resulting in a deletion fragment containing *pho8Δ::LEU2*. The resulting *pho8Δ* strains were then transformed with the Pho8Δ60 expression plasmid pCC5 (76). This truncated Pho8 is missing its vacuolar signal peptide and therefore remains in the cytosol after synthesis. Pho8Δ60 travels to the vacuole only through autophagy where it assumes its enzymatic activity. This activity can be measured and correlates to the autophagic activity.

The assay method was performed according to Noda *et al.* (94) with following modifications. Logarithmically grown cells were washed with water and then resuspended in SD(-N) medium. One OD_{600} cells were harvested at each indicated time point and washed once with water. The cells were then suspended in 200 µl of assay buffer (250 mM Tris-HCl, pH 9.0, 10 mM $MgSO_4$, 10 µM $ZnSO_4$) and disrupted by vortexing with glass beads. After centrifugation, 50 µl of the supernatant was added to 500 µl of assay buffer and 50 µl of 55 mM α-naphtylphosphate. After incubating for 15 min at 30 °C, 500 µl of 2 M glycine-NaOH (pH 11.0) was added to stop the reaction. Fluorescence intensity was measured after excitation at 345 nm and emission at 472 nm. Protein concentration was determined via the BCA method (Pierce).

4   Results

The completion of the genomic sequencing of the yeast *Saccharomyces cerevisiae* and the generation of a collection of deletion mutants opened new means of enciphering the meaning and function of genes. This allows a better discovery and study of processes and pathways within this organism. These results can then be correlated to higher organisms.

During this study a collection of viable deletion strains, in which each mutant consists of an individual gene replaced by the kanamycin resistance gene, was obtained and the individual mutants were examined in the following reverse genetic screen.
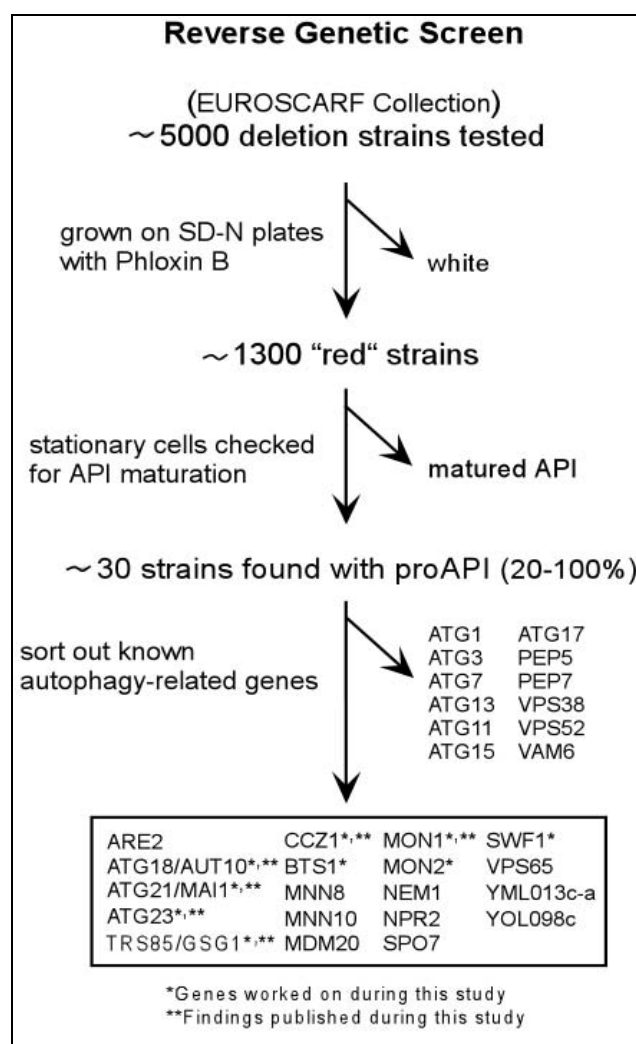
Figure 4-1 Scheme of the reverse genetic screen

4.1   A reverse genetic screen identified novel autophagy related genes

In the beginning it was assumed that yeast cells need the autophagic process to survive stress situations. Autophagy mutants are known to have a reduced viability when grown in minimal media. In a worldwide effort, 'The Yeast Deletion Project', a collection of deletion mutants was created.

This enabled the screening of all viable single open reading frame (ORF) deletion mutants within the yeast *Saccharomyces cerevisiae* (~5000 from ~6000 genes). This collection was obtained from Euroscarf, Frankfurt. These deletion mutants were grown on agar plates lacking nitrogen sources (SD(-N) plates) for several days. As a result, yeast strains that were unable to survive on plates lacking nitrogen sources died earlier than the wild type strain. In order to ease the selection of strains that had problems, the dye phloxin B was added to the plates before pouring.

Phloxin B can only penetrate dead cells, thus a correlation between survival ability and an uptake of phloxin B was made. Mutant strains stained darker than the wild type strain were scored as possible autophagy mutants. After screening approximately 5000 ORF deletions about 1300 deletion strains were classified as "red".

As I began my studies in autophagy H. Barth and M. Thumm (49) had just completed this red/white classification. A second selection procedure was then developed to single out which genes truly affected autophagy or the related Cvt pathway. Autophagy offers the cell protection; in addition, autophagy and the Cvt pathway are also selective transporters of the cargo protein aminopeptidase I (Ape1). Aminopeptidase I is transported from the endoplasmic reticulum to the vacuole by way of the Cvt pathway during vegetative conditions and through autophagy during starvation. Within Cvt vesicles or autophagosomes Ape1 is transported in a dodecameric pro-form to the vacuole where the vacuolar enzyme is matured to its active form. Every missing protein that is involved in this transport causes Ape1 to remain in its immature pro-form. This difference can be distinguished through Western blot analysis. When separated in an acrylamide gel containing SDS, proaminopeptidase I runs at a molecular weight of 61 kDa; the mature form runs at 50 kDa. It was then the responsibility of H. Barth and myself to check the maturation of Ape1 of the remaining 1300 "red" strains.

The selected strains were inoculated in 750 µl YPD contained within a 24-well micro titer plate and grown while shaken overnight at 30 °C. The cultures were processed for immunoblotting by way of alkaline lysis and dissolved in 150 µl Laemmli buffer. The samples were loaded onto a 7.5 % SDS-PAGE gel, run at 150 V and semi-dry blotted onto a PVDF membrane. The membrane was coated in milk powder dissolved in PBS-T

buffer. After washing, the membrane was incubated with a rabbit anti-Ape1 antibody (1: 5,000 in PBS-T) and then with a second antibody horseradish peroxidase conjugated goat anti-rabbit (1: 5,000 in PBS-T). The membrane blot was developed with the ECL® detection kit and the strains with proaminopeptidase I bands were identified. Those genes known to be a part of autophagy or related pathways were removed, leaving 19 strains for further examination. This study concentrates on six genes unknown to autophagy and the Cvt pathway: *ATG18/AUT10*, *ATG21/MAI1*, *ATG23*, *TRS85/GSG1*, *CCZ1* and *MON1*.

4.2   *ATG18* and *ATG21* two homolog genes with different functions

The two open reading frames *YFR021w* and *YPL100w* were identified[16] in the two-stepped screen described above. Both Genes were unable to process aminopeptidase I to its mature form and had noticeable amounts of proaminopeptidase I when examined by Western immunoblot analysis. After the initial identification of *YFR021w* and *YPL100w* these ORFs were examined in the *Saccharomyces cerevisiae Genome Database* (SGD). The databank described the ORFs to be novel genes of unknown function. The genomic sequences were downloaded and entered in a BLAST search. Surprisingly, *YFR021w*, *YPL100w* and a third ORF *YGR223c* were all found to be homolog to one another. *YFR021w* and *YGR223c* were found to be 19 % and 14 % identical to *YPL100w*, respectively (82). Interestingly, these homologues belong to three subfamilies in a phylogenetic analysis using the program Clustal (95). Each subfamily contains one yeast homologue and uniquely YPL100w is the only representative of its subfamily, *Figure 4-2*.

---

[16] *ATG18* and *ATG21* were cooperatively studied by H. Barth und K. Meiling-Wesse; C. Voss also performed some experiments.
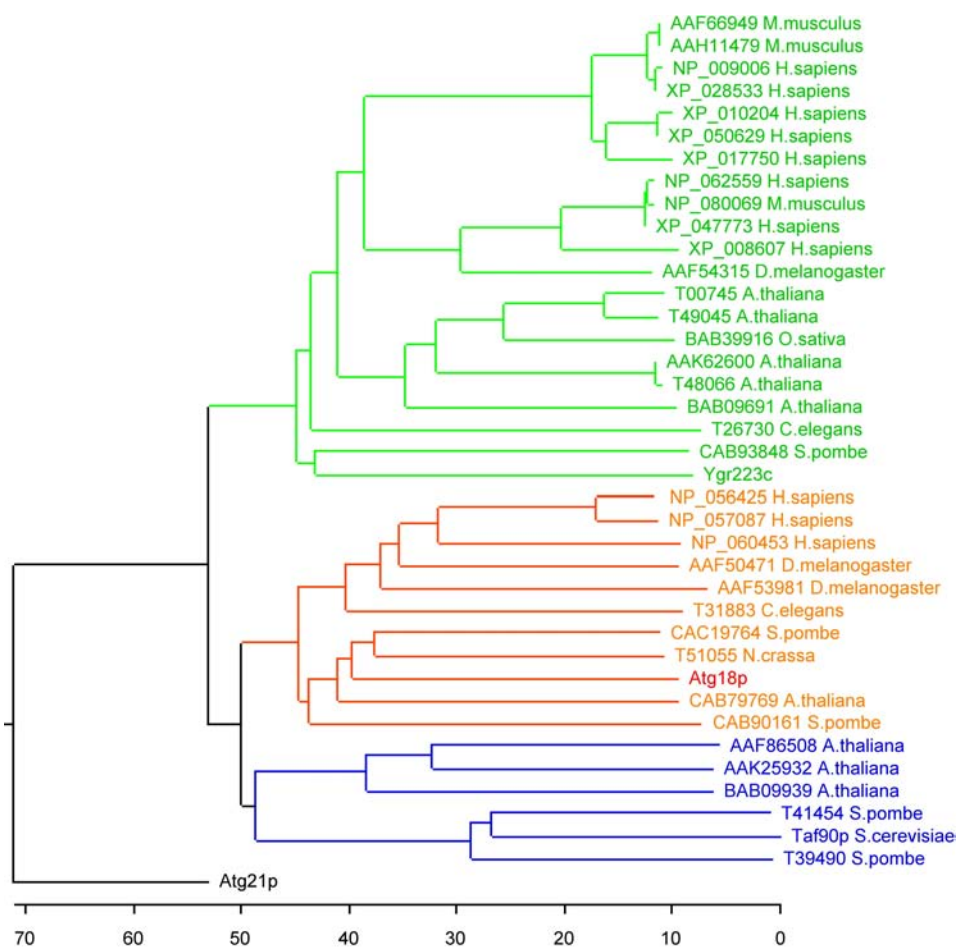
Figure 4-2 Phylogenetic analysis reveals that the homologues belong to three separate subfamilies.

4.2.1 Ape1 maturation is inhibited in *yfr021wΔ*; in *ypl100wΔ* Ape1 is immature only the vegetative state

To reconfirm the involvement of YFR021w and YPL100w in autophagy, Ape1 maturation in *yfr021wΔ* and *ypl100wΔ* strains was re-examined. This time the strains were examined not only under vegetative conditions, but also under nitrogen starvation. *yfr021wΔ* and *ypl100wΔ* cells were grown in YPD and aliquots were extracted during the stationary growth phase (A_{600} ~4-8). Cells in the stationary phase were then starved in potassium acetate for 4 hours and an aliquot was extracted. Additionally, *atg12Δ* and the wild type strain were also examined as controls. Atg12 is known to be involved in the autophagosome and Cvt vesicle formation. Lack of Atg12 prevents Ape1 from being transported to the vacuole, thus Ape1 should be in its immature pro-form. As seen in *Figure 4-3*, *yfr021wΔ* and *ypl100wΔ* both are unable to mature Ape1 under vegetative conditions. During nitrogen starvation, where autophagy is induced, only *ypl100wΔ* can mature Ape1. Considering this, *YFR021w* was called *AUT10*, for being involved in

autophagy and *YPL100w* was termed *MAI1*, for its problem in the <u>Ma</u>turation of <u>Am</u>inopeptidase <u>I</u> during the Cvt pathway. Later on, a unified nomenclature was implemented for all <u>Au</u>to<u>T</u>opha<u>G</u>y related genes (96), thus *AUT10* became *ATG18* and *MAI1* became *ATG21*.
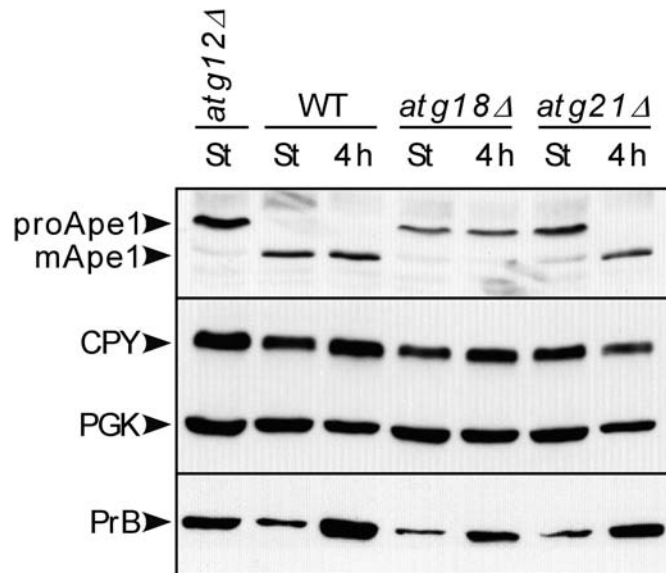
Figure 4-3 *ATG18* **is involved in autophagy whereas** *ATG21* **is only involved in the Cvt pathway. Aliquots of** *atg18Δ* **and** *atg21Δ* **probed with anti-Ape1 antibodies show that** *atg18Δ* **is defective in maturation of Ape1 under both vegetative and starvation conditions. In** *atg21Δ***, Ape1 is matured under starvation conditions; the defect in** *atg21Δ* **involves only the Cvt pathway. In both** *atg18Δ* **and** *atg21Δ* **cells carboxypeptidase Y (CPY) and proteinase B (PrB) are matured. (PGK) is shown as a quantity control for the amount of protein between aliquots.** *atg12Δ* **is a known to have a defect in ape1 maturation and WT is the wild type strain.**

To investigate if the defects in *atg18Δ* and *atg21Δ* are pleiotropic and involve other vacuolar protein transport pathways or are caused by a defect in the processing of Ape1 in the vacuole, the maturation of carboxypeptidase Y and proteinase B were controlled. Carboxypeptidase Y (*CPY*) and proteinase B (*PrB*) are proteases endogenous to the vacuole. Most proteases are sorted from the ER over the Golgi apparatus to vacuole by way of the secretory pathway. The maturation of Ape1 is dependent on the presence of PrB and Proteinase A (*PEP4*) in the vacuole. Thus defects in the secretory pathway would affect the delivery of these proteases and inhibit the maturation of Ape1. *Figure 4-3* shows that CPY and PrB are both present in a matured state. Note that proteinase B is starvation induced and therefore present after 4 h starvation in larger quantities that in the steady state.

4.2.2 Vacuolar acidification is normal in *atg18Δ* and *atg21Δ* cells

The proper formation of vacuolar proteases is dependent on the environment of the vacuole itself. These proteases are unable to degrade proteins and break down autophagic vesicles within the vacuole when the pH is not acidic (63). The vacuolar acidification was therefore examined to determine if this is a cause for the defect in the maturation of Ape1. Quinacrine is a fluorescent dye that accumulates in acidic vacuoles (89). Wild type, *vma1Δ*, *atg18Δ* and *atg21Δ* cells were investigated under stationary and starvation conditions after incubation with quinacrine. *VMA1* is a subunit of the vacuolar H(+)-ATPase. Its deletion inactivates the membrane v-ATPase and leads to a non-acidic vacuole. As seen in *Figure 4-4 atg18Δ* and *atg21Δ* both show normal vacuolar uptake of the dye quinacrine indicating that vacuolar acidification is not the cause of the inability to mature aminopeptidase I.
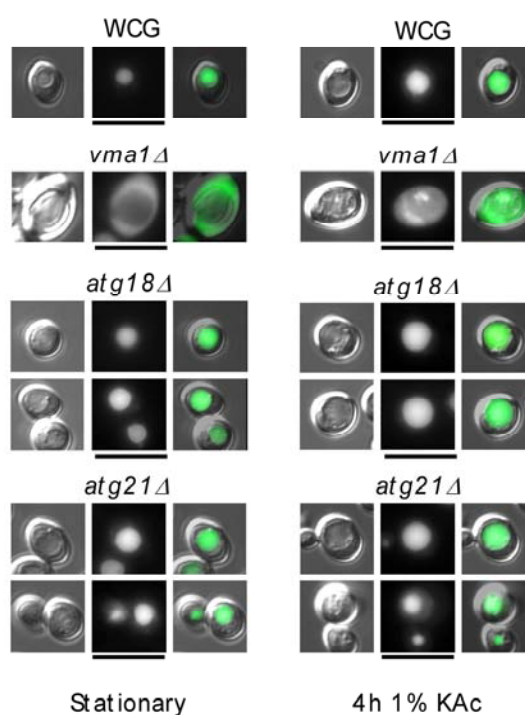
Figure 4-4 The wild type-like accumulation of the dye quinacrine in the vacuoles of *atg18Δ* and *atg21Δ* cells indicates a normal vacuolar acidification. Wild type (WCG) and v-ATPase defective *vma1Δ* cells were added as controls. The left column shows cells harvested in the stationary phase and treated with quinacrine for 5 min, washed with buffer and then viewed using a Zeiss Axioskop 2 with GFP filter. In the right column stationary cells were harvested and incubated for 4 h in 1 % potassium acetate. The starved cells were then treated with quinacrine and viewed like in the left column. The panels (from left to right) show Nomarski, fluorescence imaging and an overlay of the two pseudo colorized. Bar: 10µm.

4.2.3 *atg18Δ* does not sporulate, whereas *atg21Δ* shows reduced a sporulation rate

The yeast Saccharomyces cerevisiae can exist in a haploid and in a diploid form. The formation of four haploid gametes from a single parental diploid is part of the lifecycle of yeast and is known as sporulation (97). Yeast cells begin to sporulate when they are subject to nutrient limitation in the absence of fermentable carbon sources (98). Nutrient limitation regulates autophagy and the inability to sporulate is also an autophagic phenotype. Cells with a defect in autophagy cannot sporulate because the energy necessary to germinate or certain signaling factors are missing. Homozygote diploids (**a/α**) of *atg18Δ* and *atg21Δ* were compared to the wild type and *atg12Δ* a known gene with an autophagic defect. The strains were shifted to 1 % potassium acetate and the number of asci (tetrads) was counted after three and six days. The sporulation rate of the wild type strain was determined to be around 27 % after 3 days and about 33 % after 6 days relative to the total cells counted. Compared to the wild type, *atg12Δ* and *atg18Δ* showed no tetrad formation whatsoever, but *atg21Δ* had a reduced spore formation of 12 % after 3 days and 23 % after 6 days in potassium acetate.

4.2.4 Chromosomal deletion of *ATG18* and *ATG21*

Sometimes a specific genetic background can assist in making an experiment more interpretable. It is therefore necessary to make mutants and deletions in other genetic strains. The chromosomal deletion of *ATG18* (YHB1) in the WCG background was accomplished through homologue recombination of an *ATG18* specific kanamycin resistance gene PCR fragment. This PCR fragment was generated from the oligonucleotides fr021w-1 and fr021w-2, and the plasmid containing the resistance marker pUG6. The chromosomal deletion of *ATG21* (YHB4) was accomplished similarly with the oligonucleotides pl100w-1 and pl100w-2. H. Barth carried out both deletions.

4.2.5 The vesicle test: *atg21Δ* cells are able to form autophagosomes, whereas *atg18Δ* cells are not

To determine at which stage the autophagic process is impaired a simple microscopic test is performed, called the "vesicle test". This test was best performed using the background strain WCG. WCG has a nice enlarged vacuole allowing the formed vesicles to be easily observed using Nomarski optics. Autophagic bodies are easily recognized as spheres "dancing" within the vacuole according to Brownian movement. The tested strains were starved for 2-4 h in starvation media with and without the proteinase B inhibitor phenylmethylsulfonyl fluoride (PMSF). Strains defective in the

formation of autophagosomes have no autophagic bodies within the vacuole in the absence or presence of PMSF. Strains defective in the lysis of autophagic bodies contain vesicles within the vacuole whether or not PMSF is present. Wild type cells are able to degrade autophagic bodies in the absence of PMSF but not in its presence, thus its vacuole is empty and then full respectively. Most defects in the autophagic process occur before the autophagosome is formed or has fused with the vacuole. The only genes known to be involved with autophagy lysis are *ATG22/AUT4* and *ATG15/CVT17/AUT5*. As seen in *Figure 4-5* in the presence of PMSF *atg18Δ* behaves like *atg3Δ*, a known autophagy gene involved in formation of autophagosomes and Cvt vesicles. Whereas when observing *atg21Δ* cells autophagic bodies can be seen like in the wild type.

Figure 4-5 Vesicle test: lack of autophagic bodies within the vacuole indicates a defect in the formation of autophagosomes. In the presence of PMSF the build up of autophagic bodies (vesicles) can be seen in Wild type cells. On the contrary, in Atg3 deficient cells autophagosomes are not formed and therefore do not accumulate in the vacuole. atg21Δ cells (A) are able to form autophagosomes whereas atg18Δ (B) cells are not.

4.2.6 *atg21Δ* behaves normally when starved in medium deficient in carbon sources

Autophagy is not only induced when nitrogen sources are depleted, it is also affected by the amount of carbon nutrients present in solution. The ability to form autophagic bodies in medium depleted of carbon sources was investigated for *ATG21* and *AUT6* deleted cells. Unlike *aut6Δ*, the ability to form autophagic bodies in *atg21Δ* cells was unaffected by lack of carbon sources. The autophagic bodies in *Figure 4-6* were visualized in carbon starvation media containing PMSF in a procedure comparable to the above mentioned vesicle test.
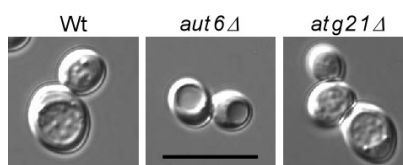
Figure 4-6 *atg21Δ* cells produce autophagic bodies normally when starved in carbon deficient media. A vesicle test performed in carbon starvation media containing PMSF showed that *atg21Δ* cells were able to form autophagosomes equally to the wild type. Cells deleted with the autophagically deficient *AUT6* gene were unable to form autophagic bodies.

4.2.7 Atg18 and Atg21 were tagged with the triple HA fusion tag

Marking a protein with a fluorescent or immunological fusion tag is a great help in localizing and characterizing a protein directly. In the case of *ATG18* and *ATG21*, these proteins were tagged with an epitope of the influenza hemagglutinin protein or HA-tag. Three HA-tags combined with the His5 protein from *Schizosaccharomyces pombe* were chromosomally integrated into the C-terminal end of the two Atg-proteins. This was done similarly to the chromosomal deletion by H. Barth. For Atg18-HA in the WCG background (YHB3) a PCR product created from the plasmid p3xHA-HIS5 and the oligonucleotides YFR-HA-1 and YFR-HA-2 was integrated. Atg21-HA was also constructed in the WCG background (YHB5) using the p3xHA-HIS5 plasmid and the oligonucleotides PL100w-HA-1 and PL100w-HA-2. Both transformants were selected on CM-His plates and correct integration was confirmed through Southern blot analysis. The expression of the tagged protein was controlled with Western blot analysis as seen in *Figure 4-7*. Atg18-HA has a molecular size of about 60 kDa when separated on a SDS-PAGE gel; Atg21-HA has approximately the same size. Both are visible when probed against anti-HA antibodies as seen in *Figure 4-7* (A) lanes 2 and 3 for Atg18-HA and (B) lanes 1 and 2 for Atg21-HA. Both proteins are functional; Ape1 is matured in both cases. PGK is shown as a loading control.
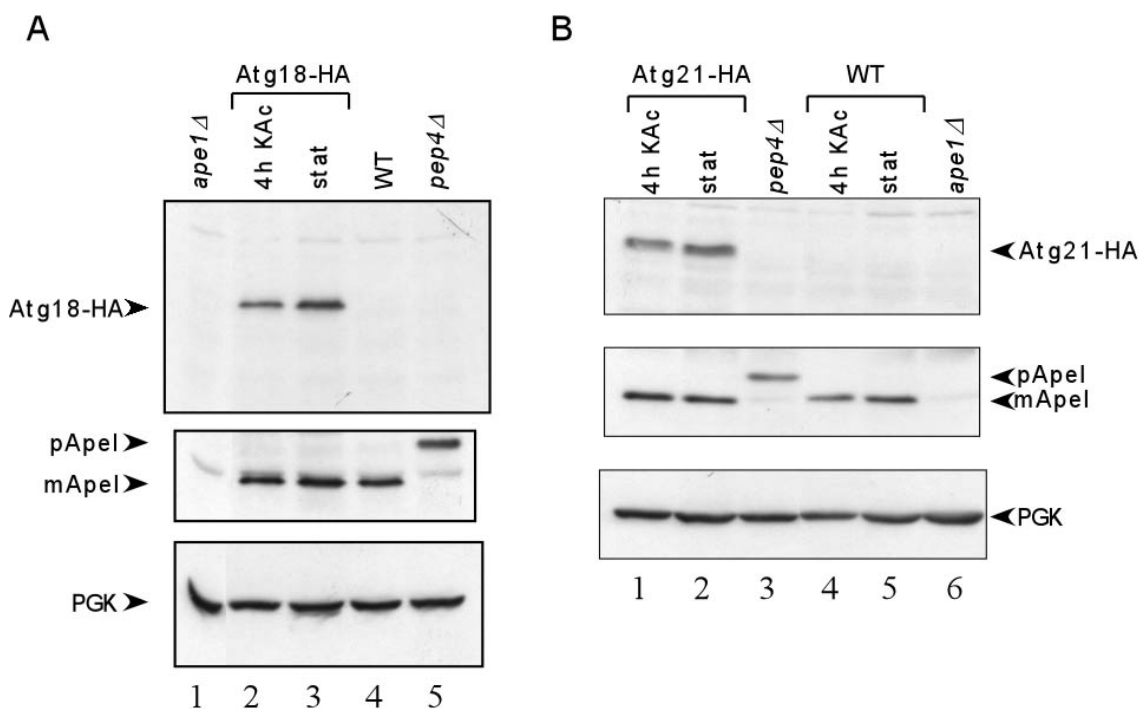
Figure 4-7 Expression of Atg18-HA and Atg21-HA from the chromosome. Atg18-HA (A, lanes 2,3) and Atg21-HA (B, lanes 1,2) are detectable in a Western blot analysis. Ape1 is matured in these samples and shows that Atg18-HA and Atg21-HA are functional. The wild type (WT), *ape1Δ*, and *pep4Δ* are shown as Ape1 maturation controls. PGK demonstrates that equal amounts of protein were loaded.

4.2.8 Indirect immunofluorescence of Atg18-HA localizes to points in the cytosol and along the vacuolar membrane; Atg21-HA localizes mainly to the vacuolar membrane near the nucleus.

Even without a direct fluorescing tag, proteins can be localized using indirect immunofluorescence. The cells to be visualized are grown, and starved if necessary. Subsequently, the cell wall of the cells is spheroplasted and then fixated with formaldehyde. The fixed cells then are attached to a slide that has been prepared with poly-L-lysine. After washing with buffer and incubating with a rabbit anti-HA antibody, the cells are washed and incubated further with a second antibody, an anti-rabbit antibody conjugated to the fluorescent marker CY3. CY3 excites a red signal under a fluorescent microscope. The excess second antibody is then washed away and the cells are treated with Citifluor containing DAPI. A cover slip is placed on top and fixed and sealed with nail polish.
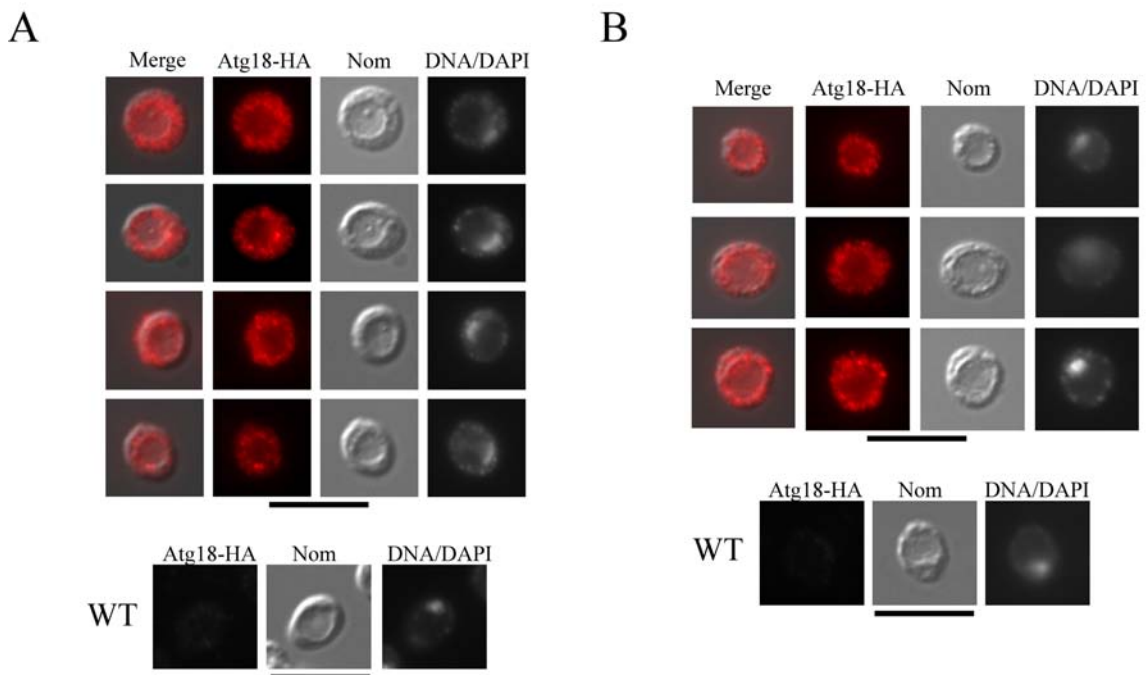
Figure 4-8 Atg18-HA was expressed from the chromosome under the control of its native promoter. Atg18-HA was localized to punctated structures around the vacuolar membrane and in the cytosol. Fixed Atg18-HA cells (A: stationary cells; B: cells starved for 4 h in 1 % potassium acetate) were probed with anti-HA antibodies and visualized by indirect immunofluorescence microscopy. Wild type cells lacking a HA-Tag were included. From left to right: an overlay of Nomarski and immunofluorescence (Merge), immunofluorescence (Atg18-HA), Nomarski (Nom) and nuclear staining with DAPI (DNA/DAPI). Bar 10μm. Done by H. Barth (50).

In *Figure 4-8* Atg18-HA was localize to the cytosol and points on the vacuolar membrane. There seems to be no dependence on the nutrient state as there is no difference in the pattern of Atg18-HA in panel A or B. The localization of Atg21-HA in *Figure 4-9* is somewhat more defined. Atg21-HA seems to be clustered mostly along the vacuolar membrane. In starved cells Atg21-HA is often seen next to or sometimes embracing the nucleus.
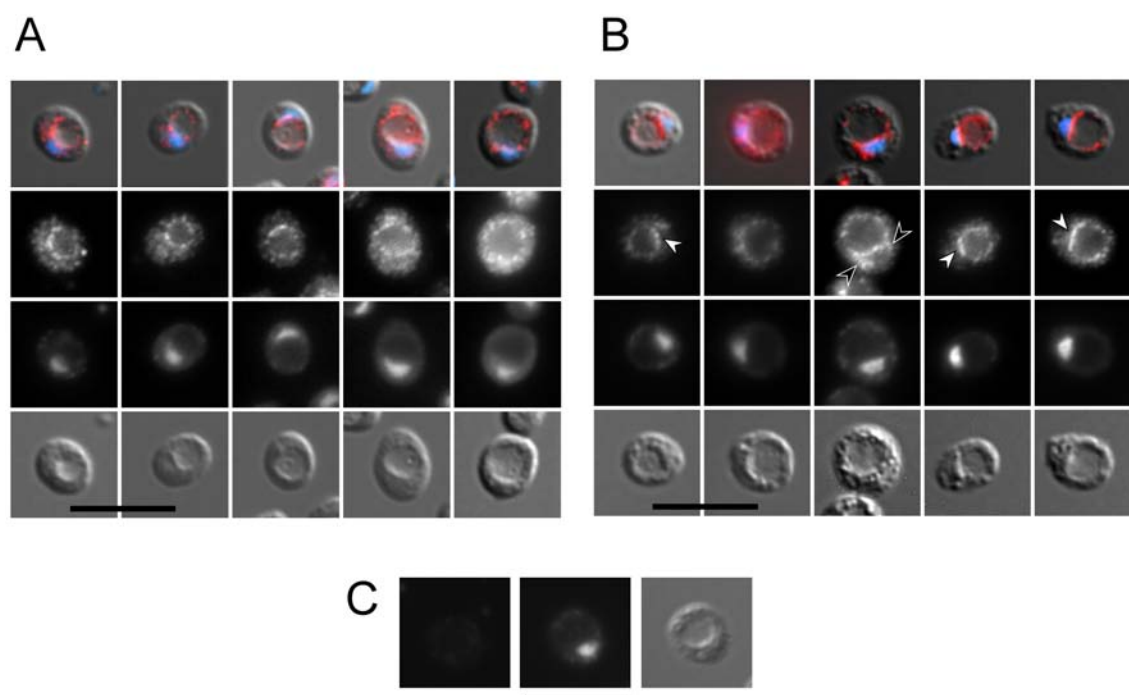
Figure 4-9 Atg21-HA chromosomally expressed from its endogenous promoter was visualized with antibodies against HA using indirect immunofluorescence. White arrowheads show regions where Atg21-HA appears concentrated near the nucleus. Black arrowheads point to offshoots that seem to protrude toward the nucleus. In general, Atg21-HA is located in areas near the vacuolar membrane. Panel A shows fixed stationary cells. Panel B displays cells that were starved for 4 h in 1 % potassium acetate and then fixed. Frames from top to bottom: a colorized overlay of Atg21-HA immunofluorescence (red), nucleus staining with DAPI (blue) and Nomarski; Atg21-HA immunofluorescence; nucleus staining with DAPI; and Nomarski. Panel C is a wild type cell without HA-tagging. Bar 10 μm. Done by H. Barth (82).

4.2.9 Atg21-HA is a peripheral membrane protein

After observing that Atg21-HA is located on or near the vacuolar membrane, a membrane association experiment was carried out by H. Barth. Aliquots of spheroplasted Atg21-HA cells were mixed with different solutions that solubilize proteins differently and centrifuged in a Beckman TL-100 ultracentrifuge at 100,000 xg. Potassium acetate, an ionic salt, releases peripheral proteins that are ionically bound to

membranes by weakening ionic interactions. Sodium carbonate, pH 11.5, also releases peripheral membrane proteins that are affected by extreme pH values. Chaotropic agents, such as urea, destabilize hydrophobic interactions and breaks hydrogen bonds promoting the solubility of hydrophobic residues in solution (99). Triton X-100 is a detergent that disrupts all membranes releasing peripheral and integral membrane proteins. Atg21-HA is loosely bound to membranes (*Figure 4-10*). In buffer it is only partially pelletable. Like the known peripheral membrane protein from the 60 kDa subunit of v-ATPase complex (Vma2), the membrane bound fraction of Atg21-HA was solubilized by potassium acetate, sodium carbonate, urea and triton X-100. The 100 kDa subunit of v-ATPase complex (Vph1) was a control for integral membrane proteins and 3-phosphogycerate kinase (PGK) is a soluble cytosolic protein.
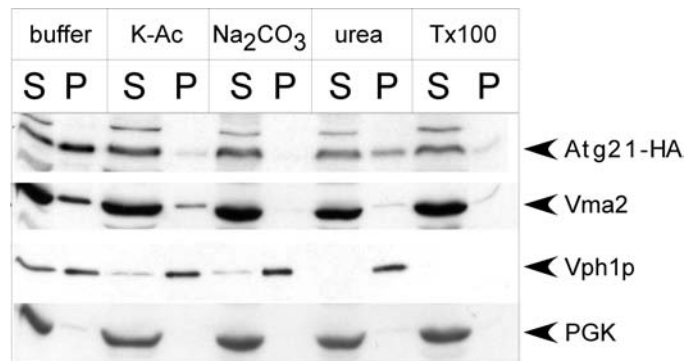
Figure 4-10 Atg21-HA is a peripheral membrane protein. Aliquots of spheroplasted Atg21-HA cells were mixed with equal amounts of buffer, potassium acetate (K-Ac), sodium carbonate (Na₂Co₃), urea and triton X-100 (Tx100) and centrifuged at 100,000 xg. After centrifuging, the samples were divided into supernatant (S) and pellet (P) fractions and processed for immunoblotting. Controls were Vma2 a peripheral membrane protein, Vph1p an integral membrane protein and PGK a soluble cytosolic protein.

4.2.10 Atg21 deleted cells form the dodecameric Cvt complex normally

The glycerol gradient separates protein conglomerates. This experiment was used as a tool to determinate if proApe1 correctly consolidates to a dodecameric form. Wild type and *atg21Δ* cells were lysed and placed on top of a 20-50 % glycerol step gradient. The gradient was centrifuged at 20,000 xg for 4 h at 15 °C. Afterwards the gradient was divided into ten fractions from top to bottom, precipitated and analyzed by Western blotting. When compared to the wild type (WCG) the protein bands of fatty acid synthase (FAS), aminopeptidase I (Ape1) and 3-phosphoglycerate kinase (PGK) fractionated in *atg21Δ* into the same lanes (*Figure 4-11*). FAS is a large conglomerate; PGK is a single protein that is cytosolic.
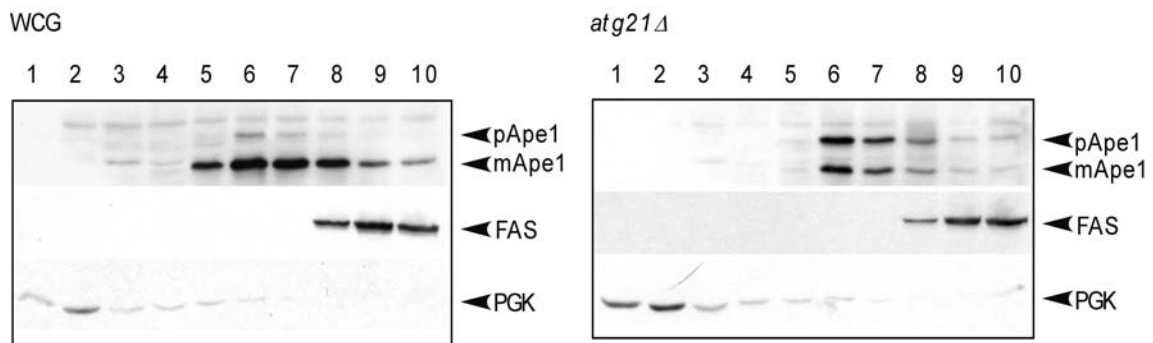
Figure 4-11 The glycerol gradient shows that in *atg21Δ* Ape1 peaks in the same fractions as in wild type cells (WCG). Aminopeptidase I organizes itself in the dodecamer form in both the wild type and in *atg21Δ*. Lysed *atg21Δ* and wild type cells were layered on top of glycerol gradients (20-50 %) and centrifuged in a Beckman ultracentrifuge TL-100 (TLS-55 rotor) at 20,000 xg for 4 h and 15 °C. The gradient was then divided into ten fractions from top to bottom, TCA precipitated, separated on a SDS-PAGE and blotted. The membrane was probed with antibodies against Aminopeptidase I (Ape1, p pro-form, m mature-form, molecular mass of 600 kDa), fatty acid synthase (FAS, molecular mass of 2,400 kDa) and 3-phosphoglycerate kinase (PGK, molecular mass 45 kDa).

4.2.11 Aminopeptidase I is not protected from proteases in vegetative *atg21Δ* cells

Aminopeptidase I is transported to the vacuole inside Cvt vesicles during vegetative conditions and in autophagosomes during periods of nutrient limitation. The protease protection assay is a simplified means of determining whether or not proApe1 is contained within these transport vesicles. When it is within aminopeptidase I is protected from the added proteases and remains in the pro-form. Ape1 is accessible, when it is outside the transport vesicles or the vesicle are improperly formed, it is seen in a matured or semi-matured state (Ape1*). *atg1Δ* and *atg3Δ* are examples of mutants were the formation of Cvt vesicles and autophagosomes is disrupted. *YPT7* is important in the docking and fusion of vesicles with the vacuole. *ypt7Δ* cells are unable to mature Ape1, because Ape1 is never released into the vacuole. When the protease is added to the reaction in the presence of triton x-100 membranes are disrupted and Ape1 is pseudo-matured.

For this and the following experiments *YPT7* was chromosomally deleted using the excised *ypt7::HIS3* fragment obtained from T. Lazar. In the WCG background this resulted in YKMW10 (*ypt7Δ*). This was repeated in the strains *atg1Δ*, *atg3Δ* and *atg21Δ* yielding the respective strains: YCV4 (*atg1Δ ypt7Δ*), YKMW16 (*atg3Δ ypt7Δ*) and YKMW19 (*atg21Δ ypt7Δ*). As seen in *Figure 4-12* proApe1 is protease accessible in *atg21Δ* cells. Like *atg1Δ* it is possible that *ATG21* is involved in the formation of Cvt vesicles.
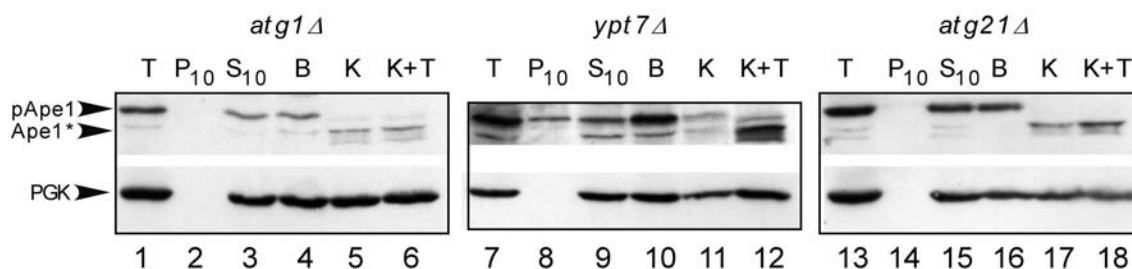
Figure 4-12 Ape1 is accessible to added proteases in *atg21Δ* cells. *atg1Δ*, *ypt7Δ* and *atg21Δ* cells were spheroplasted divided into four aliquots and subjected to centrifugation by 10,000 xg (T, S$_{10}$, P$_{10}$: lanes 1-3, 7-9, and 13-15), buffer (B: lanes 4, 10 and 16), proteinase K (K: lanes 5, 11 and 17) and to proteinase K plus triton X-100 (K+T: lanes 6, 12 and 18). *atg1Δ* is unable to form completed vesicles, thus Ape1 is accessible to cleavage by proteinase K, lane 5. *YPT7* participates in the fusion of vesicles with the vacuolar membrane. *ypt7Δ* vesicles cannot enter the vacuolar lumen; therefore Ape1 remains in its unmodified state when proteinase K is present, lane 11. In lane 17, *atg21Δ* cells are accessible to proteinase K digestion, thus in *atg21Δ* cells, transport vesicles are either not formed or Ape1 is contained outside of these vesicles. (pApe1 is pro-Ape1 and Ape1* is a digested form of Ape1, but not necessarily the mature Ape1-form.) PGK is shown as a spheroplasting and loading control. If the cells were not completely spheroplasted, PGK would be pelleted in whole cells in P$_{10}$.

To discover if Ape1 is matured in *atg21Δ* cells as a result of normal processing in the vacuole, a second protease protection assay was performed. In *atg3Δ* and *atg21Δ* cells the *YPT7* gene was deleted. This epistatic experiment was used to see if a loss of Atg21 effects the maturation of Ape1 before fusion with the vacuole. *atg3Δ ypt7Δ* cells are unable to form autophagosomes and Cvt vesicles; other transport vesicles cannot enter the vacuole due to the absence of Ypt7. In *ypt7Δ* cells all vesicles, including autophagosomes, remain outside the vacuole. In stationary *atg21Δ ypt7Δ* cells, as seen in *Figure 4-13* part A, Ape1 is processed by proteinase K, similar to *atg3Δ ypt7Δ* cells. In stationary *ypt7Δ* cells Ape1 remains protected inside Cvt vesicles; Ape1 was also pelletable inside these Cvt vesicles (lane 8).
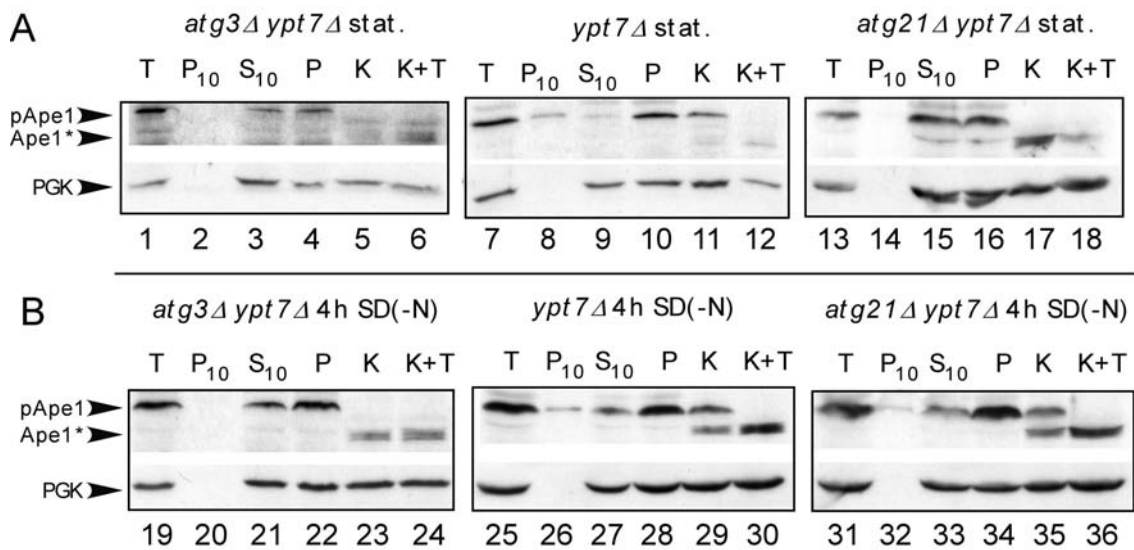
Figure 4-13 In an epistatic protease protection experiment Ape1 is accessible to proteinase K in (A) stationary but not (B) starved *atg21Δ ypt7Δ* cells. Membranes were immunoblotted with antibodies against proApe1. In Stationary (lanes 1-6) and starved (lanes 19-24) *atg3Δ ypt7Δ* cells Cvt vesicles and autophagosomes are not formed and Ape1 is acesssible to proteases. Cvt vesicles and autophagosomes are prevented from entering the vacuole in *ypt7Δ* cells. Cvt vesicles pelleted at 10,000 xg can be seen in lane 8. Autophagosomes pelleted can also be seen in lanes 26 and 32. In lanes 29 and 35 some of the autophagosmes formed lysed and Ape1 was partly accessible. Ape1 was mostly protected from proteinase K, therefore autophagosomes were formed. The membrane was additionally immunoblotted with anti-PGK antibodies as control for the absence of whole unspheroplasted cells and the amount of protein loaded onto the membrane. Aminopeptidase I is a resident vacuolar hydrolase. It is not readily processed by extrogenously added proteinase but is converted into a psuedo-mature form (Ape1*). pApe1 stand for proAminopeptidase I.

The same strains were observed after starvation for 4 h in SD(-N), *Figure 4-13* part B. After autophagy was induced, Ape1 was still accessible in *atg3Δ ypt7Δ* cells but not in *atg21Δ ypt7Δ*. In both *ypt7Δ* and *atg21Δ ypt7Δ* cells Ape1 containing autophagosomes were pelletable at 10,000 xg. After adding proteinase K Ape1 was generally inaccessible, but some of the autophagosomes were lysed.

4.2.12 Cell fractionation reveals that Cvt vesicles are not formed in *atg21Δ ypt7Δ* cells

ATG21 deleted cells show defects in the Cvt pathway. The questions still unanswered are if Cvt vesicles are formed or not, and if Cvt vesicles are formed is Ape1 simply not contained within them. C. Voss tried to answer this question with a cell fractionation.
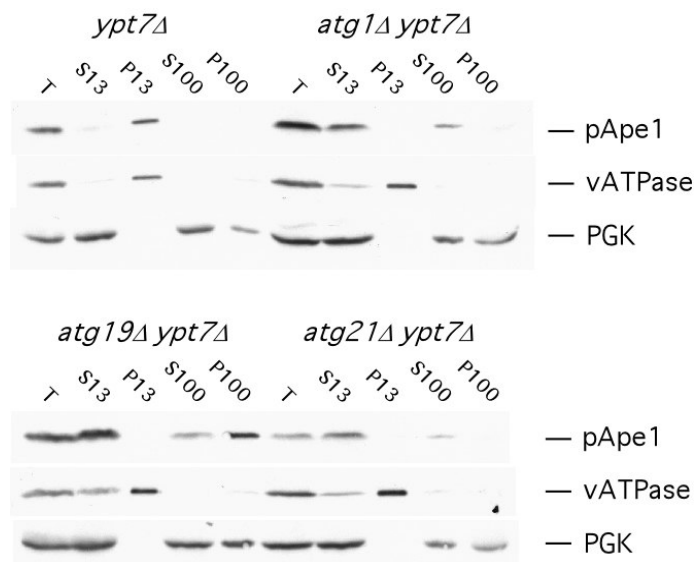
Figure 4-14 Cell fractionation reveals that Cvt vesicles are not formed in *atg21Δ ypt7Δ* cells. Stationary cells were hypotonically lysed and aliquoted into two fractions. One fraction was kept as a control for the total (T) protein processed. The other fraction was centrifuged by 13,000 xg then divided into pellet (P13) and supernatant (S13) fractions. About 60 % of the supernatant (S13) fraction was then centrifuged at 100,000 xg and also divide into pellet (P100) and supernatant (S100) fractions. The other 40 % was retained as the S13 fraction. The fractions were processed for immunoblotting. Probing with anti-proaminopeptidase I (pApe1) antibodies shows that I *ypt7Δ* cells Ape1 is almost completely contained within pelletable vesicles, seen in P13. The absence of Ape1 in the P13 fractions of *atg1Δ ypt7Δ*, *atg19Δ ypt7Δ* and *atg21Δ ypt7Δ* indicate that Ape1 is not contained within Cvt vesicles. v-ATPase (vATPase) is a vacuolar integral membrane protein used as a control for large pelletable proteins. 3-Phosphoglycerate kinase (PGK) is a cytosolic protein used as a control for the absence of whole cells.

atg21Δ ypt7Δ cells were hypotonically lysed and compared to *atg3Δ ypt7Δ*, *ypt7Δ* and *atg19Δ ypt7Δ* cells after centrifugation at 13,000 xg and 100,000 xg. The ability to pellet Ape1 at relatively low speeds was the deciding factor. It is known that in *ypt7Δ* cells Ape1 travels normally within Cvt vesicles to the vacuole, but these vesicles cannot fuse with the vacuolar membrane and thus Ape1 is trapped inside these Cvt vesicles. Likewise it is known that in *atg1Δ ypt7Δ* cells Cvt vesicles are not formed and Ape1 is not contained within vesicles. Similarly, in *atg19Δ ypt7Δ* cells Ape1 is not contained within Cvt vesicles, but Cvt vesicles are formed normally as a result of the missing Ape1-binding receptor. When comparing these three cases with *atg21Δ ypt7Δ*, in *Figure 4-14*, a definite lack of pelletable Ape1 in low speed centrifugation (P13) is noticed and at higher speeds (P100) very little Ape1 is pelletable. Therefore it was concluded that *atg21Δ ypt7Δ* resembles *atg1Δ ypt7Δ* and it is unlikely that Cvt vesicles are properly formed. v-ATPase is a integral vacuolar membrane protein and is completely pelletable at 13,000 xg. PGK is a cytosolic protein and a control for the quality of the lysis.

4.2.13 Autophagy is reduced in *atg21Δ* cells

Alkaline phosphatase (ALP) is a resident vacuolar hydrolase. It is expressed in the cytosol and transported via its own pathway to the vacuole, where it is matured to its active form. The *PHO8* gene contains a signal peptide that sends it to the vacuole to be processed. A modified version of this protein was utilized to measure the autophagic activity (94). A truncate version of pho8Δ60 (pCC5, (76)) was expressed within strains deleted in *pho8Δ* and the strain being examined. This truncated Pho8 remains within the cytosol until it is unselectively transported within autophagosomes to the vacuole. Once in the vacuole Pho8 is matured to its active form. The autophagic activity can be determined indirectly by the ALP activity. The ALP activity examined in *pho8Δ* (wild type), *atg15Δ pho8Δ* and *atg21Δ pho8Δ* cells. The logarithmically grown strains containing pho8Δ60 were shifted to SD(-N) starvation media; at 0, 2, 4 and 6 hours a sample was examined and its ALP activity determined, *Figure 4-15*. The enzyme activity of the wild type was set to 100 %. In *atg15Δ* cells lysis of autophagosomes is defective, therefore pho8Δ60 is not released and is inactive. In *atg21Δ pho8Δ* cells autophagy was reduced to 35 %.
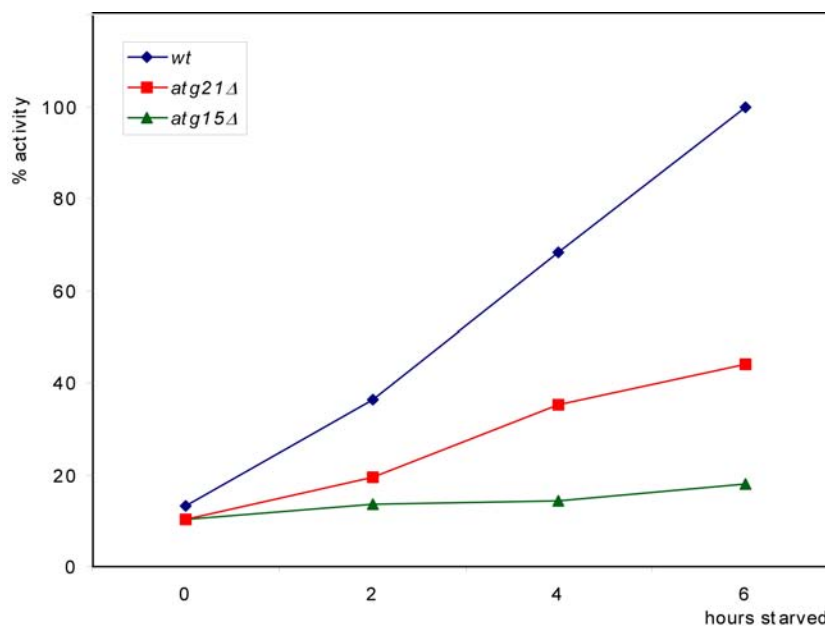
Figure 4-15 Using the ALP Assay *atg21Δ* cells show a reduced rate of autophagy. *PHO8* (alkaline phosphatase, ALP) deleted strains were transformed with the cytosolic Pho8Δ60. Being a vacuolar enzyme, it remains inactive until transported into the vacuole where it is matured. This truncated Pho8 stays within the cytosol until it is transported in autophagosomes. This transport is unspecific and fully dependent on the rate of autophagy. At the shown intervals samples of starving strains were taken, lysed and the activity of ALP was measured. This activity was directly correlated to the autophagic activity.

This reduced autophagic activity was also seen during the maturation of Ape1, *Figure 4-16*. Samples of wild type, *pep4Δ* and *atg21Δ* cells were taken before and at intervals after they were starved in 1 % potassium acetate (KAc). The amount of proApe1 in *atg21Δ* decreased slowly after shifting to KAc compared to the wild type, where Ape1 was only found in the matured form. In *atg1Δ* cells the formation of Cvt vesicles and autophagosomes is impaired. Ape1 is not transported to the vacuole and therefore cannot be processed, thus only proApe1 is seen.
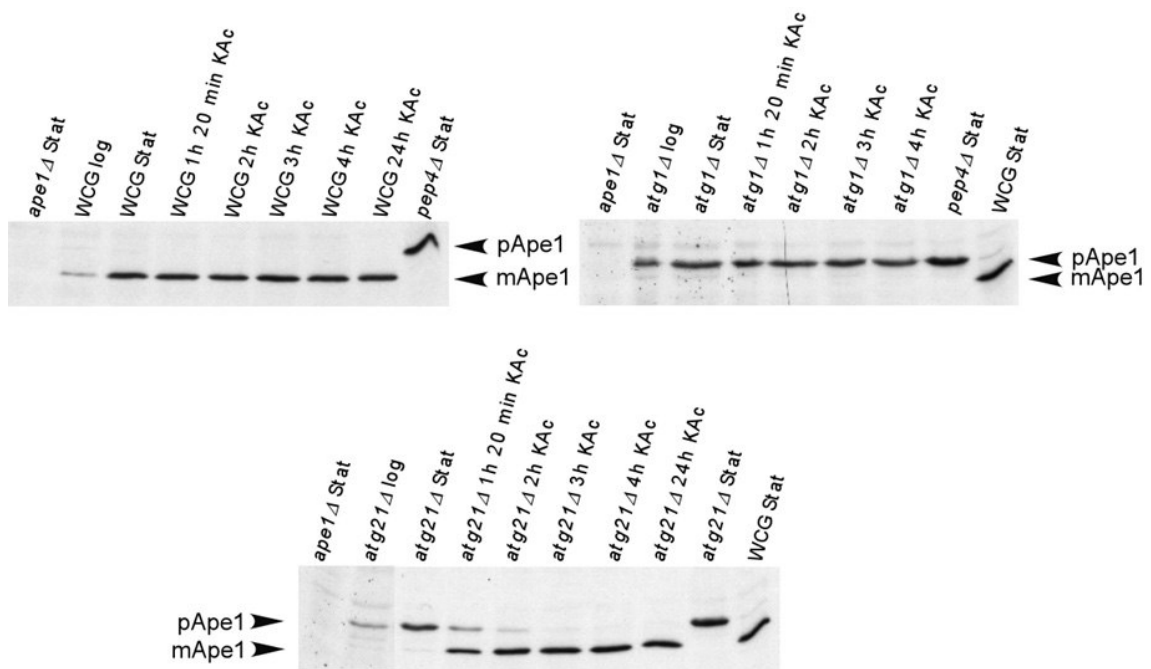
Figure 4-16 A reduced rate of autophagy is also seen during the maturation of Ape1. The strains were grown to a logarithmic phase where a sample was taken then allowed to grow to a stationary phase. There a second fraction was taken and the remaining cells were shifted to 1 % potassium acetate (KAc). There after a sample was removed hourly for four hours and the remaining cells were starved for 24 h total before sampling. The samples were processed for immunoblotting and probe with anti-aminopeptidase I [pro- (pApe1) and mature (mApe1) aminopeptidase I]. The wild type contained mature Ape1 at all times, whereas in *atg1Δ* cells, whose defect is in formation of Cvt vesicles and autophagosomes, Ape1 remained unprocessed in all fractions. Cells lacking *ATG21* have pro-Ape1 under vegetative conditions. After shifting to starvation conditions *atg21Δ* cells, unlike wild type cells, process aminopeptidase I slowly. Only after 4 h is the *atg21Δ* sample completely matured.

4.2.14 Direct fluorescence proteins localize Atg21 in relation to known autophagic proteins

Direct fluorescent protein tags are becoming the pick of the litter. This is because the fixation process of indirect immunofluorescence can distort the cell framework and falsify the true localization of the protein being investigated. Another problem is that the background fluorescence is often difficult to control. Direct fluorescence has many advantages, protein localization can be observed in live cells. Under the right

conditions, these proteins can be observed continuously over longer time frames. Though this is also possible in indirect immunofluorescence, using complimentary fluorescing tags many proteins can be observed simultaneously. The most common fluorescent protein tag is the green fluorescent protein (GFP) from the jellyfish *Aequorea victoria*. Through selected mutations this fluorescent tag is available in yellow (YFP) and cyan (CFP). Other fluorescent tags from other species give range to many other colors.

4.2.14.1   The creation of a YFP-tagged Atg21 protein

During this study, different proteins were tagged with fluorescent proteins. Atg21 was combined with YFP; Ape1 was combined separately with both YFP and CFP. *Figure 4-17* shows that the created fusion protein ATG21-YFP (pkmw16) is active; it complements the deletion mutant's inability to mature Ape1.
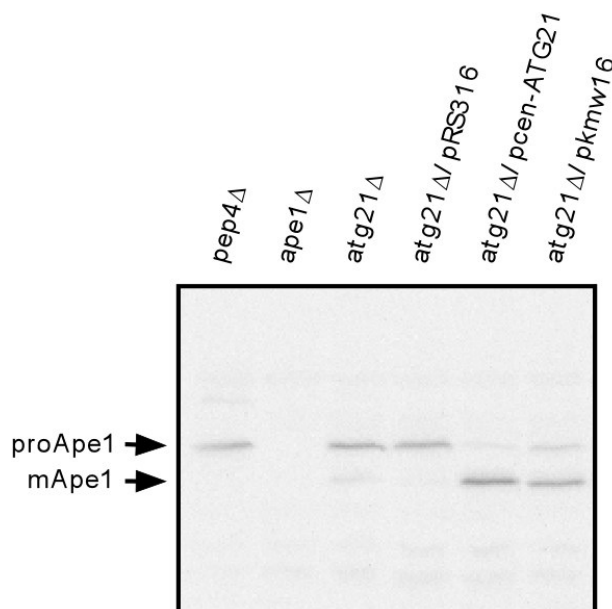
Figure 4-17 *atg21Δ* **cells are complemented by the Atg21-YFP plasmid.** *atg21Δ* **cells were transformed with an empty plasmid (pRS316), a centromeric plasmid containing ATG21 (pcen-ATG21) and a centromeric plasmid containing the ATG21-YFP fusion protein (pkmw16).**

Other GFP, CFP and YFP constructs were also obtained from cooperating laboratories. These constructs were very useful in localizing Atg21 in relationship to other known proteins. Fluorescent dyes also helped with orientation around the yeast cell, for example the vacuolar membrane dye FM4-64 or the dye Hoechst 44422 used to stain the nucleus in live cells (similar to DAPI). These combined with the created fluorescent-tagged proteins lead to a greater understanding of Atg21.

4.2.14.2 Visualization of Atg21-YFP in *ATG* and *ATG* related strains
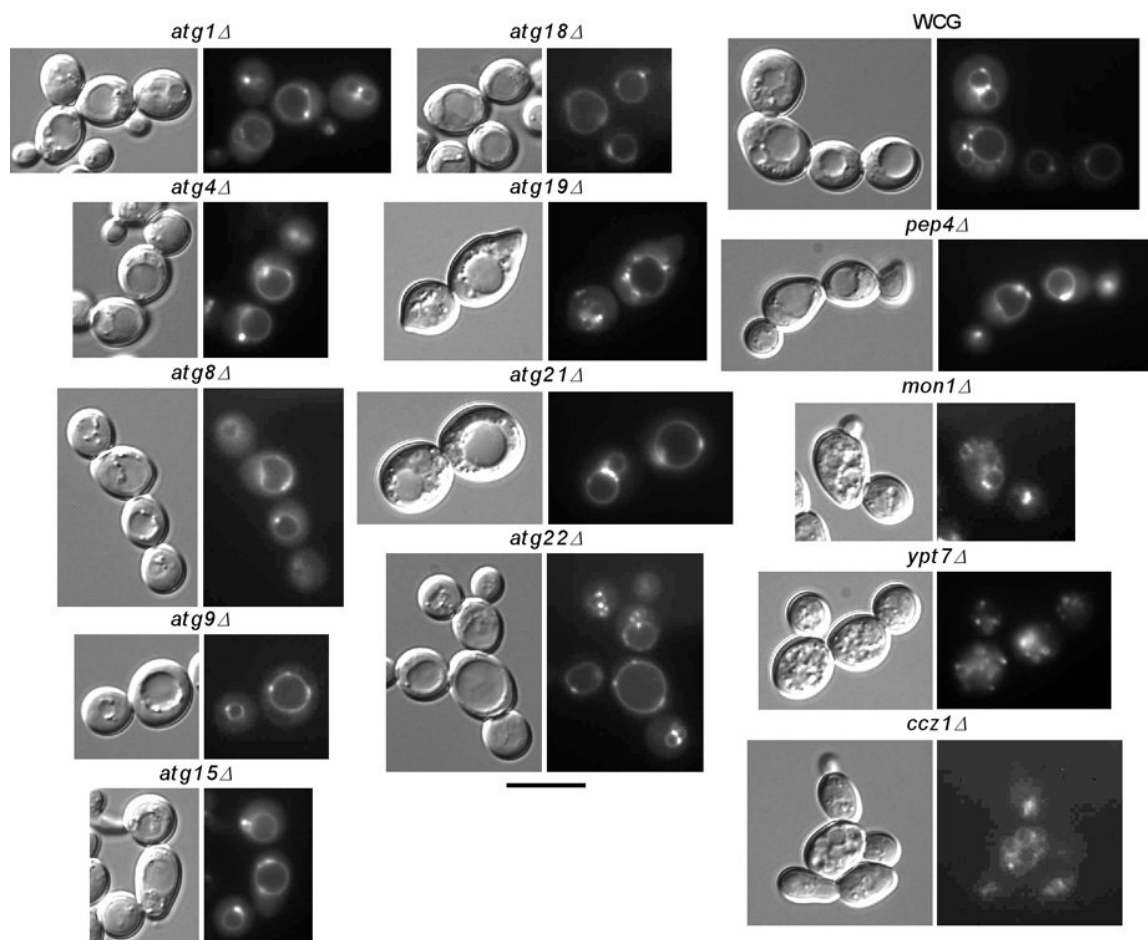
Figure 4-18 The fluorescently tagged Atg21 protein, Atg21-YFP, shows no location deviation in several ATG deleted and autophagy related strains compared to the wild type strain (WCG), bar 10 µm.

Atg21-YFP, under the control of its endogenous promoter, was viewed in several *ATG* deleted strains, *Figure 4-18*. In these *ATG* deleted and autophagy related strains no deviation was seen when compared to the wild type. Atg21-YFP was located at the vacuolar membrane and to points on the vacuolar rim. In strains with vacuolar fusion difficulties, such as *ypt7Δ*, Atg21-YFP was also located comparable to the wild type.
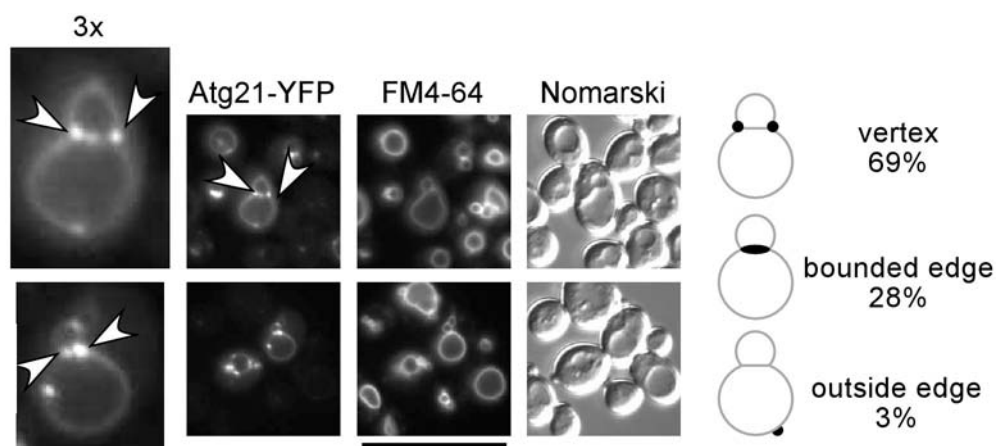
Figure 4-19 Atg21-YFP is located at the vertices of two or more vacuoles as seen in combination with FM4-64, a vacuolar membrane dye. The arrowheads indicate points were Atg21-YFP seem to concentrate. The schematic to the right indicates the percentage of punctae located at these points. 94 cells were scored, bar 10 μm.

After counting many cells it was noticed that Atg21-YFP is often located on the vertices of two or more vacuoles. Of the 94 cells counted, 68% of the Atg21-YFP points were at the vacuolar vertices and 28% were located on the bounded edge of two vacuoles, see *Figure 4-19*. Only 3 % were located not at these connecting points when two or more vacuoles were sited. 97 % of the Atg21-YFP punctae were located adjacent to two or more vacuoles. This localization pattern is reminiscent of the Vps class C-HOPS complex (58).

Interestingly, Atg21-YFP seemed to be transported in vesicles to the vacuole after longer starvation periods. *Figure 4-20* shows Atg21-YFP in *atg15Δ* cells after two days in CM-Ura medium; here fluorescent vesicles are seen moving about with in the vacuole. Cells defective in *ATG15* cannot lyse the autophagosomes that enter into the vacuole. As a result, autophagic bodies collect within the vacuole.
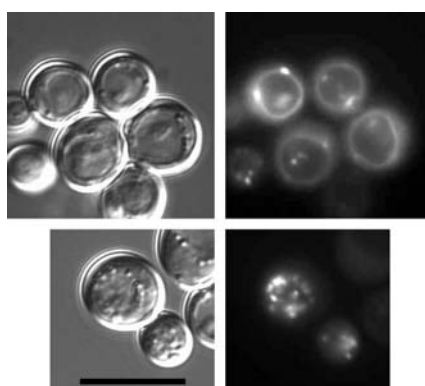
Figure 4-20 In *atg15Δ* cells, Atg21-YFP collects within the vacuole in a vesicle-like pattern. *atg15Δ* cells expressed with Atg21-YFP were grown in CM-Ura and after two days moving vesicles were observed within the vacuole: Nomarski images (left) and fluorescence (right), bar 10 μm.

4.2.14.3 Atg21-YFP is not always located adjacent to the nuclear-vacuolar junction

Since Atg21-HA was seen to be located near the nucleus at the nuclear-vacuolar junction. Atg21-YFP was examined in relation to *NVJ1*. Nvj1 is an integral membrane protein that localizes to the boundary between the nucleus and the vacuole, the nuclear-vacuolar junction (70). Nvj1-CFP was expressed under the control of the copper promoter CUP1. After viewing many cells, *Figure 4-21*, statistically only half of the punctae appear to be localized adjacent to these junctions. Since each cell usually contains more than one point this may or may not be relevant to the location of Atg21.
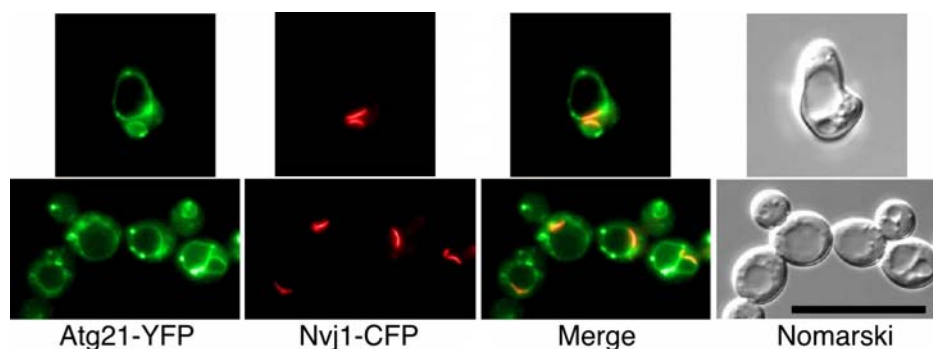
Figure 4-21 Only half of the Atg21-YFP punctae (green) are located near the nuclear-vacuolar junction shown as Nvj1-CFP (red), bar 10 μm.

4.2.14.4 The PAS is not necessarily near the nuclear-vacuolar junction

The PreAutophagosomal Structure (PAS) is known to be located at the vacuolar membrane but its location relative to other organelles was yet unknown. Ape1-YFP was used as a reference point for the PAS' location. The nucleus was stained with Hoechst 44422 and the nuclear-vacuolar junction was visualized with Nvj1-CFP. As indicated by the white arrowheads in *Figure 4-22* the PAS is not always located adjacent to the nuclear-vacuolar junction. Though when taken as a whole, more often than not it is found somewhere within the vicinity of the nuclear-vacuolar junction and the nucleus. No differences in the relevant locations of Ape1-YFP and Nvj1-CFP were seen when comparing the wild type with *atg21Δ* cells (not shown).
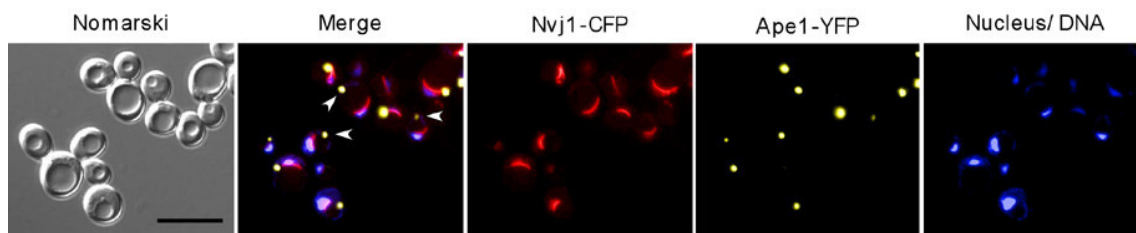
Figure 4-22 The PAS is not always located adjacent to the nuclear-vacuolar junction. Live cells expressing Ape1-YFP (yellow) and Nvj1-CFP (red) were visualized using direct fluorescence. The nucleus (blue) was also seen after staining the cells with Hoechst 44422. Though the PAS was often seen adjacent to the nuclear-vacuolar junction, white arrowheads indicate cells where they were not seen near one another. The PAS was represented by Ape1-YFP and the nuclear-vacuolar junction was represented by Nvj1-CFP. Nvj1-CFP was expressed under the control of the copper promotor CUP1, whereas Ape1-YFP was expressed under its endogenous promotor. Bar 10 μm.

4.2.14.5 Atg21-YFP generally does not colocalize with the preautophagosomal structure

The last question asked about Atg21-YFP was if it co-localize with the PAS. The Atg21-YFP punctae localize to the vacuolar membrane, as does the preautophagosomal structure. So this was an interesting question. Ape1-CFP was again used as the fluorescent PAS marker. Localization of Atg21-YFP relative to Ape1-CFP was observed in *atg21Δ* cells. In *Figure 4-23*, Atg21-YFP is pseudo-colorized with green whereas Ape1-CFP is shown in red. As indicated by the white arrowheads some of the Atg21 punctae colocalize with the PAS, but generally there were more noncolocalizing punctae than those that did.
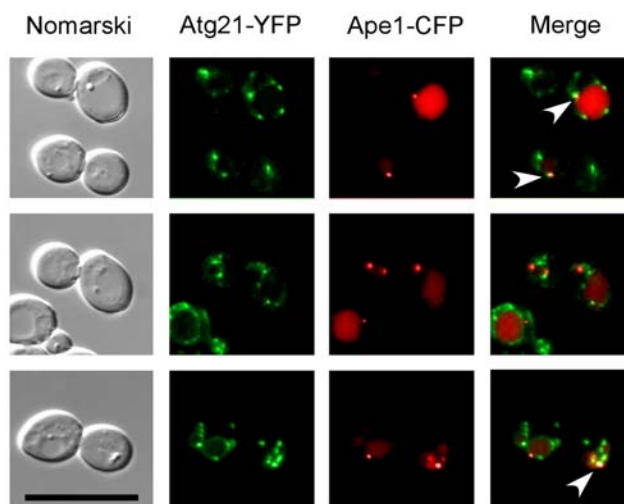
Figure 4-23 Atg21-YFP and proaminopeptidase I-CFP were visualized in *atg21Δ* cells. Atg21-YFP is pseudo-colorized with green and Ape1-CFP is pseudo-colorized red. Ape1-CFP was used as a fluorescent marker for the preautophagosomal structure (PAS). As indicated by the white arrowheads some but not all of the Atg21 punctae colocalize with the PAS. Aminopeptidase I is a vacuolar hydrolase that is transported to the vacuole. Ape1-CFP entering the vacuole causes it to fluoresce. Bar 10μm

4.2.15 Localization of different GFP-tagged proteins to the preautophagosomal structure in *atg21Δ* cells

Autophagosomes and Cvt vesicles are thought to form (de novo) from an unknown organelle called the preautophagosomal structure or PAS. This dot-like organelle is located at the vacuolar membrane. Proteins that comprise Cvt vesicles and autophagosomes seem to collect at this point before forming the transport vesicle. Three proteins involved in the formation of Cvt vesicles and autophagosomes were chosen and localized with GFP-tagged versions.

Atg9 is an integral membrane protein that is involved in the formation of both Cvt vesicles and autophagosomes. It localizes mainly to the PAS but also has a peripheral pool at the mitochondria (100). The percentage of cells with GFP-Atg9 at the PAS was determined in both growing and starved wild type, *atg1Δ*, *atg21Δ* and *atg18Δ* cells, *Figure 4-24*. In about 80 % of growing cells GFP-Atg9 was localized to a point on the vacuolar membrane, the PAS, regardless of strain. In starved cells the amount of GFP-Atg9 localizing to the PAS was reduced to 25 % in the wild type, *atg18Δ* and *atg21Δ* cells; in starved *atg1Δ* cells the percentage remained high at 75 %. GFP-Atg9 is recycled from the PAS dependent on an Atg1-Atg13 complex, therefore the amount of GFP-Atg9 in *atg1Δ* cells residing at the PAS remains high.
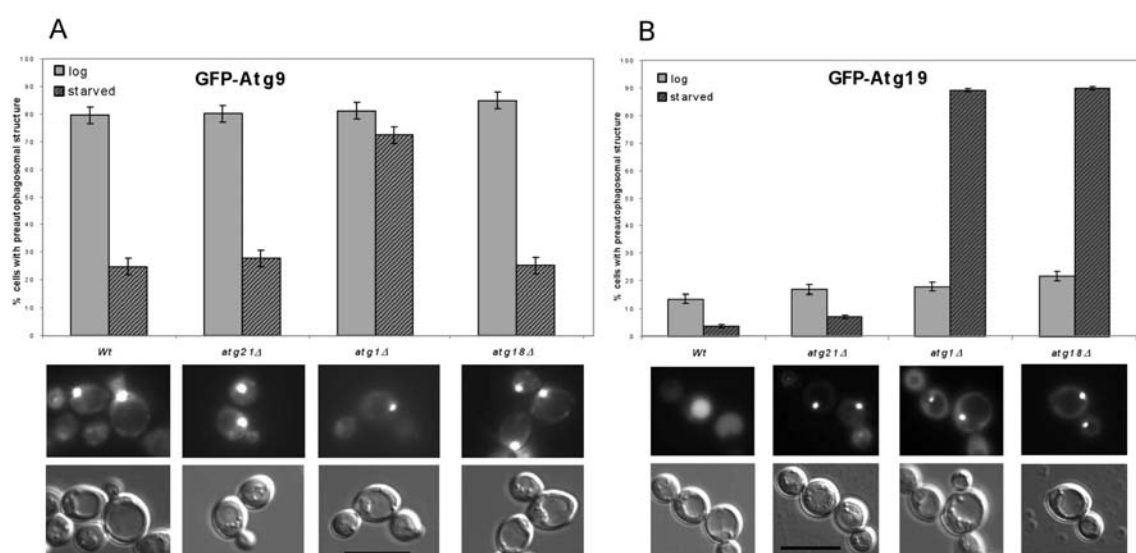
Figure 4-24 Growing *atg21Δ* cells recruit (A) GFP-Atg9 and (B) GFP-Atg19 to the PAS. The bar diagram show the results of scoring cells where GFP-Atg9 or GFP-Atg19 are recruited to the preautophagosomal structure (PAS). The percentage results from the number of cells with a fluorescent point on the vacuolar membrane compared to the total cells counted. Atg19-GFP travels to the vacuole where GFP is freed from Atg19. In *atg1Δ* and *atg18Δ* GFP-Atg19 is recruited to the PAS but due to a defect in autophagy GFP-Atg19 remains outside the vacuole. GFP-Atg9 in *atg21Δ* and *atg18Δ* localize to the PAS similar to the wild type, bar 10 μm.

Atg19 is also recruited to the PAS; it is the receptor protein for Ape1. Ape1 is sequestered to the PAS were it is packed into Cvt vesicles and autophagosomes. GFP-Atg19 localizes to the PAS in about 15 % of the growing cells counted. In starved cells a decrease in the localization of GFP-Atg19 to the PAS was noticed in wild type and *atg21Δ* cells; a fluorescent point was seen in only about 5 % of the cells. This was also due to the fact that Atg19 travels with the transport vesicles and is lysed in the vacuole. In starved *atg1Δ* and *atg18Δ* cells a dramatic increase to almost 90 % was seen. This is probably due to the recruitment of Atg19 to the PAS but without the formation of autophagosomes that can transport Atg19 to the vacuole.
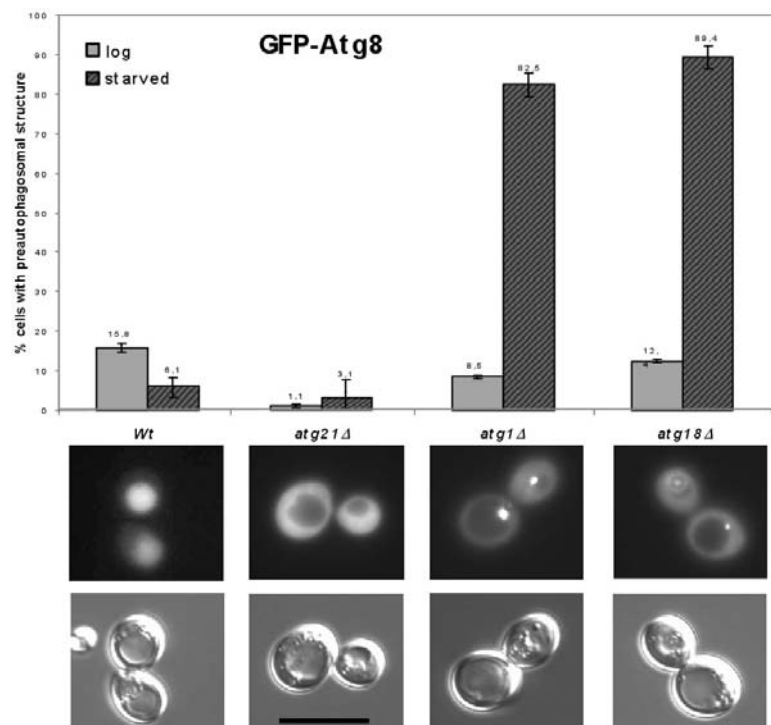
Figure 4-25 Growing *atg21Δ* cells are defective in the recruitment of GFP-Atg8 to the PAS. The bar diagram shows the results of tallying cells where Atg8-GFP is recruited to the Preautophagosomal Structure (PAS). The percentage results from the number of cells with a fluorescent point on the vacuolar membrane compared to the total cells counted. Atg8-GFP travels to the vacuole where GFP is freed from Atg8. In *atg1Δ* and *atg18Δ* Atg8-GFP is recruited to the PAS but due to a defect in autophagy Atg8-GFP remains outside the vacuole, bar 10 μm.

The third protein Atg8 is involved in the elongation of autophagosomes. It is synthesized in the cytosol, where Atg4 activates it by removing its carboxyterminal amino acid. In a second step activated Atg8 is covalently coupled to the membrane lipid phosphatidylethanolamine (PE), dependent on an ubiquitin-like conjugate system involving Atg3 and Atg7. This membrane bound Atg8 is also contained at the PAS until it is utilized for vesicle formation. Interestingly, GFP-Atg8 showed almost no recruitment to the PAS in growing cells. In only 1 % of the cells counted GFP-Atg8 was seen at this perivacuolar point. In wild type, *atg18Δ* and *atg1Δ* cells GFP-Atg8 was seen

at the PAS though in small amounts of 8 – 15 %. In cells starved for 4 h, less GFP-Atg8 was localized to the PAS but this was due to the transport and degradation of GFP-Atg8 into the vacuole. *atg21Δ* cells showed a slight increase of PAS localization (3 %), though it was obvious that GFP-Atg8 remained mostly cytosolic, see *Figure 4-25*. GFP-Atg8 localization at the PAS was significantly increased in *atg1Δ* and *atg18Δ* cells for similar reasons as explained for the accumulation of GFP-Atg19.

4.2.16 Defects in the degradation of GFP-Atg8 is an indicator for a reduced autophagic rate
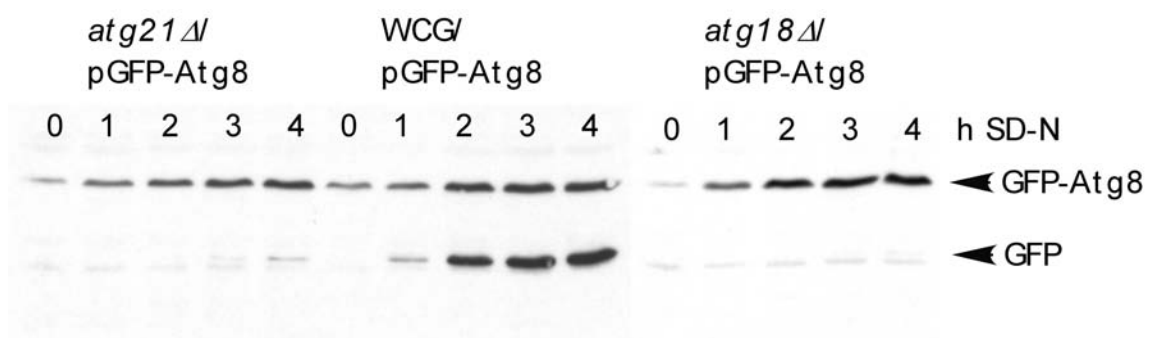
Figure 4-26 The inability to degrade GFP-Atg8 is an indicator of a defect in autophagy. *atg21Δ*, *atg18Δ* and the wild type (WCG) were transformed with the GFP-Atg8 plasmid. The cells were shifted to starvation medium, SD(-N), and hourly samples were taken and processed for immunoblotting. The membrane was probed with anti-GFP antibodies. *atg18Δ* cells shows a complete block in the degradation of GFP-Atg8 whereas in *atg21Δ* cells a small amount of free GFP is observed after three hours.

Another test for autophagy is to observe the degradation of GFP-Atg8. Atg8 is conjugated to the lipid membrane protein phosphatidylethanolamine (PE) and is integrated into the inside and outside membrane of autophagosomes. The protein Atg4 removes Atg8 attached outside of the completed autophagosomes. Atg8 attached to PE on the inner membrane travels to the vacuole and is degraded. Therefore, GFP-tagged Atg8 travels within the autophagosomes and GFP is released from GFP-Atg8 when the autophagic body is degraded in the vacuole. GFP being quite proteolysis resistant accumulates in the vacuole. This process can be examined by western analysis. As seen in *Figure 4-26*, the amount of GFP-Atg8 increases the longer the cells are starved. In the wild type (WCG) GFP-Atg8 is properly transported to the vacuole and GFP is progressively released. *ATG18* deleted cells release no free GFP, though the amount of GFP-Atg8 increases. The amount of free GFP in *ATG21* deleted cells is very small, first arriving after three hours of starvation. This is reminiscent of the decreased autophagic rate observed during the ALP assay and the lag in the maturation of aminopeptidase I in *atg21Δ* cells.

4.2.17 *atg21Δ* cells are delayed in the conjugation of Atg8 to phosphatidylethanolamine
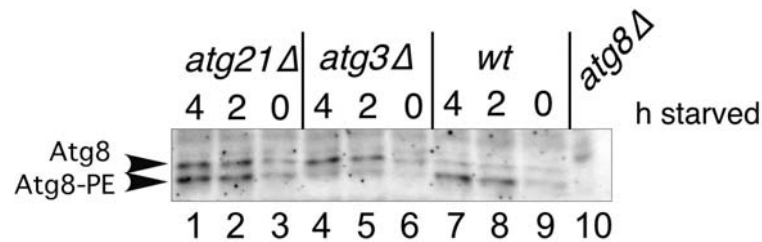
Figure 4-27 Compared to the wild type (wt) significant amounts of Atg8 remains non-conjugated to phosphatidylethanolamine (PE) in *atg21Δ* cells. Atg3 is the conjugating enzyme for Atg8; in *atg3Δ* cells Atg8 remains unconjugated to PE. Samples of *atg21Δ*, *atg3Δ* and the wild type were taken at the indicated times after shifting to SD(-N). The samples were separated using a SDS-PAGE containing urea.

In *Figure 4-25* it was shown that GFP-Atg8 accumulates in the cytosol and is not recruited to the PAS compared to the wild type. Therefore the question was asked whether or not Atg8 is conjugated to phosphatidylethanolamine. The lipid-coupled form of Atg8 shows a higher mobility than the free form of Atg8 in SDS-PAGEs containing urea (43). This attribute was used to analyze the lipidation of Atg8 in *atg21Δ*. In lanes 1-3 of *Figure 4-27* performed by C. Voss, *atg21Δ* appears to have a significant amount of free Atg8, whereas in wild type cells (lanes 7-9) almost all Atg8 is lipidated. *atg3Δ* was used as a control; *ATG3* is the E2-like enzyme required for the lipidation of Atg8. Due to the increased amount of free Atg8, *atg21Δ* cells appear to have a defect in the conjugation of Atg8 to phosphatidylethanolamine.

4.2.18 The expression level of Atg8 is normal

Atg8 is one of the few proteins whose expression is induced by starvation. To determine if the reduced Atg8-PE formation is due to a reduced amount of Atg8, the induction of Atg8 was examined. Wild type and *atg21Δ* cells were grown and shifted to SD(-N) medium. After the shift, samples were taken hourly and processed for immunoblotting against the Atg8 protein. *atg21Δ* and the wild type show no significant differences in their induction rate as seen in *Figure 4-28*, examined by C.Voss.
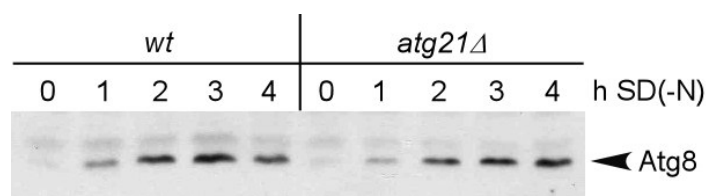
Figure 4-28 The induction of Atg8 in *atg21Δ* is normal. The strains were grown and shifted to SD(-N) medium. After the indicated hours samples were taken and processed for immunoblotting. The membrane was probed with anti-Atg8 antibodies.

4.2.19 Overexpression of Atg8 in *atg21Δ* cells does not reconstitute the defect in maturation of Ape1

Since Atg8 is expressed normally in *atg21Δ* cells but is not able to localize to the preautophagosomal structure, the question was: if Atg8 is overexpressed in *atg21Δ* cells will that alleviate *atg21Δ*'s inability to mature Ape1? Therefore Atg8 expressed from a 2μ-plasmid was transformed into *atg21Δ* cells. As a control, an empty 2μ-vector was also transferred into *atg21Δ* cells. The cells were then grown to a stationary phase and then shifted to SD(-N) medium. Samples from vegetative and starvation conditions were probed for the maturation of Ape1. The overexpression of Atg8 had no effect on the Ape1 maturation, as seen in *Figure 4-29* from H. Barth.
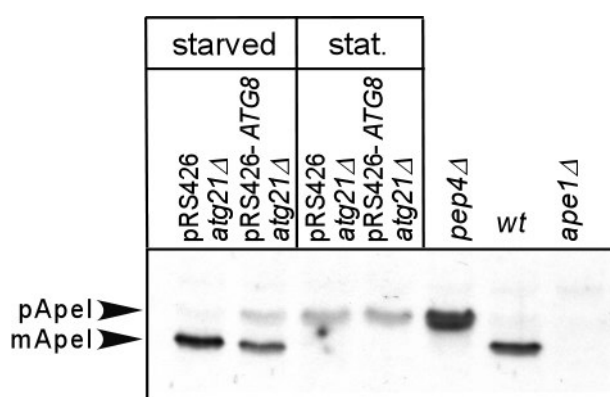
Figure 4-29 The overexpression of Atg8 in stationary and starved *atg21Δ* cells has no effect on the maturation of aminopeptidase I. *atg21Δ* cells were transformed with an empty 2μ plasmid (pRS426) and the 2μ plasmid containing Atg8. The starved cells were shifted to SD(-N) for 5 hours.

4.2.20 The decreased lipidation of Atg8 in *atg21Δ* has no effect on the autophagosomal size

With the help of electron microscopy we are able to look into the yeast cell more detailedly. *Figure 4-30* the formed autophagosomes in *ypt7Δ* and *atg21Δ ypt7Δ* cells were compared in sized. The cells were grown to mid-logarithmic phase and then starved for four hours in SD(-N) starvation media. The cells were then harvested and fixed with a 1 % potassium permanganate solution (91). The fixed cells were then Epon embedded and examined by E.-L. Eskelinen (University of Kiel, Kiel Germany). The images were taken with a Zeiss EM 900 transmission electron microscope. The relative size of the autophagosomes was determined by measuring the mean area of the autophagosomes through point counting from the 12,000x magnified photographs. Surprisingly, the autophagosomes formed in *atg21Δ* cells were not limited in size by the reduced lipidation of Atg8, though fewer autophagosomes were created. *YPT7* deleted cells were used due to the phenotype that all transport vesicles are blocked from entering the vacuole. The autophagosomes accumulated in the cytosol can then be easily compared.
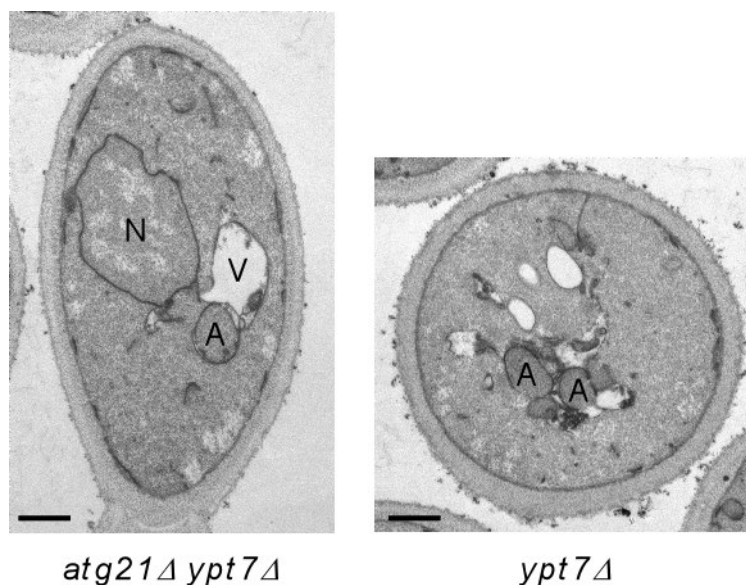
atg21Δ ypt7Δ   *ypt7Δ*

Figure 4-30 Although the lipidation of Atg8 in *atg21Δ* is retarded, the autophagosomes created are of normal size as seen in *atg21Δ ypt7Δ* and *ypt7Δ* cells. *ypt7Δ* and *atg21Δ ypt7Δ* cells were starved for 4 h in SD(-N) and then fixated with permanganate and Epon embedded. The images (12,000x magnification) were taken with a Zeiss EM 900 transmission electron microscope. V, vacuole; N, nucleus; A, autophagosome; bar 0.6 μm.

4.2.21 Atg21 seems to localize to a separate compartment in an optiprep gradient

To identify the possible compartment to which Atg21 localizes, H. Barth and myself performed equilibrium centrifugations in an Optiprep gradient. The gradient was created using Optiprep solution in the concentrations from 0-50%. Hypotonically lysed Atg21-HA cells were centrifuged at high speed and the resulting pellet fraction was placed on top of the Optiprep gradient. The gradient centrifuged for 16 h at 140,000 xg and 4 °C was then divided into thirteen equal fractions from top to bottom and processed for immunoblotting, *Figure 4-31*. Atg21-HA peaked in fractions 3 and 4 unlike the other marker proteins. The vacuolar membrane localized to fractions 1 and 2, as indicated by the proteins v-ATPase and Vac8 both found at the vacuolar membrane. Pep12, fractions 7 and 8, was used as a marker for the perivacuolar compartment and Dpm1, fraction 10, marked the endoplasmic reticulum.
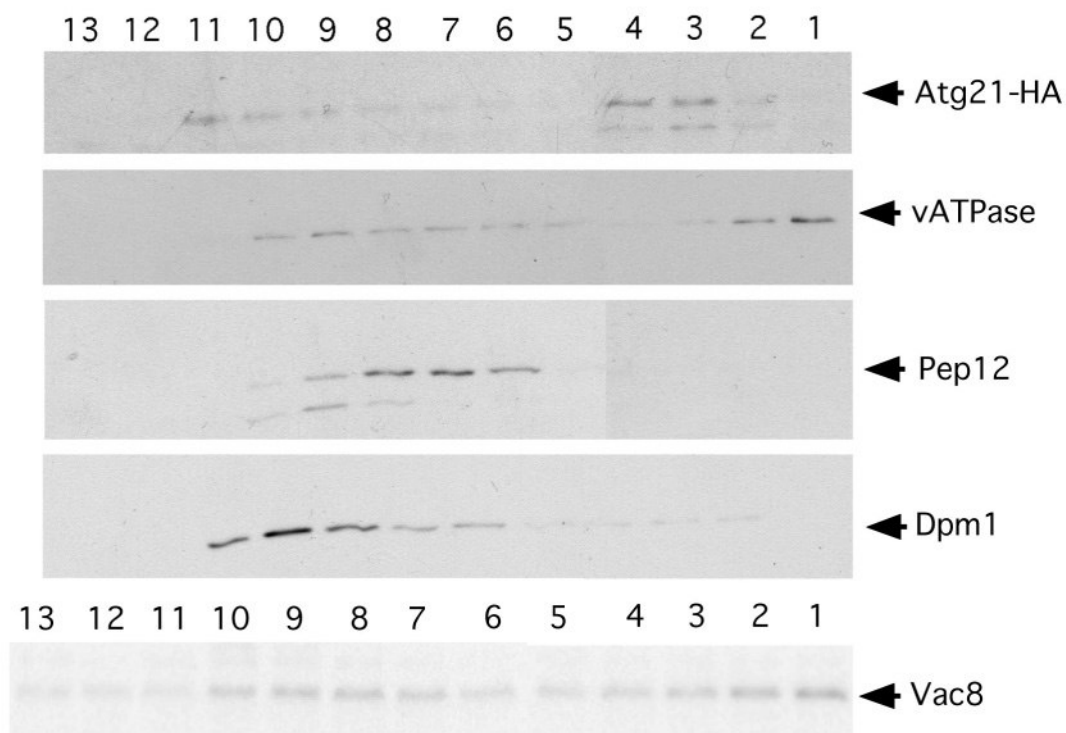
Figure 4-31 In a Optiprep gradient the location of Atg21-HA was compared to other known compartmental proteins. Atg21-HA cells were spheroplasted and hypotonically lysed. The lysate was centrifuged at 100,000 xg and the pellet fraction was layered onto an Optiprep gradient and separated for 16 h at 140,000 xg. Thirteen fraction were removed from top to bottom and immunoblotted with antibodies against HA, vacuolar ATPase (vATPase, 100 kDa subunit, vacuolar membrane marker), Pep12 (perivacuolar compartment marker), Dpm1 (endoplasmic reticulum marker) and Vac8 (located at the nucleus vacuolar junction). Atg21-HA peaked in fractions 3 and 4 unlike any of the other protein markers.

4.3 CCZ1 and MON1 two genes involved in the fusion of Cvt vesicles and autophagosomes with the vacuole

CCZ1 and *MON1* were also identified in the second part of the reverse genetic screen. The deletion of either one of the genes leads to a disruption of the maturation of aminopeptidase I. This defect in the maturation of Ape1 was further examined under vegetative and starvation conditions in *Figure 4-32*. Under both conditions only proApe1 was observed, both autophagy and the Cvt pathway are affected. The maturation of proteinase B (PrB) and carboxypeptidase Y (CPY) were also slightly affected by the deletion of *MON1* or *CCZ1*.
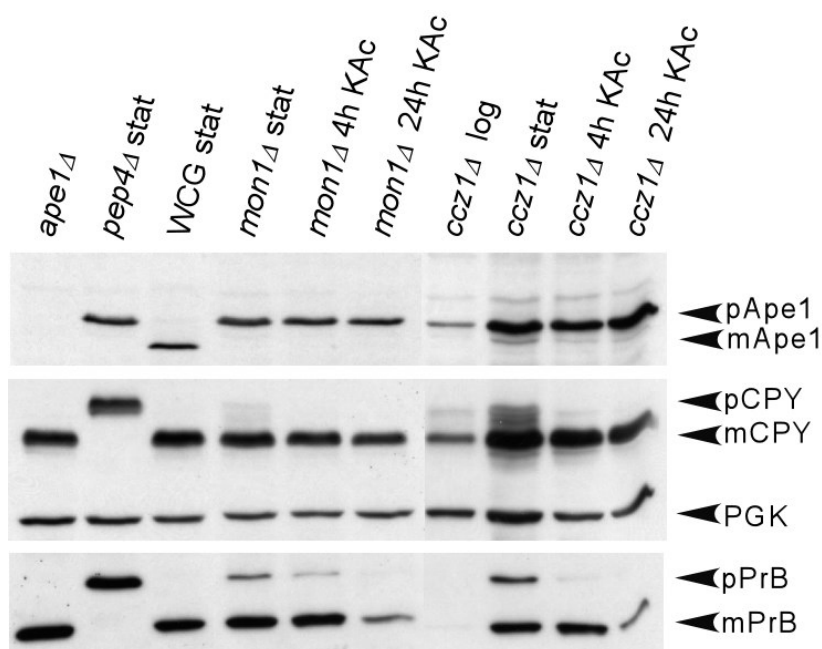
Figure 4-32 Maturation of Aminopeptidase I is defective in *MON1* and *CCZ1* deleted cells. Deletions in the *MON1* or *CCZ1* locus affect the maturation of aminopeptidase I (Ape1), carboxypeptidase Y (CPY) and proteinase B (PrB). Cells from *mon1Δ* and *ccz1Δ* were grown and shifted to starvation media (KAc). Samples were taken at different growth phases and after 4 and 24 hours in KAc. The samples were compared to the wild type strain (WCG) and proteinase A (*pep4Δ*) deleted cells. 3-Phosphogycerate kinase (PGK) was probed as a loading control.

4.3.1 Cross complementation shows that *CVT16* and *CCZ1* are allelic

To investigate if the novel genes found were ones from a previous screen, *CCZ1* and *MON1* were crossed with "unknown" Cvt strains (48). These Cvt mutants were identified by their defect in the maturation of aminopeptidase I. This defect is common in both the identified novel deletion mutants and the "unknown" Cvt mutants. This common defect was used to check for allelisms. *MON1* was not allelic to the Cvt point mutants *cvt3-1*, *6-1*, *11-1*, *13-1*, *14-1*, *15-1* or *16-1*. Though when *ccz1Δ* was crossed

with the Cvt point mutant *cvt16-1* the defect in the maturation of Ape1 was not complemented as seen in *Figure 4-33*. Therefore, *CVT16* is identical with *CCZ1*.
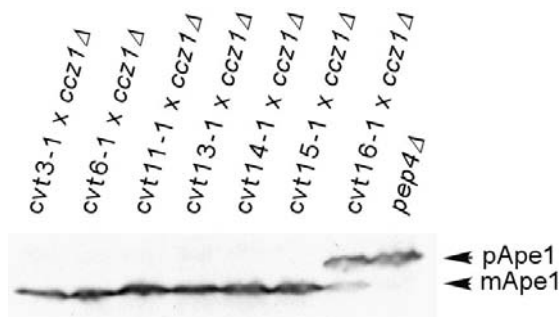
Figure 4-33 *CVT16* **is identical with** *CCZ1*. **"Unknown" Cvt mutants were conjugated with** *ccz1Δ* **and cultures were tested for the complementation of aminopeptidase I.** *cvt16-1* **did not complement the defect in** *ccz1Δ*, **they are therefore allelic.** *pep4Δ* **was used as a control for immature Ape1.**

4.3.2 Vacuolar acidification of *ccz1Δ* cells is normal

The vacuolar acidification was examined in *ccz1Δ* cells to determine if the necessary pH for the proper formation of vacuolar proteases was given. These proteases, such as Ape1, are unable to degrade proteins and break down autophagic vesicles within the vacuole when the pH is not acidic (63). This was therefore checked to determine if this is a cause for the defect in the maturation of Ape1. Quinacrine is a fluorescent dye that accumulates in acidic vacuoles (89). Wild type, *vma1Δ* and *ccz1Δ* cells were investigated under stationary and starvation conditions after incubation with quinacrine. *VMA1* is a subunit of the vacuolar H(+)-ATPase. Its deletion inactivates the membrane v-ATPase and leads to a non-acidic vacuole. As seen in *Figure 4-34* though *ccz1Δ* has fragmented vacuoles these show normal vacuolar uptake of the dye quinacrine indicating that vacuolar acidification is not the cause of the inability to mature aminopeptidase I.
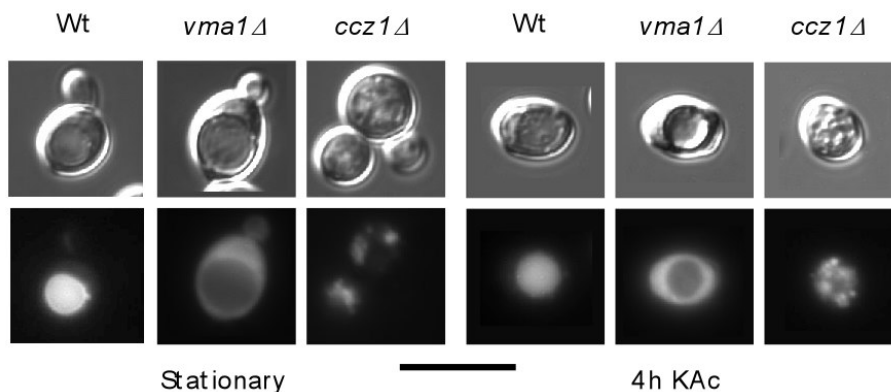
Figure 4-34 Vacuolar acidification of *CCZ1* **deleted cells is normal. WT is the wild type and** *vma1Δ* **has a defective v-ATPase subunit. Though** *ccz1Δ* **has fragmented vacuoles, these vacuoles are stained by the dye quinacrine which fluoresces in an acidic enviroment. Bar 10 μm.**

4.3.3 Both *CCZ1* and *MON1* deleted cells cannot sporulate

Autophagy is a process by which under starvation conditions the cell can glean energy to survive by breaking down proteins in the vacuole. Sporulation is a process that yeast cells also undergo when they recognize that the nutrients needed to grow are missing over longer periods of time. Diploid cells can convert themselves into four ascospores called asci or a tetrad. In cells defective in autophagy this sporulation process is impeded; the cells do not have enough energy to undergo sporulation.
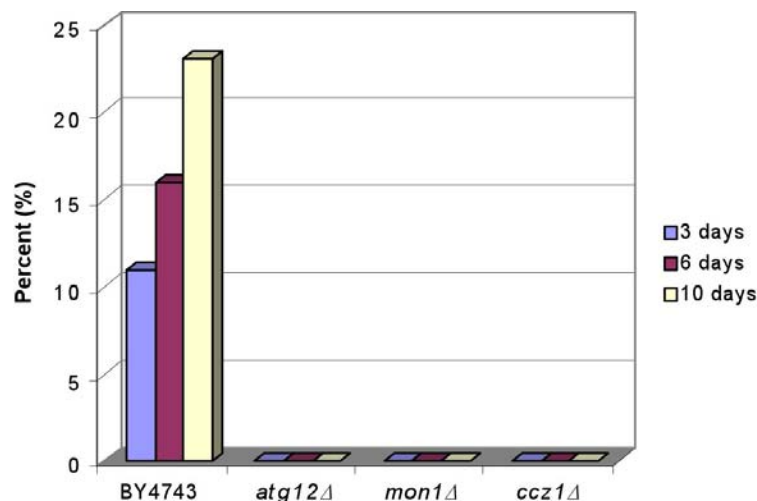
Figure 4-35 Both *MON1* and *CCZ1* deficient cells cannot sporulate. Cells were shifted to 1 % potassium acetate and samples were examined under the microscope for tetrads after 3, 6 and 10 days. The percentage was determined by the number of tetrads counted compared to the total number of cells scored. BY4743 was the wild type strain and *atg12Δ* is a known to play a role in autophagy.

Cells lacking *MON1* and *CCZ1* were examined for their ability to sporulate, along with the wild type BY4743 and *atg12Δ* cells. Like *atg12Δ*, *ccz1Δ* and *mon1Δ* cells were unable to form a single tetrad (*Figure 4-35*). This is a good indication that autophagy is completely impaired in these strains, keeping in mind that when only the related Cvt pathway is blocked, as in *atg21Δ* cells, some tetrads still form.

4.3.4 Autophagic bodies are not present in starved *mon1Δ* and *ccz1Δ* cells

As with *ATG18* and *ATG21*, *CCZ1* and *MON1* were chromosomally deleted in the WCG background to assist in their examination. WCG is a helpful background for experiments such as the vesicle test, because the vacuole tends to be slightly larger and can be clearly seen under the light microscope. Using a PCR fragment constructed from the plasmid pUG6 and the oligonucleotide pairs s-MON1/ as-MON1 and s-CCZ1/ as-CCZ1 the *MON1* and *CCZ1* genes were respectively deleted in the WCG background.

The knockouts were tested for their inability to mature Ape1 and the presence of fragmented vacuoles. Both strains YKMW7 (*ccz1Δ*) and YKMW2 (*mon1Δ*) were controlled by Southern blot analysis (not shown).
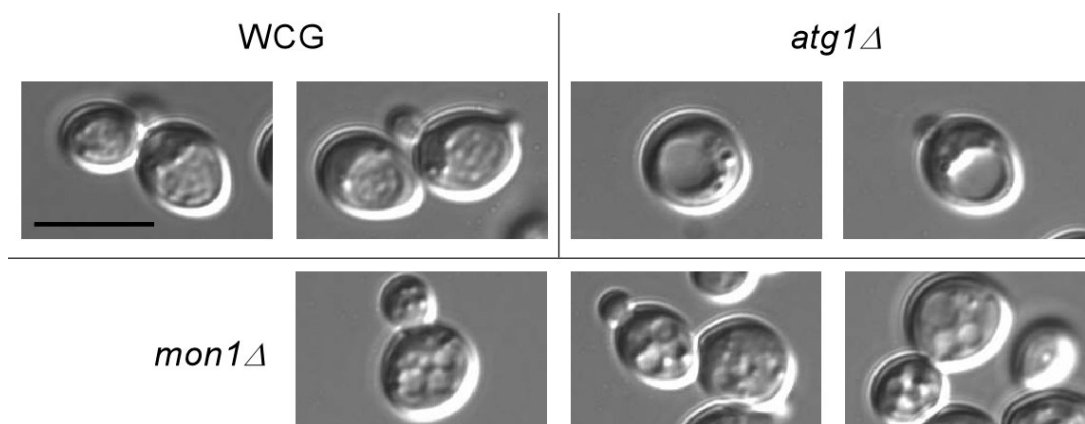
Figure 4-36 *mon1Δ* cells shows no formation of autophagic bodies. Wild type (WCG), *atg1Δ* and *mon1Δ* cells were starved for 4 h in SD(-N) starvation media containing the proteinase B inhibitor PMSF. *mon1Δ* cells contained fragmented vacuoles, but no autophagic bodies were observed within them, as seen in the wild type. *atg1Δ* cells cannot form autophagosomes or Cvt vesicles, therefore the vacuoles of these cells remain empty.

The so called "vesicle test" was carried out with the cells from the wild type (WCG), *atg1Δ*, *ccz1Δ* and *mon1Δ*. This involved shifting the cells to a starvation medium containing the proteinase B inhibitor phenylmethylsulfonyl fluoride (PMSF). Under these conditions the wild type collects autophagic bodies within its vacuole. The vesicles, only visible because the inhibited proteinase B is unable to lyse the autophagic bodies, are seen "dancing" around the vacuole due to Brownian movement. In the control strain *atg1Δ*, autophagosomes are not formed and therefore they cannot be present within the vacuole. The characteristic fragmented vacuoles of *mon1Δ* and *ccz1Δ* are easily seen under the microscope using Nomarski optics. Autophagic bodies were not seen within *ccz1Δ* (not shown) and *mon1Δ* cells (*Figure 4-36*) during the vesicle test.

4.3.5 In *mon1Δ* and *ccz1Δ* cells aminopeptidase I is not accessible to extraneous proteases

A proteinase protection assay was utilized to determine whether or not aminopeptidase I was property enclosed by a vesicular membrane. Proaminopeptidase I is transported to the vacuole within Cvt vesicles during vegetative conditions and in autophagosomes during periods of starvation. After the vesicle or autophagic body is lysed within the vacuole, proaminopeptidase I is matured to its active form. This transport and processing is examined in the protease protection assay. When pro-Ape1 is not recruited and enclosed within these cargo-vesicles it is accessible to extraneously added proteases

and is processed to a pseudo-matured state. On the other hand, if the packaging of pro-Ape1 occurs normally, then aminopeptidase I remains in the pro-form. *mon1Δ* and *ccz1Δ* were compared to the strains *atg1Δ* and *ypt7Δ*. In *atg1Δ* cells Ape1 is accessible to proteases as seen in *Figure 4-37* in lane 5. Cells without *ATG1* cannot form Cvt vesicles or autophagosomes; therefore pro-Ape1 remains within the cytosol and is not protected. In *ypt7Δ* cells both Cvt vesicles (Part A, lane 5) and autophagosomes (Part B, lane 5) are properly formed, nevertheless pro-Ape1 is not properly processed because these cargo-vesicles remain outside of the digestive vacuole. Cells lacking *MON1* and *CCZ1* were found to be similar to *ypt7Δ* cells.
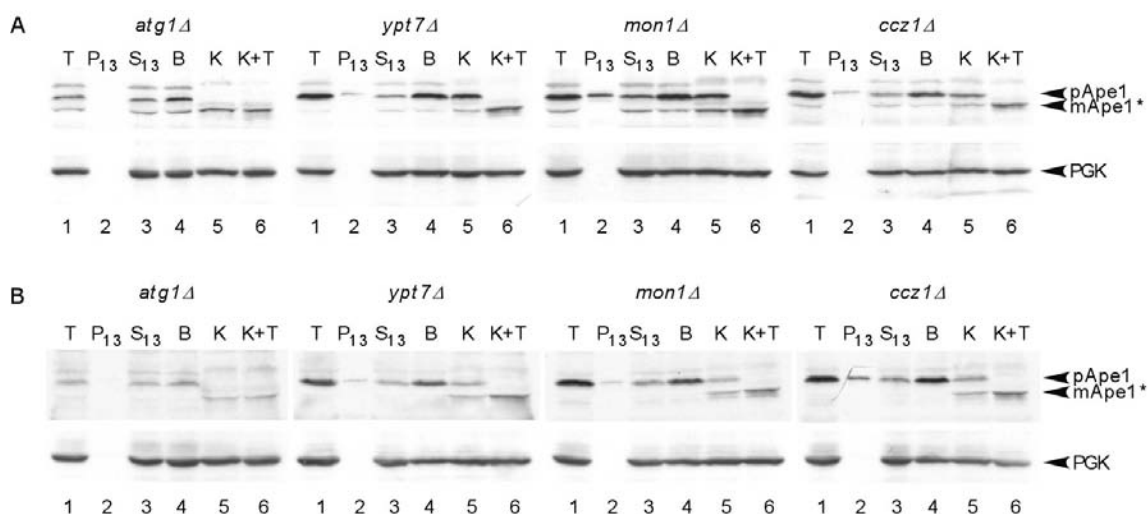
Figure 4-37 In both *mon1Δ* and *ccz1Δ* cells aminopeptidase I (Ape1) is contained within protective Cvt vesicles and autophagosomes as examined in a protease protection experiment. Hypotonically lysed cells were examined in the stationary phase (A) and after 4h of starvation (B) for the accessibility of proApe1 to extraneously added proteinase K. In *atg1Δ* Cvt vesicles and autophagosomes are absent; cytosolic proApe1 is accessible to proteases. In *ypt7Δ* all transport vesicles are blocked from entering the vacuole; proApe1 is protected within these vesicles. Three aliquots of each strain were treated simultaneously. In the first, used as a control, equal amounts of lysate was mixed with buffer (B, lanes 4). In the second, lysate was mixed with an equal amount of proteinase K solution (K, lanes 5). In the last aliquot, lysate was mixed with proteinase K and triton X-100 (K+T, lanes 6). Protected proteins can be accessed by proteases because triton X-100 is a detergent that disrupts membranes. *mon1Δ* and *ccz1Δ* show similarities to *ypt7Δ* cells; proApe1 is protected within Cvt vesicles (A) and autophagosomes (B). In lanes 1 (T) a sample of the total amount of cell material is shown. An equal amount of lysate was centrifuged at 13,000 xg yielding a pellet fraction (P$_{13}$, lanes 2) and a supernatant fraction (S$_{13}$, lanes 3). In these fractions, immunoblotting against PGK was important in order to exclude the possibility of contaminating whole cells. Ape1, a vacuolar hydrolase, is pseudo-matured by proteinase K as indicate by mApe1*.

4.3.6 Pho8Δ60 is not activated during the ALP Assay in *ccz1Δ* and *mon1Δ* cells

Autophagic ability can be measured through an activity test, termed the ALP assay. Developed by Noda *et al.* (94) it uses the measurability of the activation of the enzyme alkaline phosphatase (ALP). The first step is the deletion of the native ALP protein

Pho8. An inactive Pho8 is generated. Due to a signalling sequence it is targeted to the vacuole were it is processed and activated. *PHO8* was deleted from the wild type, *atg15Δ*, *mon1Δ* and *ccz1Δ* strains using homologue recombination. The deletion fragment, created from the *pho8Δ::LEU2* plasmid pGF10 (75) cut with the enzymes Stu1 and BamH1, was transformed into YKMW7 (*ccz1Δ*) and YKMW2 (*mon1Δ*) this yielded the strains YKMW20 (*ccz1Δ pho8Δ*), YKMW22 (*mon1Δ pho8Δ*), respectively. The strains *atg15Δ pho8Δ* (YUE63) and *pho8Δ* (YUE66) were created similarly by U. Epple.

These *pho8Δ::LEU2* strains were transformed with the Pho8Δ60 expression plasmid pCC5 (76) and the ALP assay performed. The ALP assay utilizes the phosphatase activity of Pho8 to activate a fluorophore, whose increase in fluorescence can be photometerically measured. Unlike the wild type (WCG), *ccz1Δ* and *mon1Δ* cells show no activation of the truncated alkaline phosphatase over a period of four hours, *Figure 4-38*. This lack of activity indicates that the autophagic process is fully impaired as in *atg15Δ* cells.
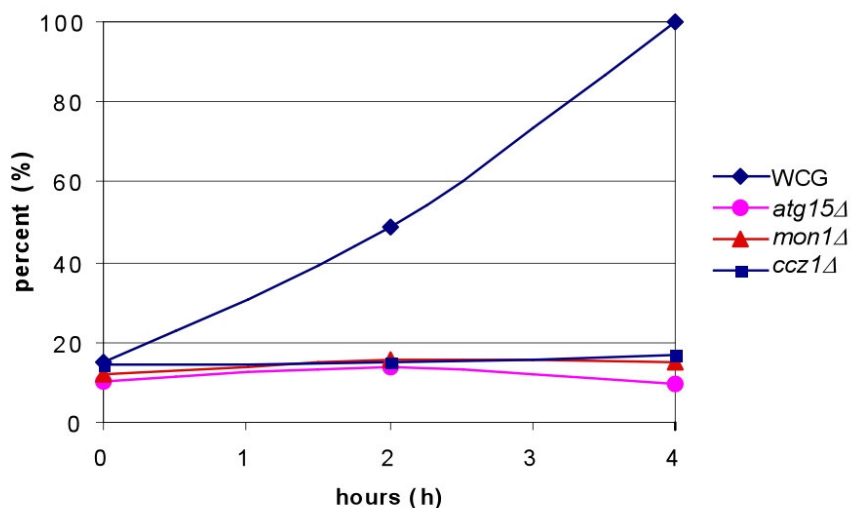
Figure 4-38 The ALP assay: *mon1Δ pho8Δ* and *ccz1Δ pho8Δ* cells are unable to transport Pho8Δ60 to the vacuole for activation. This indicated that like in *atg15Δ pho8Δ* cells autophagy is impaired. In the mutants to be investigated, the vacuolar alkaline phosphatase gene (*PHO8*) was deleted. These strains were then transformed with the truncated form Pho8Δ60, which remains in the cytosol. The truncated form can only be activated after it is transported to the vacuole by autophagy. In the vacuole it is matured and activated. The ALP activity in the wild type (WCG) was defined as 100 percent activity.

4.3.7 GFP-Atg8 exists as fluorescent points outside of the vacuole

Atg8 is another cargo protein of autophagy. Atg8 is involved in the biogenesis of Cvt vesicles and autophagosomes. In an ubiquitin like conjugating system Atg8 is covalently bound to the lipid phosphatidylethanolamine and is integrated into the inner and outer membrane of Cvt vesicles and autophagosomes. Atg4 removes excess Atg8 found outside of the completed transport vesicles, but Atg8 trapped inside the vesicles is transported into the vacuole where it is degraded. By observing the fluorescently tagged Atg8, GFP-Atg8, more information on the degree of blockage that occurs in *ccz1Δ* and *mon1Δ* cells can be gleaned. GFP-Atg8 expressed under the control of its native promoter from a centromeric plasmid was transformed into the wild type, *ypt7Δ*, *ccz1Δ* and *mon1Δ* cells.
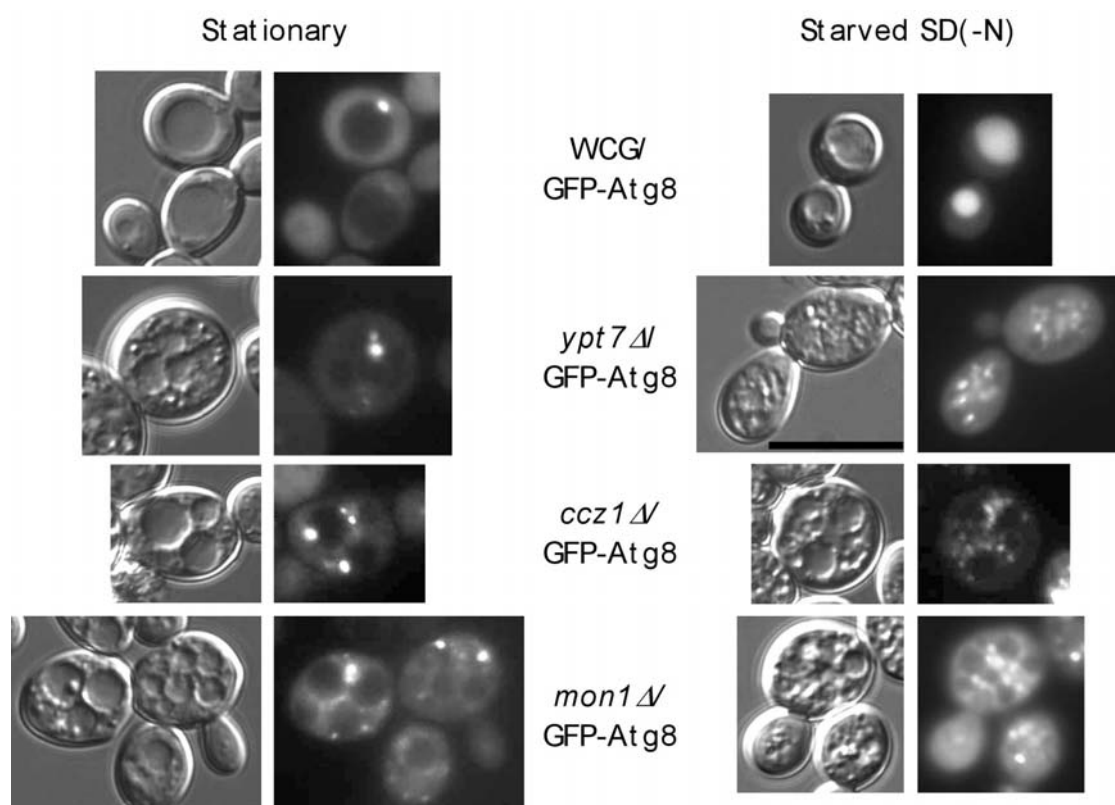
Figure 4-39 GFP-Atg8 transformed into the above cells was observed under stationary and starvation conditions. The within the pairs the left image was taken using Nomarski optics and the right with fluorescence. In wild type (WCG) cells GFP-Atg8 is formed in the cytosol and concentrates at the point-like PAS. After starvation GFP-Atg8 is integrated into the membrane of autophagosomes and is transported into the vacuole. There the autophagosome is degraded releasing the protease resistant GFP protein; this is seen to accumulate in the vacuole. In starved *ypt7Δ*, *ccz1Δ* and *mon1Δ* cells GFP-Atg8 accumulated in punctated structures outside of the vacuoles. Bar 10µm

Using fluorescent microscopy GFP-Atg8 was observed under vegetative and starvation conditions within these strains, *Figure 4-39*. In vegetative wild type cells GFP-Atg8 is seen in the cytosol and concentrated at the PAS. When these cells are starved the fluorescent GFP-Atg8 is transported into the vacuole and free GFP accumulates there. GFP is fairly protease resistant. In *ypt7Δ* cells the fusion of transport vesicles with the vacuole is impaired, therefore, GFP-Atg8 remains outside of the vacuole. This is clearly seen in starved cells. There many autophagosomes accumulate outside of the vacuole but the vacuole itself remained unstained. *MON1* and *CCZ1* deleted cells also shared with *ypt7Δ* its characteristic fragmented vacuoles. This gives us some insight that *CCZ1* and *MON1* may be involved in the fusion of smaller vacuoles, Cvt vesicles and autophagosomes with the vacuole.

4.3.8 In Western blot analysis GFP-Atg8 is not degraded in *ccz1Δ* and *mon1Δ* cells

Observing GFP-Atg8 in *ccz1Δ* and *mon1Δ* cells using Western blot analysis also revealed how disturbed the autophagic process was. The accumulation of GFP set free through the degradation of GFP-Atg8 is an indicator that autophagosomes enter the vacuole and are lysed normally. The strains examined were transformed with the centromeric plasmid GFP-Atg8 under the control of its native promoter. In *Figure 4-40*, GFP-Atg8 is induced normally in the wild type (WCG). GFP-Atg8 is transported into the vacuole and degraded increasingly with each hour of starvation. With each increment more GFP is released. In the following strains, autophagy is inhibited. *ATG18* is known to have an autophagic defect and *YPT7* is known to play a role in the docking and fusion of all transport vesicles with the vacuole. When these genes are missing autophagosomes are unable to be transported into the vacuole, thus GFP is not released from Atg8 through degradation. In cells lacking *CCZ1* and *MON1* a similar defect in autophagy is seen.
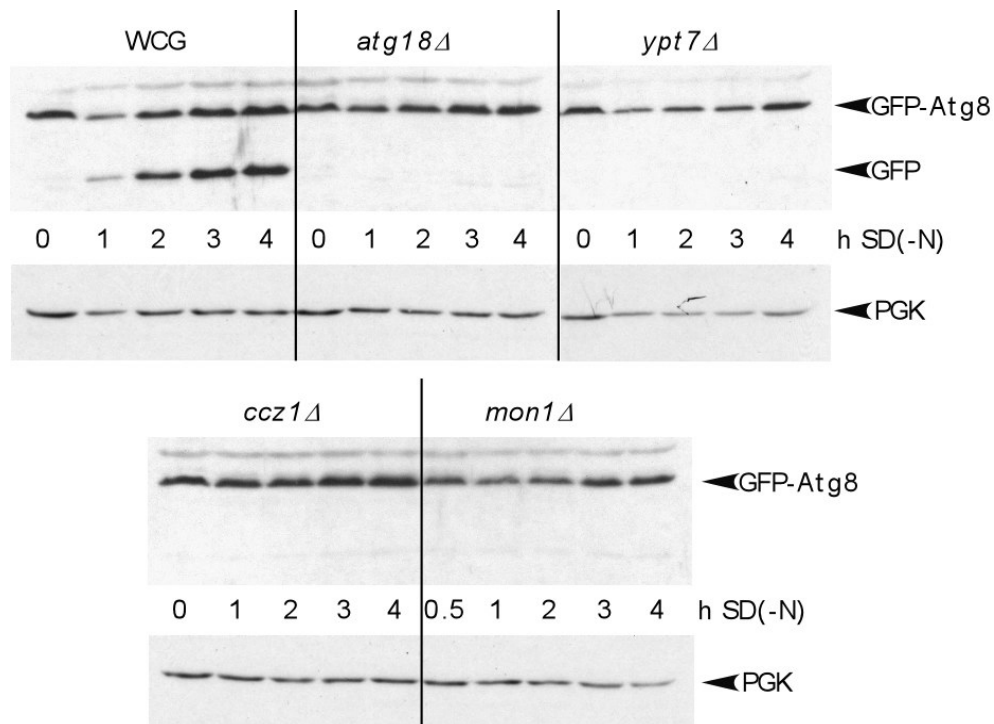
Figure 4-40 GFP-Atg8 degradation: Strains transformed with GFP-Atg8 expressed under the control of its native promoter were shifted to SD(-N) starvation media. After the indicated intervals samples were harvested and processed for immunoblotting. The membrane was probed with anti-GFP antibodies and anti-PGK antibodies. PGK was shown as a loading control. The wild type (WCG) transported autophagosomes normally to the vacuole, where they were degraded, setting free the fairly protease resistant GFP. *atg18Δ*, *ypt7Δ*, *ccz1Δ* and *mon1Δ* cells all showed a defect in the transport of GFP-Atg8 into the vacuole. Though GFP-Atg8 was expressed normally, it was not degraded indicated by the absence of free GFP.

4.4 *ATG23* and *TRS85* two genes also involved in the Cvt pathway

4.4.1 *TRS85/ GSG1* (78)

4.4.1.1 *TRS85* deleted cells show a block in the maturation of aminopeptidase I during vegetative conditions

Originally, *GSG1/YDR108W* was discovered and termed *general sporulation gene 1* because diploid cells lacking Gsg1 fail to sporulate (101). We found *GSG1* in the phloxin screen and identified it after the aminopeptidase I screen. A deletion strain in the genetic background WCG was created integrating a PCR fragment formed from the plasmid pUG6 and the oligonucleotide primers s-GSG1 and as-GSG1. The knockout YKMW1 was confirmed through Southern blot analysis. *gsg1Δ* cells are unable to mature proaminopeptidase I during vegetative conditions where the Cvt pathway is active, see *Figure 4-41*. The absence of *GSG1*, though, did not have an affect on the

transport and maturation of carboxypeptidase Y or proteinase B, the enzyme needed to lyse Cvt vesicles and autophagosomes. Pep4 activates PrB, when it is missing pApe1 remains within unlysed Cvt vesicles and autophagosomes.
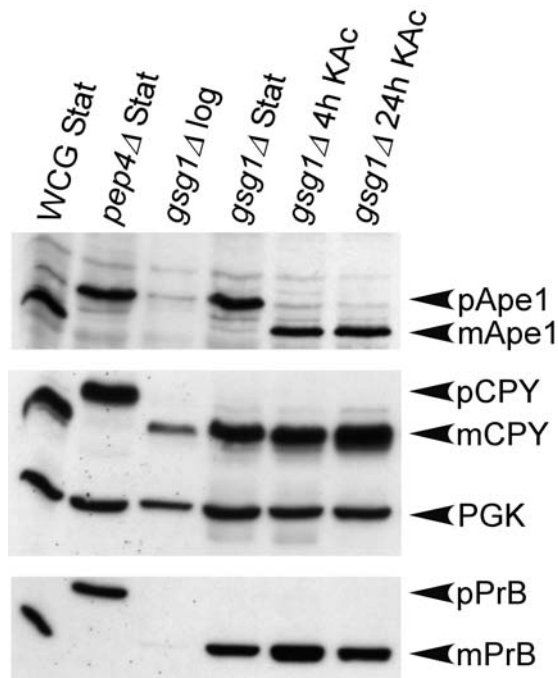
Figure 4-41 The maturation of aminopeptidase I (Ape1) in *gsg1Δ* cells is impaired during vegetative conditions (log, Stat). The maturation of carboxypeptidase Y (CPY) and proteinase B (PrB) are not influenced by the deletion of *GSG1*. The wild type (WCG) matures Ape1 normally were as in *pep4Δ* cells the maturation of Ape1 is blocked at the activation step. PGK is a cytosolic protein used as a control for the amount of protein loaded onto the gel.

As noticed in *atg21Δ* cells after shifting to starvation media, *gsg1Δ* cells have a delay in the maturation of Ape1 which is not seen the wild type, *Figure 4-42*.
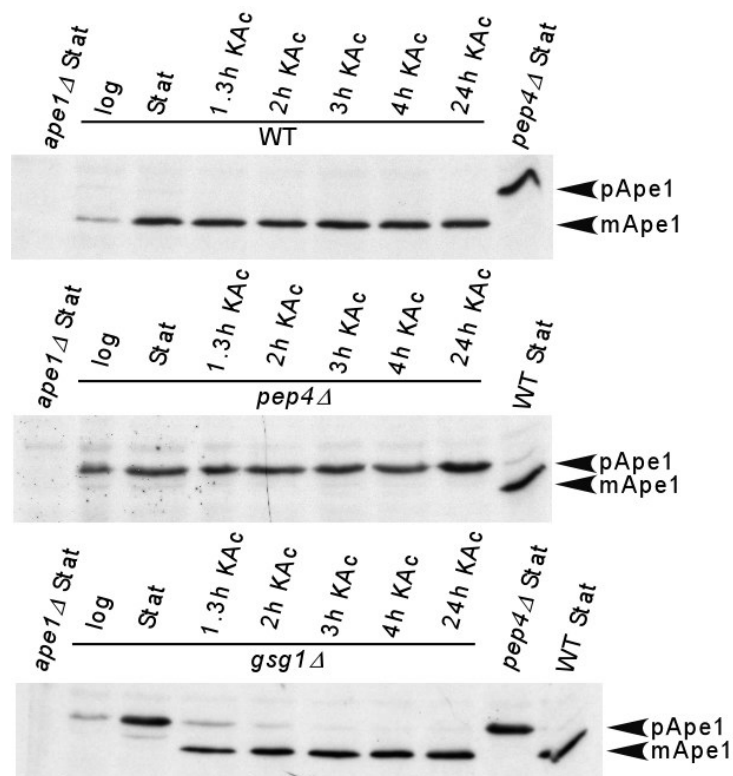
Figure 4-42 *gsg1Δ* cells mature aminopeptidase I slower than the wild type (WT) after shifting to starvation media. The wild type, *pep4Δ* and *gsg1Δ* cells were grown to and aliquots were taken from the logarithmic and stationary phases. The remaining stationary cells were shifted to potassium acetate (KAc) and aliquots were removed at the indicated times. All aliquots were processed for immunoblotting and probed with Ape1 antibodies.

4.4.1.2 Viable TRAPPs

GSG1 is also known under the name *TRS85*. The name *TRS85* comes from it being a 85 kDa component of the TRAPP I and II complex involved in the ER-to-Golgi and Golgi transport (102). Since *GSG1/TRS85* was shown to have a complete blockage in the maturation of aminopeptidase I during vegetative conditions, it was logical to check the remaining viable TRAPPs for their involvement in the Cvt and or autophagic pathways. *TRS33* and *TRS65* along with *GSG1/TRS85* deleted cells were grown to stationary phase and then shifted to SD(-N) starvation medium for four hours. The cells were then prepared for Ape1 immunoblotting. The results in *Figure 4-43* show that in *trs33Δ* and *trs65Δ* cells there is little to no blockage in the maturation of Ape1. These TRAPP genes unlike *TRS85* have no influence on the Cvt pathway or autophagy.
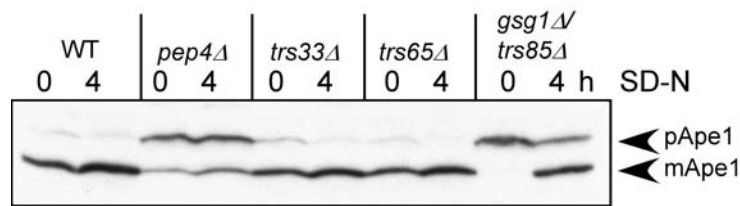
Figure 4-43 Of the viable proteins in the TRAPP complexes, the maturation of Ape1 is only impaired in *trs85Δ* cells. The indicated strains were grown to stationary phase and then shifted to SD(-N) starvation medium. Aliquots were removed at the indicated times. The maturation of Ape1 is minimally affected by deletion of the TRAPP genes *TRS33* and *TRS65* compared to the deletion of *TRS85/GSG1*.

4.4.1.3 Cross complementation

As in the case of *MON1* and *CCZ1*, the *TRS85* deletion strain was conjugated with "unknown" Cvt deletion strains and examined for non-complementing aminopeptidase I maturation. *TRS85* was not allelic to any of the "unknown" Cvt strains. All conjugations produced strains that matured Ape1.

4.4.1.4 Vacuolar acidification in *trs85Δ* is normal

An acidic vacuolar pH is one criterion that vacuolar proteases need to mature and process proteins. Aminopeptidase I is a vacuolar proteases, therefore the vacuolar acidification was examined to determine if the block in maturation was caused by inadequate acidification in *trs85Δ* cells. In *Figure 4-44*, *vma1Δ*, wild type (WCG) and *trs85Δ* cells were treated with the dye quinacrine. Quinacrine is transported into acidic vacuoles. In *vma1Δ* cells, a subunit of the (H+) vacuolar ATPase is deleted, thus inhibiting the acidification of the vacuole. In *TRS85* deleted cells the vacuolar pH is normal under both the stationary and starved (4h KAc) conditions.
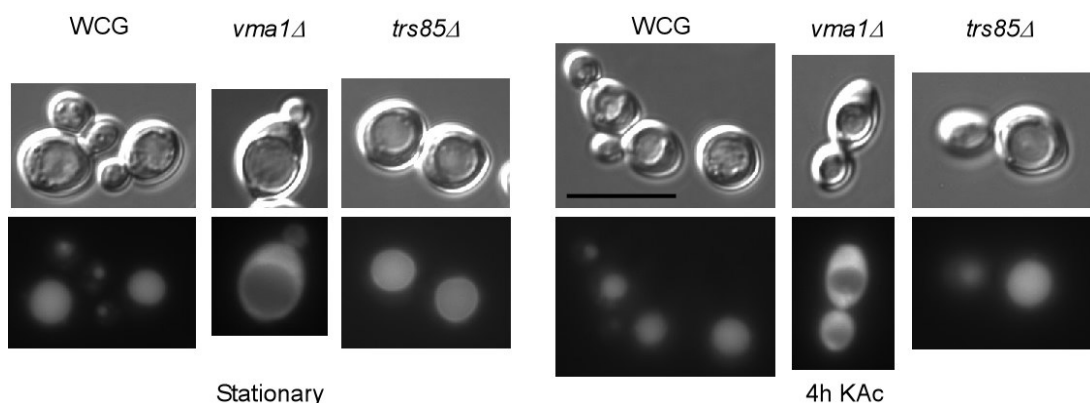
Figure 4-44 The vacuolar uptake of the dye quinacrine is a good indicator that a strain has a correct vacuolar acidification. This is seen in the wild type (WCG) and in *trs85Δ* cells during stationary phase and after 4 hours of starvation. *vma1Δ* is missing a subunit of the vacuolar ATPase which pumps protons into the vacuole; the vacuole is therefore not acidic.

4.4.1.5 In *TRS85* deleted cells autophagic bodies accumulate within the vacuole
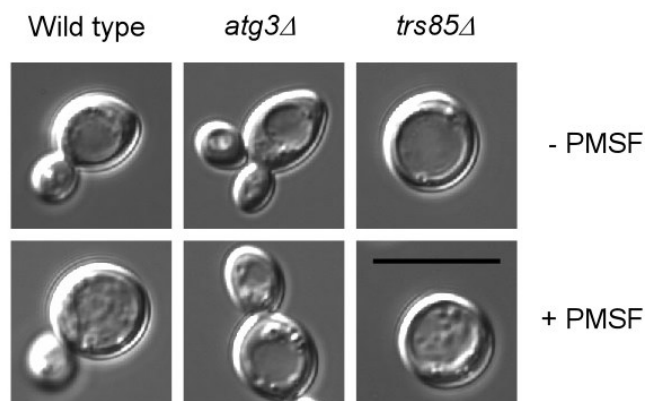
Figure 4-45 Autophagy is functional in *trs85Δ* cells as indicated by the accumulation of autophagic bodies within the vacuole after starving in media containing PMSF. PMSF (phenylmethylsulfonyl fluoride) prevents autophagic bodies from being lysed in the vacuole. In the absence of PMSF autophagic bodies are degraded normally. The absence of *ATG3* influences the formation of autophagosomes. In *atg3Δ* cells the vacuole remains empty for lack of autophagic body formation both with and without PMSF.

The accumulation of autophagic bodies in the vacuole after the addition of the protease B inhibitor PMSF indicates that autophagy is functioning properly; this is seen in *Figure 4-45* in the wild type and in *trs85Δ* cells. The strains were grown and shifted to starvation media. The absence of autophagic bodies when PMSF is not added is proof that autophagic bodies are properly lysed. Both the wild type and *trs85Δ* cells degrade autophagic bodies normally. *atg3Δ* is an example of a strain that influences the formation of autophagosomes. Here autophagic bodies are absent with and without PMSF.

4.4.1.6   Sporulation in *trs85Δ* cells is reduced
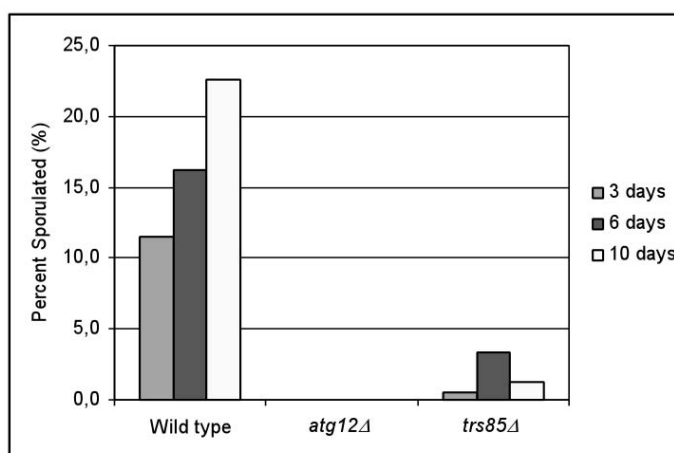
Figure 4-46 The sporulation of *trs85Δ* cells is reduced compared to the wild type. Atg12 is an important part of the autophagic process without it cells do not have enough energy to sporulate.

The inability to produce spores (tetrads) is a phenotype of strains with an autophagic defect. It is thought that without autophagy yeast cells cannot produce enough energy to sporulate. Without the ability to sporulate these cells have a reduced survival under stress conditions such as starvation. Stationary cells were shifted to starvation medium and examined under a light microscope after 3, 6 and 10 days. The amount of tetrads and dyads were scored and the percentage determined compared to the total cells counted. The wild type shows a steady increase in the percentage of spores (*Figure 4-46*), whereas in the autophagy mutant *atg12Δ* spores were completely absent. In *trs85Δ* cells sporulation was significantly reduced as also seen in *atg21Δ* cells. *TRS85* was identified for its inability to sporulate (101), this small difference in reduced sporulation or inability to sporulate may be dependent on our method of scoring spores. Here tetrads and dyads were counted as spores. This reduced ability to sporulate was also noted in Engelbrecht *et al*, 1998 (103).

4.4.1.7 In a protease protection experiment aminopeptidase I was accessible to extraneously added proteases in *trs85Δ*

Aminopeptidase I is transported to the vacuole inside Cvt vesicles during vegetative conditions and in autophagosomes during periods of nutrient limitation. The protease protection assay is a simplified means of determining whether or not proApe1 is contained within these transport vesicles. Like with the previous novel genes, stationary *trs85Δ* cells were treated with proteinase K along with *atg1Δ* and *ypt7Δ* as controls. Cells were spheroplasted and hypotonically lysed and three aliquots of lysate were mixed with equal amounts of buffer (lane 4), protease K (lane 5) and protease K containing triton X-100 (lane 6), seen in *Figure 4-47*. Aminopeptidase I is normally transported to the vacuole within protective transport vesicles, called Cvt vesicles during vegetative conditions. When these vesicles are not formed as in the case of *atg1Δ*, proApe1 (pApe1) is accessible to externally added proteases and is pseudo-matured (m*Ape1). In *ypt7Δ* cells, aminopeptidase I is protected within these vesicles. Ape1 is not degraded because vesicles in *ypt7Δ* cells are unable to merge with the vacuole trapping proApe1 within them. When triton X-100 is added to the mixture membranes are disassociated, this accesses proApe1 to proteases causing it to become pseudo-matured (lane 6). *TRS85* deleted cells behaved similarly to *atg1Δ* cells; proApe1 is accessible to added proteinase K. This indicates that either Cvt vesicles are not formed or Ape1 is located outside of these Cvt vesicles.
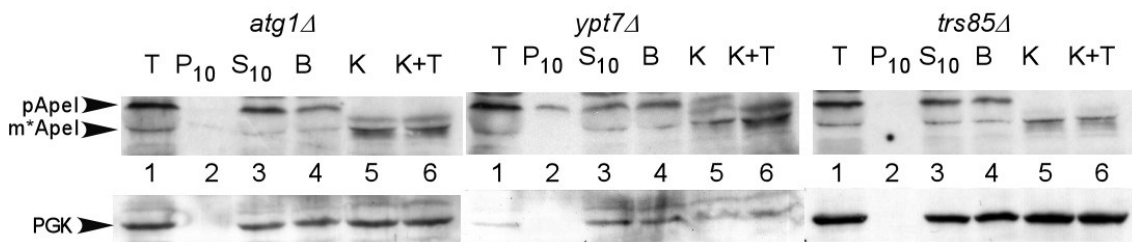
Figure 4-47 In a protease protection assay Ape1 is accessible to extraneously added proteinase K in *trs85Δ* **cells.** *atg1Δ*, *ypt7Δ* **and** *trs85Δ* **cells were spheroplasted divided into four aliquots and subjected to centrifugation by 10,000 xg (T, S_{10}, P_{10}: lanes 1-3), buffer (B: lanes 4), proteinase K (K: lanes 5) and to proteinase K plus triton X-100 (K+T: lanes 6).** *atg1Δ* **unable to form completed vesicles allows Ape1 to be accessible to cleavage by proteinase K.** *YPT7* **participates in the fusion of vesicles with the vacuolar membrane.** *ypt7Δ* **vesicles cannot enter the vacuolar lumen and Ape1 remains unmodified when proteinase K is present. In lane 5 of** *trs85Δ* **cells are accessible to proteinase K digestion. pApe1 is pro-Ape1 and Ape1* is a digested form of Ape1, but not necessarily the mature Ape1-form. PGK is shown as a spheroplasting and loading control. If the cells were not completely spheroplasted, PGK would be pelleted in whole cells in P_{13}.**

As in the case of YKMW19 (*atg21Δ ypt7Δ*), *YPT7* was deleted in *trs85Δ* cells using the *ypt7::HIS3* deletion plasmid yielding YKMW18 (*trs85Δ ypt7Δ*). The epistatic protease protection assay, *Figure 4-48*, was performed only in stationary cells, because *trs85Δ* contains only mature Ape1 after four hours of starvation. The epistatic assay gives insight into whether or not the pseudo-maturation of Ape1 occurs inside or outside of the vacuole. In all strains deleted in *YPT7* Cvt vesicles and autophagosomes remain outside of the vacuole. In stationary *ypt7Δ* cells completed Cvt vesicles protect proApe1 from extraneously added proteases. In stationary *atg3Δ ypt7Δ* Cvt vesicles are not formed and proApe1 is found in the cytosol where it is accessible to extraneously added proteases. ProApe1 in stationary *trs85Δ ypt7Δ* cells is accessible to extraneously added proteinase K (lane 5), indicating a possible defect in the formation of Cvt vesicles or closed Cvt vesicles.
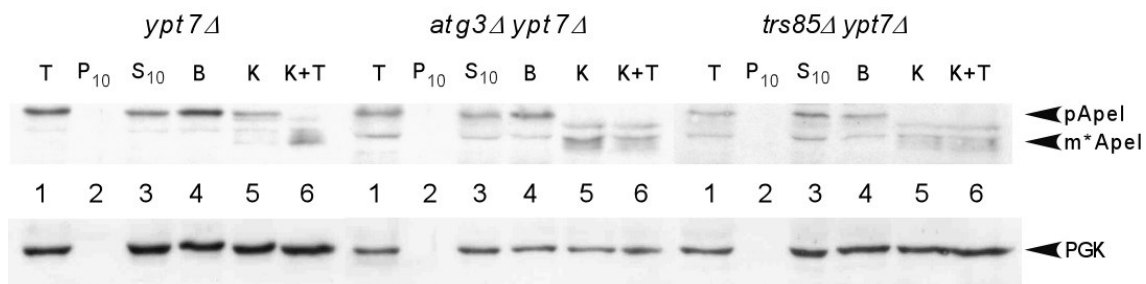
Figure 4-48 In an epistatic protease protection assay *trs85Δ ypt7Δ* **shows Ape1 pseudo-maturation. Lysed spheroplasts from** *ypt7Δ*, *atg3Δ ypt7Δ*, **and** *trs85Δ ypt7Δ* **were divided into five aliquots. The first, T (total, lane 1) shows the amount of protein per aliquot. The second aliquot was centrifuged by 10,000 xg and divided into P_{10} (pellet, lane 2) and S_{10} (supernatant, lane 3) fractions. The third fraction B (lane 4) was mixed with buffer. The forth aliquot (lane 5) was mixed with buffer containing proteinase K. The fifth aliquot (lane 6) was mixed with buffer containing proteinase K and triton X-100. The proteins were precipitated with TCA and processed for immunoblotting with Ape1 and PGK antibodies. pApe1 equals proApe1 and m*Ape1 is pseudo-matured Ape1.**

4.4.1.8 Autophagy is reduced in *trs85Δ* cells

The rate of autophagy can be quantified by utilizing the alkaline phosphatase (ALP) assay (94). This assay alters the original cytosolic to vacuolar pathway of alkaline phosphatase by truncating the vacuolar targeting sequence found in the first sixty base pairs of the PHO8 gene. In order to achieve this the chromosomal *PHO8* was deleted in the strains investigated and a plasmid carrying the truncated Pho8Δ60 was transformed. ALP is a vacuolar enzyme that remains inactive outside of the vacuole. This feature is the basis of the ALP assay. Autophagy sequesters its cargo unspecifically from the cytosol. Therefore the amount of ALP transported and activated in the vacuole is directly proportional to the rate of the autophagic process.
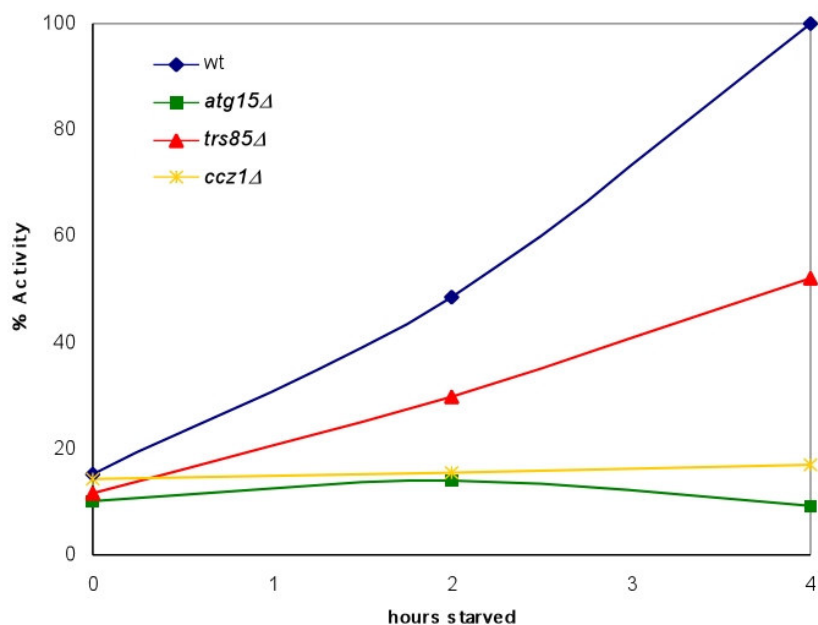
Figure 4-49 The autophagic rate was reduced by one half in *trs85Δ* cells. Strains lacking the original vacuolar *PHO8* gene but transformed with a cytosolic truncated version of it were compared in the alkaline phosphatase (ALP) assay. Pho8Δ60 remains inactive in the cytosol until it is transported via autophagy to the vacuole. The activity of the truncated ALP was measured after two and four hours of starvation. The activity of Pho8Δ60 is proportional to the autophagic rate. The amount of wild type activity was set to 100 % activity. *atg15Δ* and *ccz1Δ* are two genes known to affect autophagy.

The strains examined *pho8Δ* (wild type), *atg15Δ pho8Δ*, *ccz1Δ pho8Δ* and *trs85Δ pho8Δ* were all transformed with the pho8Δ60 plasmid and grown and shifted to starvation media. Before shifting, and after two and four hours of starvation H. Barth took samples of the cells being investigated and measured their alkaline phosphatase activity and the protein content. The amount of activity measured by the wild type was set to 100 %. Compared to the wild type in *Figure 4-49*, *trs85Δ* cells showed a decrease in the autophagic rate of approximately 50 %. *atg15Δ* cells are defective in the lysis of the

pho8Δ60 containing autophagic bodies and in *ccz1Δ* cells autophagosomes cannot fuse with the vacuole. Both of these control strains show no increase of the autophagic rate after autophagy is induced.

Another way to visualize the rate of autophagy is by observing the degradation of GFP-Atg8 in the cells being investigated. The wild type (WCG), *atg18Δ* and *trs85Δ* were transformed with the plasmid GFP-Atg8. Atg8 is a protein that is covalently attached to the inner and outer membrane of autophagosomes. After the autophagosome is completed Atg4 cleaves the Atg8 from the outer membrane. The Atg8 on the inner membrane is then transported with the autophagosome to the vacuole where it is degraded. Using the green fluorescent protein tag (GFP) to mark Atg8, the transport and degradation of GFP-Atg8 can be observed in Western blot analysis. The protease resistance of GFP aids the visualization, as one can observe and quantify the increase in the amount of free GFP.
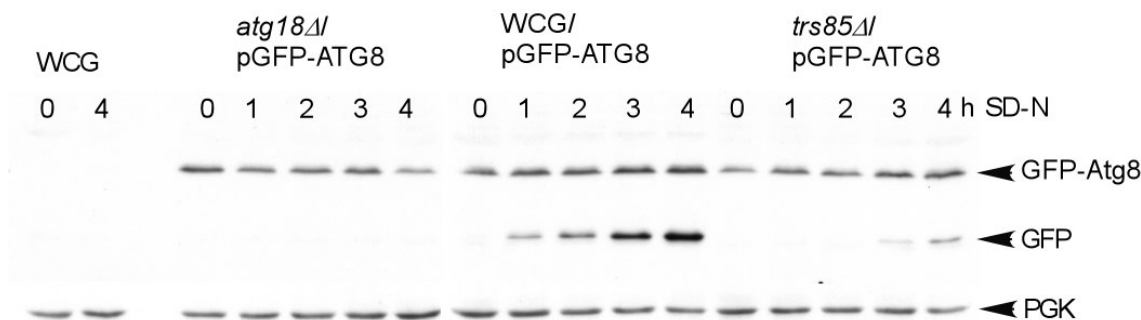
Figure 4-50 *trs85Δ* cells slowly transport and release GFP-Atg8 to the vacuole; autophagy is reduced. WCG (wild type), *atg18Δ* and *trs85Δ* cells were transformed with the plasmid GFP-Atg8 and samples were taken after the indicated times in SD(-N) starvation medium. The samples were processed for immunoblotting and probed with anti-GFP antibodies. The wild type degrades GFP-Atg8 continuously as indicated by the increase in free GFP over time. *atg18Δ* has a defect in autophagy and a degradation of GFP-Atg8 is not seen. The degradation of GFP-Atg8 in *trs85Δ* cells is delayed. Free GFP is first present after 3-4 hours of starvation. PGK was probed to examine the amount of protein loaded.

In *Figure 4-50* the strains were grown and shifted to SD(-N) medium and aliquots were taken hourly and processed for Western blot analysis. The aliquots of WCG (with and without the GFP-Atg8 plasmid), *atg18Δ* and *trs85Δ* were probed with anti-GFP and anti-PGK antibodies. In *atg18Δ* a defect in autophagy prevents Atg8-GFP from reaching the vacuole, thus no free GFP is observed. In wild type cells, a steady increase of free GFP is seen. In *trs85Δ* cells a release of GFP is only observed after 3-4 hours and the amount is dramatically reduced. This observation correlates with the reduced rate of autophagy seen in the ALP assay.

4.4.1.9 Localization of different GFP-tagged proteins to the preautophagosomal structure in *trs85Δ* cells

The preautophagosomal structure or PAS is the origin of autophagosomes and Cvt vesicles. This dot-like organelle is located at the vacuolar membrane. Proteins that comprise Cvt vesicles and autophagosomes collect at this point before forming the transport vesicle. Three proteins involved in the formation of Cvt vesicles and autophagosomes were chosen and localized with GFP-tagged versions, Atg9, Atg19 and Atg8.
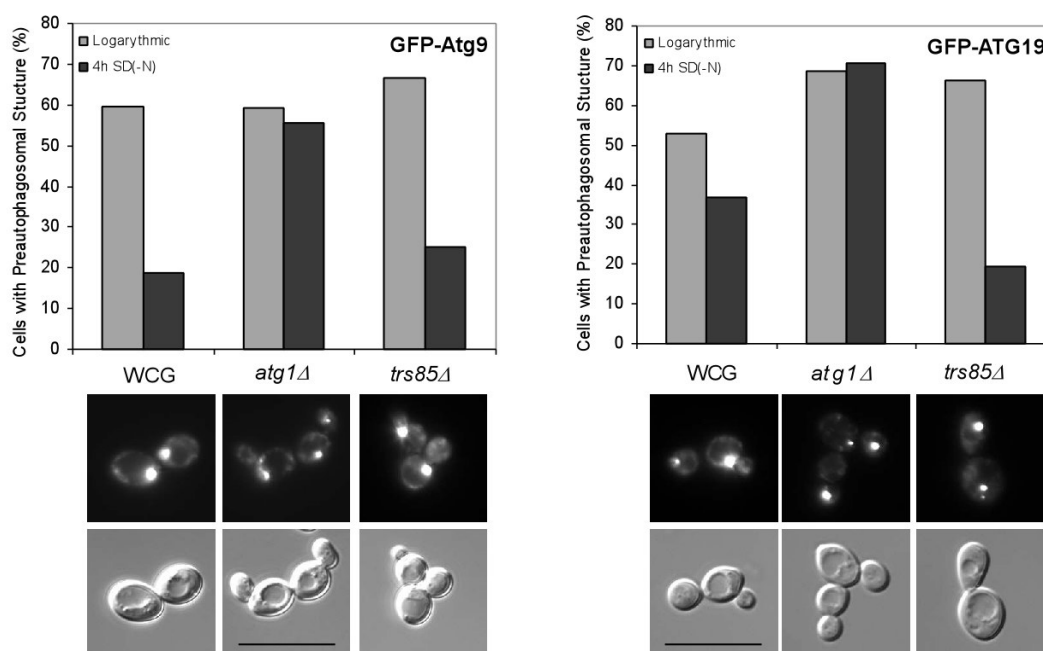
Figure 4-51 Growing *trs85Δ* cells recruit GFP-Atg9 (left) and GFP-Atg19 (right) to the PAS. The bar diagram show the results of scoring growing and starved cells where GFP-Atg9 or GFP-Atg19 are recruited to the preautophagosomal Structure (PAS). The percentage results from the number of cells with a fluorescent point on the vacuolar membrane compared to the total cells counted. In *atg1Δ* GFP-Atg19 is recruited to the PAS but due to a defect in autophagy GFP-Atg19 remains outside the vacuole. GFP-Atg9 in *trs85Δ* localizes to the PAS similar to the wild type. GFP-Atg9 counts remain high in starved *atg1Δ* cells because of a defect in the recycling of Atg9 from the PAS, bar 10 μm.

Atg9 is an integral membrane protein that is involved with the formation of both Cvt vesicles and autophagosomes. It localizes mainly to the PAS but also has a cytosolic portion (100). The percentage of cells with GFP-Atg9 at the PAS was determined in both growing and starved wild type, *atg1Δ* and *trs85Δ* cells, *Figure 4-51* (left). In 60-70 % of all growing strains GFP-Atg9 was localized to a point on the vacuolar membrane, the PAS. In starved cells the amount of GFP-Atg9 localizing to the PAS was reduced to about 20 % in the wild type and 25 % in *trs85Δ* cells. In starved *atg1Δ* cells the percentage remained high at 55 % due to a defect in the Atg1-Atg13 Atg9-recycling complex.

Atg19 is the receptor protein for Cvt complex (55). It localizes to the PAS and is then packed along with the Cvt complex into the transport Cvt vesicles or autophagosomes. GFP-Atg19 therefore collects at the PAS and is then transported into the vacuole. In the wild type free GFP is often seen as the vesicles are lysed in the vacuole (not shown). GFP-Atg19 that localized to the vacuolar membrane was tallied and presented as a percentage of the total cells counted, *Figure 4-51* (right). In growing wild type, *atg1Δ* and *trs85Δ* cells about 50-70 % of the cells had GFP-Atg19 at the PAS. In starved wild type and *trs85Δ* cells the percentage was dramatically reduced as GFP-Atg19 was transported via autophagy into the vacuole. In starved *atg1Δ* a decrease in the localization to the PAS was not seen because a defect in the formation of autophagosomes prevents GFP-Atg19 from being transported into the vacuole.
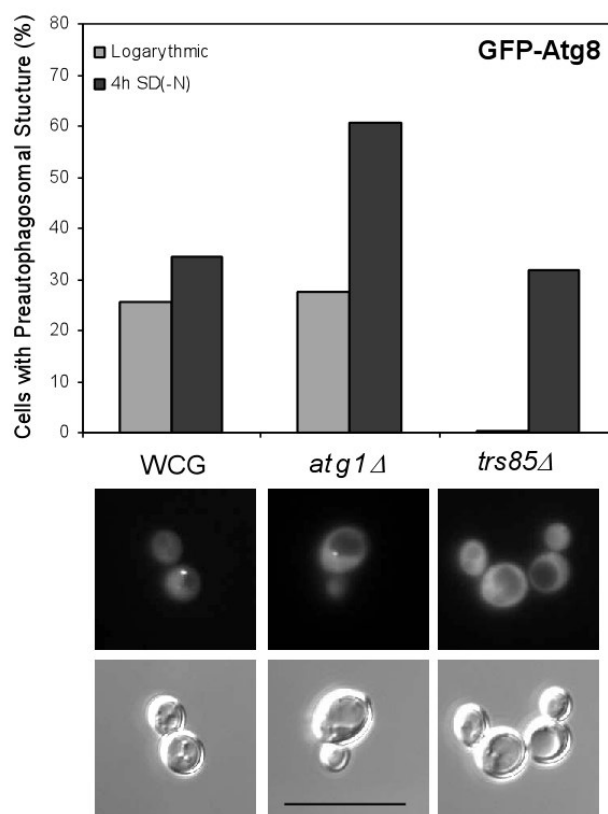
Figure 4-52 GFP-Atg8 does not localize to the PAS in vegetative *trs85Δ* cells. In growing and starved cells the percentage of cells with GFP-Atg8 at the vacuolar membrane was determined, as seen in the bar graph. In growing wild type and *atg1Δ* cells about 25 % of the cells had GFP-Atg8 located at the PAS, whereas in *trs85Δ* no accumulation of GFP-Atg8 was seen. In starving cells this defect was not seen and wild type accumulation of GFP-Atg8 was localized to the PAS. Photos show examples of growing cells, bar 10 μm.

GFP-Atg8 also accumulates at the PAS and is necessary for the formation of Cvt vesicles and autophagosomes. In about 25 % of the growing wild type and *atg1Δ* cells GFP-Atg8 was localized to the vacuolar membrane at the PAS, see *Figure 4-52*. In cells lacking *trs85Δ*, GFP-Atg8 was only seen cytosolically; no GFP-Atg8 was visualized as

a dot. After shifting to starvation medium normal values (about 30 %) of *trs85Δ* cells with GFP-Atg8 at the PAS were seen. In *atg1Δ* cells the percentage of cells with GFP-Atg8 at the PAS was elevated (60 %) due to the block in autophagosome formation and an accumulation of all PAS localized proteins.

4.4.1.10 The conjugation of Atg8 to phosphatidylethanolamine is normal in cells lacking *TRS85*

In a identical procedure to WCG, *TRS85* was knocked out in the genetic SEY6211 background using the same PCR fragment as in section 4.3.5. The product of the homologue recombination yielded YKMW28 (*SEY6211 trs85::KAN*) which was controlled by Southern blot analysis.
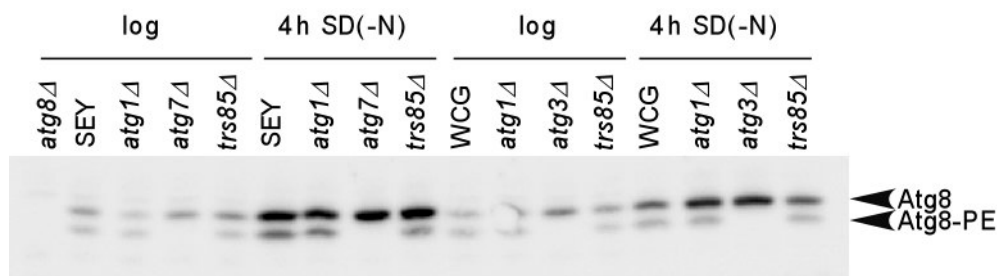
Figure 4-53 Cells lacking TRS85 have wild type amounts of Atg8-Phosphatidylethanolamine (PE). Logarithmic and starved cells were harvested, processed for immunoblotting and separated in a SDS-PAGE containing urea. Blots were then probed with antibodies against Atg8. Cells were examined in the genetic background SEY6211 and in WCG, but no differences in the formation of Atg8-PE was seen in *trs85Δ* cells compared to the wild type. *atg7Δ* and *atg3Δ* are directly involved in the conjugation of Atg8 to phosphatidylethanolamine.

Since the localization of GFP-Atg8 to the PAS was disrupted in *trs85Δ* an examination of a possible cause for this problem was carried out. Atg8 is part of a ubiquitin-like conjugation system. Atg8 is modified by Atg4, this activated form temporary coupled to its E1 enzyme Atg7. Atg7 conjugates Atg8 to Atg3, its E2 enzyme, where it is finally conjugated to phosphatidylethanolamine (PE) located in a membrane. This last step is the lipidation of Atg8.

The lipidation of Atg8 was examined in the genetic backgrounds WCG and SEY6211. *atg1Δ* a protein part of the signal switch between the Cvt pathway and autophagy was also examined. Deletion mutants of the E1 (*atg7Δ*) and E2 (*atg3Δ*) enzymes were examined as controls.

trs85Δ and the above mentioned strains were grown to logarithmic phase and also shifted to starvation media for four hours. Samples were harvested and processed for immunoblotting. The separation of Atg8 from its PE conjugated form was carried out in

a SDS-PAGE containing 6 M urea. In *Figure 4-53* this separation is seen after probing with antibodies against Atg8. When comparing the strains in the log and starved fractions the induction of Atg8 was found to be normal. *trs85Δ* was lipidated similarly to the wild type, and in *atg3Δ* and *atg7Δ* Atg8 was not conjugated to PE.

4.4.1.11   Autophagosomes formed in starved *trs85Δ* cells are of normal size

In *trs85Δ* cells a reduced rate in autophagy was seen. This reduction is possibly caused by a reduced autophagosomal size. Under normal conditions in wild type cells autophagosomes are rarely detectable in the cytosol due to their rapid fusion with the vacuole. A defect in *YPT7* stops the vacuolar fusion of autophagosomes; therefore *trs85Δ ypt7Δ* cells were used to determine the size of autophagosomes. *ypt7Δ* and *trs85Δ ypt7Δ* cells were starved for nitrogen and prepared for electron microscopy. The mean area of the autophagosomes was estimated. A correlation between the autophagosomal size and the mean area of the autophagosomes was made. Quantifying the area of autophagosomes appears more accurate than measuring their diameter, since autophagosomes are not perfectly round.
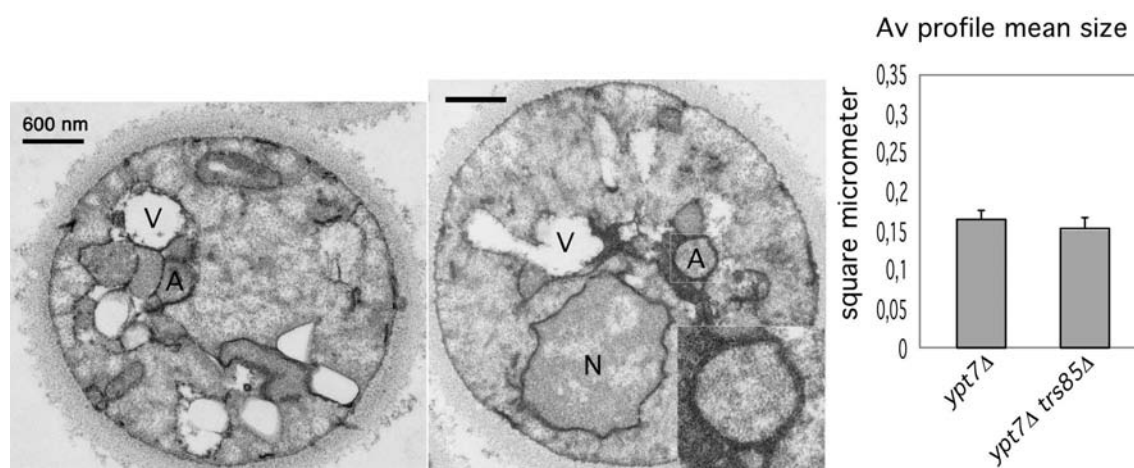
Figure 4-54 *trs85Δ* cells form normal sized autophagosomes. *trs85Δ* (left) and *trs85Δ ypt7Δ* (middle) cells were fixed with potassium permanganate and Epon embedded. The autophagosome area was compared in electron micrographs of both strains and the average size displayed in the table to the right. A autophagosome from the *trs85Δ ypt7Δ* cell was magnified 2.5x (lower right panel) and it shows no abnormal formations. Bar 600 nm.

On the left side of *Figure 4-54* we see an average *ypt7Δ* cell with autophagosomes (A) waiting outside of the vacuole (V); (N) stands for nucleus. In the middle we compare a *trs85Δ ypt7Δ* cell and see a perfectly formed autophagosome located in the cytosol. This autophagosome is magnified 2.5 fold in the lower right hand corner. The average autophagosome area was calculated and displayed in the table to the right. Both *ypt7Δ* and *trs85Δ ypt7Δ* cells had an average size of 0.15-0.2 µm and no distinguishable differences could be seen.

4.4.2 *ATG23* (81)

4.4.2.1 *ATG23* deleted cells show a block in the maturation of aminopeptidase I during vegetative conditions

ATG23 was also found in the phloxin and aminopeptidase I screens. During vegetative conditions where the Cvt pathway is active *atg23Δ* cells were found to be unable to mature proaminopeptidase I. A more detailed study of the maturation of Ape1 was carried out at different growth phases. Cells lacking *ATG23* were compared to the wild type and *atg21Δ* cells in *Figure 4-55*. In the vegetative (log) and stationary growth phases *atg23Δ* and *atg21Δ* exhibited the inability to mature Ape1, but after shifting to starvation media and examination after 4 and 24 hours this inability was completely negated.
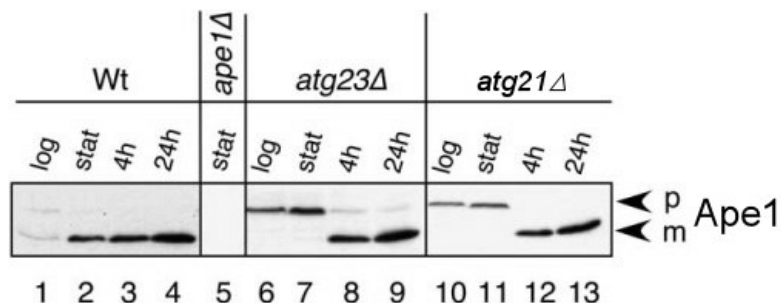
Figure 4-55 *atg23Δ* cells were unable to mature proaminopeptidase I (Ape1) during vegetative conditions. Samples of wild type (Wt), *atg23Δ* and *atg21Δ* cells were immunoblotted with antibodies against Ape1 after harvesting at logarithmic, stationary and starved phases (4 and 24 hours). After the cells were shifted to starvation media the block in the maturation of Ape1 was removed in *atg23Δ*. Wild type cells are able to process Ape1 normally during both conditions unlike *ATG21* deficient cells which also have a defect in the Cvt pathway.

The absence of *ATG23*, though, did not have an affect on the transport and maturation of carboxypeptidase Y or proteinase B, the enzyme needed to lyse Cvt vesicles and autophagic bodies. The maturation of CPY and PrB is shown in *Figure 4-56* section A. Compared to the wild type a steady state examination of the maturation of CPY in *atg23Δ* displayed no abnormal accumulation of proCPY. The induction and maturation of proteinase B is also comparable to wild type in *atg23Δ*. PrA activates PrB, when it is missing pApe1 remains within unlysed Cvt vesicles and autophagic bodies.
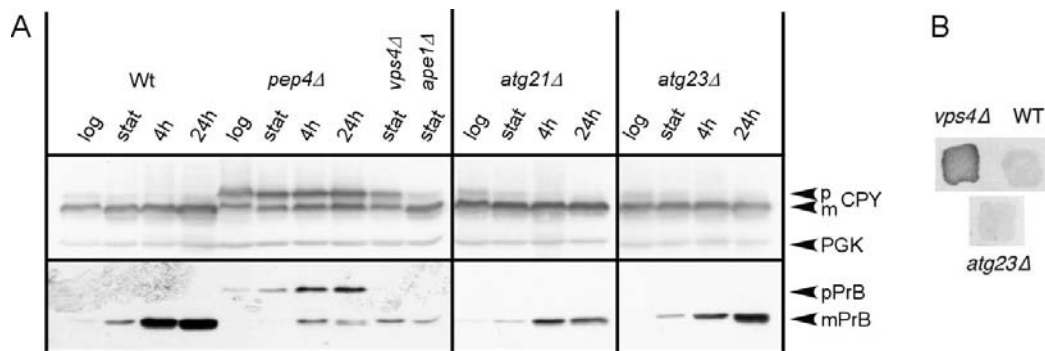
Figure 4-56 Mature vacuolar proteinase Y is detectable in *atg23Δ* cells. A: The Immunoblots of cells in the logarithmic (log) and stationary (stat) growth phase, and cells starved for 4 h or 24 h in SD(-N) medium were probed with antibodies against carboxypeptidase Y (CPY) and proteinase B (PrB). m: mature; p: pro-form. As a control *vps4Δ* cells, defective in vacuolar sorting of carboxypeptidase Y, are included. 3-Phosphoglycerate kinase (PGK) was further detected as a loading control. B: Cells were grown on nitrocellulose and after washing off the cells under running water, the nitrocellulose sheet was probed with antibodies to carboxypeptidase Y. As a control, *vps4Δ* cells, known to secrete carboxypeptidase Y, are included.

In *Figure 4-56* section B, a second test for the proper transport of CPY was controlled. When the CPY transport to the vacuole is impaired, as in the case of *vps4Δ*, CPY is secreted outside of the cell. This can be utilized to screen for strains with a CPY mislocalization. Strains are grown on a nitrocellulose membrane and then washed off under running water. The membrane is then probed with antibodies against CPY. When *atg23Δ* was compared to the wild type and *vps4Δ*, it showed wild type amounts of CPY, indicating that the transport of CPY to the vacuole was not impaired.

4.4.2.2 Vacuolar acidification in *atg23Δ* is normal

Vacuolar proteases need an acidic vacuolar pH to mature and process proteins. In *Figure 4-57*, growing *vma1Δ*, wild type (Wt) and *atg23Δ* cells were treated with the dye quinacrine. Quinacrine, a fluorescent dye, is transported into acidic vacuoles. In *vma1Δ* cells, a subunit of the (H+) vacuolar ATPase is deleted, thus inhibiting the acidification of the vacuole. In cells lacking *ATG23* the vacuolar pH is normal under stationary conditions where the aminopeptidase I maturation is blocked.
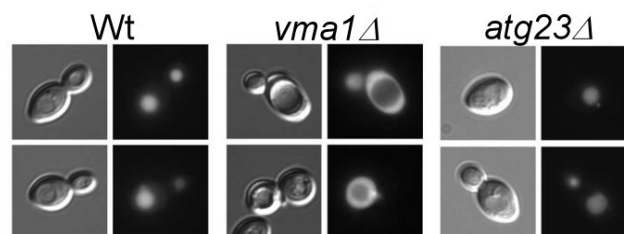
Figure 4-57 The vacuoles of growing *atg23Δ* cells have a normal acidification. Wild type, *vma1Δ* and *atg23Δ* cells were stained with the fluorescent dye quinacrine. Quinacrine fluoresces when it environmental pH is acidic. *vma1Δ*'s vacuole is nonacidic; it lacks a subunit of the vacuolar ATPase, a proton pump. Bar 10 μm.

4.4.2.3 Autophagosomes are formed in *atg23Δ* cells

A deletion strain in the genetic background WCG was created integrating a PCR fragment formed from the plasmid pUG6 and the oligonucleotide primers F-431-KAN and R-431-KAN. The knockout YFB1[17] was confirmed through Southern blot analysis.
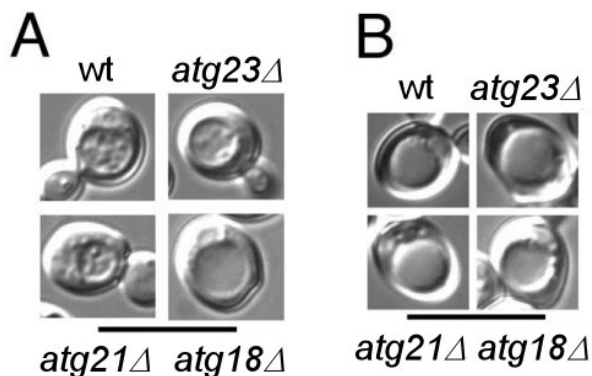
Figure 4-58 The vesicle test indicates that autophagosomes are formed in *atg23Δ* cells. The wild type, *atg21Δ*, *atg18Δ* and *atg23Δ* were grown and shifted to starvation medium (A) with and (B) without the PrB inhibitor PMSF. With PMSF autophagic bodies accumulate within the vacuole whereas without PMSF the ability to lyse autophagic bodies is distinguished. The wild type, *atg21Δ* and *atg23Δ* are able to form and lyse autophagic bodies. *atg18Δ* cells have a defect in the formation of autophagosomes and thus the vacuole remains empty. Compared to the wild type *atg23Δ* vacuoles appear to contain less autophagic bodies. Bar 10 μm.

This deletion strain was tested for its ability to accumulated autophagic bodies within the vacuole in the presence and absence of the PrB inhibitor PMSF (Vesicle Test). In *Figure 4-58* section A, *atg23Δ* had autophagic bodies, which were absent when PMSF was not added to the starvation medium, section B. This wild type behavior indicated that autophagic bodies (und autophagosomes) were formed after starvation induced autophagy (A) and were lysed under normal conditions (B). In *atg18Δ* autophagy is not functional and autophagosomes are not formed.

4.4.2.4 The degradation of GFP-Atg8 is delayed in *atg23Δ* cells

Since it seemed that there were less autophagic bodies present in the vacuole during the vesicle test a simple test for the rate of autophagy was performed. *atg23Δ* cells were transformed with the GFP-ATG8 plasmid, an autophagosomal (autophagic body) marker. GFP-Atg8 travels with the autophagosome into the vacuole, where it is released and degraded. GFP is somewhat resistant to the enzymes within the vacuole and the degradation of GFP-Atg8 to free GFP can be measured in Western blots (*Figure 4-59*) and seen using fluorescence microscopy (*Figure 4-60*).

---

[17] Created by F. Bratsika

In Western blot analysis (*Figure 4-59*, A) wild type, *ypt7Δ* and *atg23Δ* cells, containing GFP-Atg8 under the control of its native promoter, were shifted to starvation medium and observed over time. In wild type cells the amount of free GFP increased steadily immediately after the shift. In *ypt7Δ* cells where the fusion of the autophagosome with the vacuole is blocked, GFP-Atg8 is formed but remained undigested. In *atg23Δ* cells a noticeable delay in the liberation of GFP was seen. This blot was then quantified and displayed graphically in *Figure 4-59* part B, showing that after four hours only about one-third of the wild type amount of GFP was released in *atg23Δ* cells.
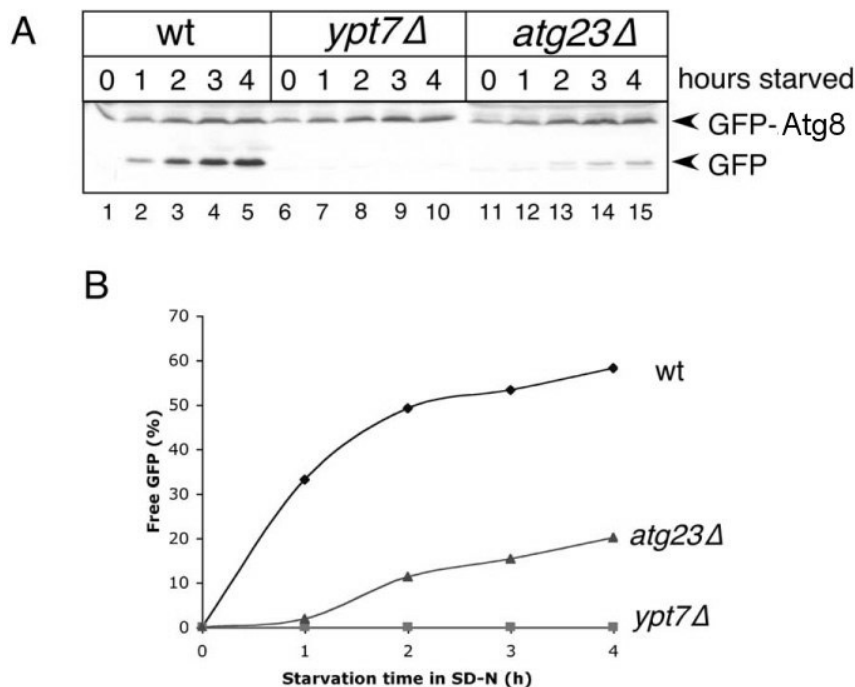
Figure 4-59 Autophagy is reduced in *atg23Δ* cells as indicated by the delayed and reduced amount of free GFP generated from the degradation of GFP-Atg8 in the vacuole. Wild type (wt), *ypt7Δ* and *atg23Δ* cells were grown and shifted to SD(-N) starvation medium. After the indicated hours of starvation a sample was removed and processed for immunoblotting. The membrane was probed with anti-Atg8 antibodies (A) and the results quantified (B) using the Fuji LAS1000 and AIDA software (Raytest); for each time point the amount of free GFP was expressed as percent of the sum of free GFP and GFP-Atg8.

The localization of GFP-Atg8 was also directly observed using fluorescence microscopy. In panel A of *Figure 4-60* GFP-Atg8 was seen localized within the cytosol and at the PAS in wild type and *ypt7Δ* logarithmic cells. In *atg23Δ* cells GFP-Atg8 was also seen in the cytosol but not localized to the PAS. In panel B after 4 h in SD(-N) the localization of GFP-Atg8 was normalized in *atg23Δ* cells. In *ypt7Δ* several dots are seen in addition to the PAS, these indicated autophagosomes that are trapped within the cytosol. In the wild type free GFP is observed in the vacuole as autophagic bodies containing GFP-Atg8 are digested.
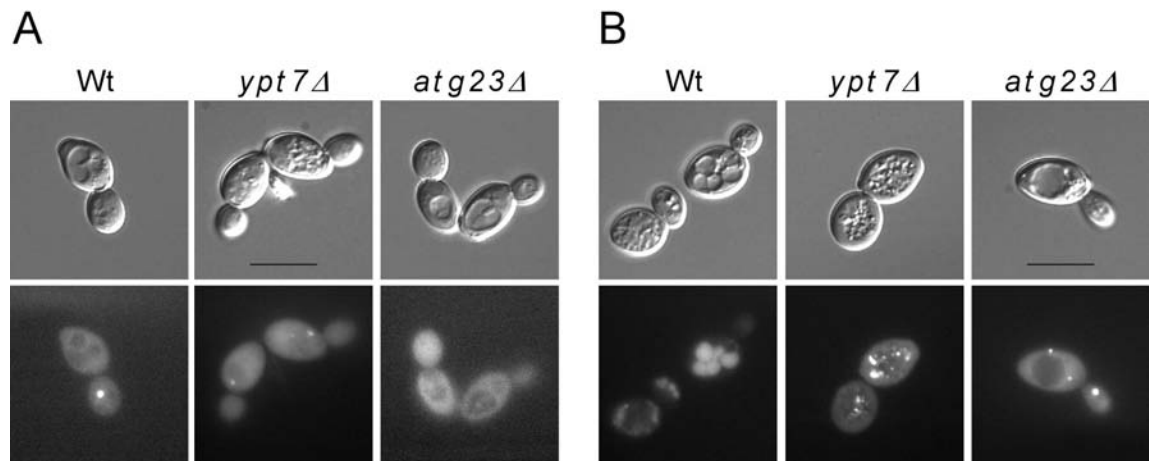
Figure 4-60 A, B: Cells expressing GFP-Atg8 from a centromeric plasmid with its own promoter were visualized in Nomarski optics (upper panels) or fluorescence microscopy (lower panels). Cells in A were grown to the exponential growth phase, cells in B were starved for 4 h in nitrogen free SD(-N) medium. Note the accumulation of GFP in the vacuoles of wild-type (Wt) cells. Bar: 10 μm.

5   Discussion

Over the years, approximately 31 genes have been identified with autophagy, six of them within this study. The proteins involved are associated with different stages of the autophagic process; these are induction, recruitment, vesicle formation, vesicle fusion, vesicle lysis and recycling. During autophagy double membrane layered vesicles are formed which transport enclosed proteins, selectively and non-selectively, to the vacuole to be lysed and degraded. The degraded material aids in the homeostasis of different building blocks. Autophagy also allows the cell to survive periods of stress and in the process disposes the cell of harmful elements, such as over-produced proteins or bacteria. The genes investigated here are of a fundamental sort they influence vesicle formation and vesicle fusion.

During the study of autophagy in the yeast *S. cerevisiae* a parallel pathway to autophagy was discovered. It was named the cytoplasm to vacuole transporting (Cvt) pathway and occurs only in yeast. Autophagy and the Cvt pathway are functionally very similar to each other; both create double membrane-bound vesicles that are transported to the vacuole. They differ in the size of their vesicles, the cargo they transport and the conditions when they are formed. Autophagosomes induced during starvation conditions contain cytosolic material and are two to six times larger in diameter than Cvt vesicles. Most of the involved genes are required in both the Cvt pathway and in autophagy alike, but some when deleted specifically disrupt only the Cvt pathway. One question is: why do some proteins only influence the Cvt pathway leaving autophagy greatly unaffected? It is the study of such genes that will help in the elucidation of the mechanism of autophagy.

Generally, transport vesicles evolve by budding off of the ER. These vesicles then traverse the Golgi apparatus to the plasma membrane or the late endosome. New vesicles then bud off and return from the plasma membrane going back either to the Golgi apparatus or travel on to the vacuole where their contents are digested. All of these transport vesicles consist of a single membrane-bound compartment, which disappears when it merges with its destination membrane organelle. Uniquely, autophagosomes and autophagic-like vesicles differ from other transport vesicles in this aspect. Here a double membrane surrounds the contents of autophagosomes and Cvt

vesicles. When they fuse with the vacuole they release a single layered vesicle into the vacuolar lumen that is later lysed dependent on a number of proteases and *Atg15*. This released vesicle is extraordinary in the cell. The following questions arise when studying autophagy: what differences allow this type of vesicle to be selectively lysed without compromising the integrity of the vacuolar membrane that surrounds it? And these double-membrane layered vesicles are autophagy-specific, but how are these double-membrane bound vesicles formed and where does the unique membrane originate?

As to the membrane origin, two theories exist. The first theory is that autophagic vesicles form from the fusion of preexisting vesicles. The second theory is that vesicles grow and mature at a certain location. The latest studies from various work groups indicate that many proteins involved in autophagy and the Cvt pathway gather at a novel organelle called the preautophagosomal structure (PAS) (34,35). Many autophagy related-proteins have been tagged with fluorescent markers and are seen at a common point located at the vacuolar membrane. These findings support the theory that autophagosomes and Cvt vesicles grow and mature at a certain location.

5.1 Four genes in this study are involved in the biogenesis of transport vesicles

5.1.1 *ATG18* and *ATG21*

During this study four genes were found that are involved in the biogenesis of the transport vesicles. Three of them are involved only in the Cvt pathway; one is involved in both the Cvt pathway and during autophagy. Of these four, one interesting pair of genes is *ATG18* and *ATG21*. They are homologues[18], but appear to have different functions. Atg18 is involved in both autophagy and the Cvt pathway, where as when missing Atg21 has been shown to cause a block only in the Cvt pathway. The differences between these two homologues can help us gain insight into the importance of their genetic differences and the influence this has on their mechanistic functions.

ATG18 and *ATG21* were identified, respectively as *YFR021w* and *YPL100w*, in a reverse genetic screen using two characteristic trademarks of autophagy, the ability to survive under starvation conditions and the maturation of the cargo protein aminopeptidase I (Ape1). Western blotting showed that the ability to mature Ape1 in YPD was impaired in both unknown ORFs. Further examination showed differences in the homologues (*Figure 4-3*) in logarithmic and stationary growing cells and in cells that were starved for 4 and 24 hours in medium without nitrogen, SD(-N). *YFR021w* had a maturation block in both stationary and starvation media so it was then named *AUT10*[19]. *YPL100w* was only blocked during vegetative growth. It matured Ape1 after shifting the cells to SD(-N), so it was named *MAI1* for its inability to Mature Aminopeptidase I during the Cvt pathway. During this study a unified nomenclature for Autophagy related genes was established thus changing their names to *ATG18* (*AUT10*) and *ATG21* (*MAI1*)[20].

The defect in autophagy of *atg18Δ* was confirmed visually by examining its ability to sporulate and form autophagosomes. Microscopically *atg18Δ* formed no spores when grown in sporulation medium. A "vesicle test" [*see Materials and Methods*] showed no

---

[18] There is also a third homologue in *S.c.*, YGR233c, but it doesn't influence either the Cvt pathway or autophagy. It was not found in our screen.

[19] AUT for AUTophagy

[20] The genes and proteins will now be named according to their actual nomenclature.

accumulation of autophagic bodies within the vacuole in *atg18Δ*. Both of these tests use autophagy inducing media. In agreement with the Western blots, *atg21Δ* accumulated autophagic bodies within the vacuole and sporulation was reduced but not impaired. In addition, the rate of autophagy was measured using an ALP assay; this showed that similar to its reduced sporulation, autophagy was also reduced but not absent in *atg21Δ* cells.

Maturation of the proteases CPY and PrB were both checked to see if other transport pathways involved were impaired, such as the dysfunction of Ape1 maturation caused by the two pathways under investigation. Both proteases were present in their mature state therefore the lack of Atg18 or Atg21 had no affect on their normal processing. An additional requirement for protease processing was also examined, the vacuolar acidification. This was found to be normal, thus the accumulation of proApe1 was not due to insufficient processing in the vacuole. At what step then, do these protein work in?

Sometimes the position of the protein within the cell can tell about what that protein does and where it operates. The HA-Tagged Atg18 and Atg21 were seen near the vacuolar membrane using indirect fluorescence. Atg21-HA was more concentrated there than Atg18-HA, which was observed as scattered punctae in the cytosol with some larger spots along the vacuolar membrane. This pattern was not distinguishable as a known organelle; therefore a stronger signal was needed to precisely locate these proteins. Atg21-YFP was created and examined with fluorescent microscopy. Though the signal of Atg21-YFP was not very strong it was clearly seen as a ring encircling the vacuole with a number of large punctae adjacent to it. This image remained the same when Atg21-YFP was visualized in a number of deletion mutants known to participate in autophagy or the Cvt pathway.

The latest studies from various work groups indicate that many proteins involved in autophagy and the Cvt pathway gather at a novel organelle called the preautophagosomal structure (PAS) (34,35). Many autophagy related-proteins have been tagged with fluorescent markers and are seen at a common point located at the vacuolar membrane. When visualized together with Ape1-CFP, which localizes to the PAS, Atg21-YFP was not found to be reliably located there. It does not seem to be a necessary part of the machinery that assembles at the PAS.

Upon closer examination together with the fluorescent vacuolar membrane marker FM4-64 the punctae of Atg21-YFP were found to concentrate at vacuolar vertices. 97 % were located at two or more vertices, and perhaps the last 3 % are at newly forming vacuoles or at ones being fused. The indirect immunofluorescence localization of Atg21-HA indicated that it was found primarily near the cell nucleus; therefore Atg21-YFP was also co-visualized with the protein Nvj1-CFP. Nvj1 is a marker for the nuclear-vacuolar junction. This finding did not result in conclusive data since Atg21-YFP punctae only localized adjacent to this area 50 % of the time. Interestingly, although Atg21-YFP is not constantly located at the PAS or the nuclear-vacuolar junction it seems to have an affect on the recruitment of Atg8 to the PAS. In *atg21Δ* cells Atg8-GFP remains cytosolic (*Figure 4-25*). As seen in a urea-containing SDS-PAGE (*Figure 4-27*), significant amounts of Atg8 are not conjugated to phosphatidylethanolamine (PE) in *atg21Δ* cells. The lipid-bound Atg8-PE is thought to be involved in the membrane-elongation of forming autophagosomes. Atg8 is also the only autophagy induced protein that is bound to autophagosomes. The formation of Atg8-PE is dependent on Atg3, its conjugating enzyme; additionally the 350-kDa Atg5/12/16 complex, which is involved in the nucleation of Cvt vesicles and autophagosomes, is also a part of the Atg8 lipidation. Is it possible that Atg21 helps relay the Atg5/12/16 complex to the Atg8-PE conjoining point? Or does it bring Atg8 to the membrane? Atg21 is a peripheral membrane protein (*Figure 4-10*). As seen in this study it is also integrated into autophagosomes after long periods of starvation. This was visualized in *atg15Δ* cells containing Atg21-YFP (Figure 4-20). In the vacuole part of the autophagic bodies can be seen dancing around. Is this a selective process or is this just the result of the invagination of vacuolar membrane into the vacuole where Atg21-YPF appears to be adjacent to? It would be interesting to see if the reduced rate of autophagy is in fact due to the hindrance of microautophagy. Though its concentration at the vacuolar vertices may mean that this is just a secondary function.

The homology found between Atg18 and Atg21 is based on a series of domains that bind phosphatidylinositol 3,5-bisphosphate (PtdIns(3,5)P_2) (33). PtdIns(3,5)P_2 is created by the protein Fab1 from PtdIns3P. PtdIns(3,5)P_2 is essential for membrane recycling from the vacuole, among other functions. A defect in Fab1 results in cells containing abnormally large vacuoles. This anomaly was used to find effector proteins for

PtdIns(3,5)P_2. Atg18/Svp1 was found to have an enlarged vacuole[21]. Mutations in its PtdIns(3,5)P_2 binding site, $_{284}$FRRG$_{287}$ to $_{284}$FTTG$_{287,}$ decreased its affinity for PtdIns(3,5)P_2 40-fold. The expression of the mutated form controlled by its own promoter did not correct the enlarged vacuole phenotype. This indicates that it must bind PtdIns(3,5)P_2 for its normal functioning in vacuolar membrane trafficking.

As a result of its known defects in autophagy (from our publications, (50)) Dove *et al.* investigated if Atg18/Svp1 needs to interact with Fab1 and/or PtdIns(3,5)P_2 in order for autophagy to function properly. In *fab1Δ* cells autophagy is not obstructed. Therefore, they hypothesize that an Atg18-PtdIns(3,5)P_2 complex interacts specifically with another protein or group of proteins and initiates membrane budding from the vacuolar surface. A second PtdIns(3,5)P_2-independent function of Atg18 affects autophagy and perhaps its affect on autophagy is due to common binding partners linking the PtdIns(3,5)P_2-dependent and independent functions of Atg18.

Another workgroup (D. Klionsky) identified Atg18/Cvt18 and associated it to autophagy, the Cvt pathway and pexophagy (104). In addition to the block in the maturation of Ape1 in *atg18Δ* cells they found that though proApe1 was membrane associated it was sensitive to extraneously added proteases. This sensitivity indicated that proApe1 is not enclosed within a protective membrane in *atg18Δ* cells when compared to wild-type cells. This implies that Atg18 is not required for the initial membrane association of proApe1 but for its sequestration or enclosure within Cvt vesicles. Their visualization of Atg18-GFP came to the same conclusion as in our study. Atg18-GFP was seen at the vacuolar membrane and at punctated structures in the cytosol. A fraction of Atg18-GFP was found to be peripherally membrane associated, though in an Optiprep gradient it did not co-fractionated with any known markers. Strangely enough, not even with the marker for the vacuolar membrane though it was visualized there in fluorescent microscopy. These findings coincide with our study of Atg21.

They further characterized Atg18's influence on other known autophagy and autophagy-like proteins and discovered that the lack of Atg18 affects the localization of Atg2-GFP in the cell. Instead of localizing to a punctated structure Atg2-GFP appeared cytosolic when observed in *atg18Δ* cells. This was similar to the pattern of Atg2-GFP in

---

[21] though this was not observed in our genetic background (WCG)

atg1Δ cells; Atg2 requires the presence of Atg1 for its recruitment to the PAS (105). Atg2 was characterized as a peripheral membrane protein that requires the interaction of Atg9 to localize to membranes (106). Atg9 is the only integral membrane protein known to be necessary for the formation and completion of autophagosomes and Cvt vesicles (72,107). Because Atg9 is not found on the membranes of these completed vesicles it must somehow be retrieved from the finished vesicles and recycled. That would explain the presence of Atg9 at the PAS and at multi-punctae within the cytosol (72,107). In *atg18Δ* cells Atg9-YFP remained at the PAS. Similar results were obtained from Atg9-YFP in a*tg2Δ* cells (100). The direct interaction of Atg9 and Atg18 was tested and indeed Atg9 seems to bind Atg18 in a pull down experiment. This binding was also dependent on the presence of either Atg1 or Atg2 (100). Atg18 was concluded to be involved in the recycling of Atg9 from the PAS. The Atg1-Atg13 complex promotes the interaction of Atg2 with Atg18. Atg2 and Atg18 then associate with Atg9. When the autophagosome or Cvt vesicle is completed Atg9 is removed from the completed vesicle and returns to a peripheral pool. (100) The association of Atg18 with Atg2 and Atg9 perhaps triggers the completion of the forming double membrane vesicles initializing the budding off of membrane containing Atg9.

5.1.2 *TRS85/GSG1*

The ORF YDR108w was first identified as a gene required for sporulation in *S. cerevisiae* and termed *GSG1* for general sporulation gene (101,103). This however did not give insight into the possible function of Gsg1. Later on Gsg1 was identified as an 85 kDa band that immunoprecipitated along with Bet3 and a number of other proteins (108). This ~800 kDa multiprotein complex termed TRAPP (transport protein particle) consists of 10 subunits and mediates the docking of transport vesicles originating from the ER (109). Along with the other TRAPP proteins *GSG1* was named *TRS85* for TRAPP subunit followed by its molecular weight. The TRAPP complex is located at the Golgi apparatus (110). The TRAPP subunits form two separate TRAPP complexes, TRAPP I and TRAPP II (102). Trs85 was found to be a component of both complexes, but in TRAPP I at substoichiometeric amounts compared to the other proteins. TRAPP I is the smaller of the two complexes having a molecular weight of ~300 kDa when compared to the ~1000 kDa TRAPP II complex. TRAPP I is involved in vesicular traffic from the ER to Golgi where it binds COP II vesicles at the *cis*-Golgi. TRAPP II

on the other hand is involved later after vesicles reach the Golgi. TRAPP I evolves with the Golgi cisternae adding the components Trs120, Trs130 and Trs65 to complete the TRAPP II complex (111). TRAPP I and II are tethering factors.

Along with two other TRAPP subunits Trs85 was determined to be non-viable for the vegetative growth of yeast (109). This trait was important for our study of autophagy. In our screen we examined a knockout mutants collection for genes that affected the maturation of Ape1, a cargo protein of both the Cvt and autophagic pathways. Naturally, we were only able to examine viable yeast cell knockouts. As seen in (*Figure 4-41*) the deletion of Trs85 lead to a complete blockage in the maturation of Ape1 in vegetative yeast cells; but when *trs85Δ* cells were shifted to the autophagy inducing medium SD(-N), the cells were able to mature Ape1. This indicates that Trs85 is necessary for the selective Cvt pathway but not during autophagy. The deletion of the two other non-viable TRAPP components, however, had no effect on Ape1 maturation (*Figure* 4-43). The transport of proApe1 was observed using fluorescence microscopy. Proaminopeptidase I tagged with a monomeric red fluorescent protein (proApe1-RFP) was observed during vegetative conditions in the wild type, *atg19Δ* and in *trs85Δ* (78). In wild type cells Ape1-RFP reaches the vacuole where it accumulates. *atg19Δ* cells are known to have a defect in the vacuolar targeting of Ape1 to the vacuole. It accumulates at a singular point outside of the vacuole. In *trs85Δ* cells proApe1-RFP also accumulates at a single point outside of the vacuole. Thus *trs85Δ* recruits the Cvt complex to the PAS but is defective in the transport of proaminopeptidase I to the vacuole preventing Ape1 proper maturation.

An effective method to examine the influence of a gene on autophagy is the "vesicle test". This indicated that compared to the wild type, *trs85Δ* has a reduced rate of autophagy. Less autophagic bodies appeared to accumulate in the vacuole when their lysis was inhibited. To better visualize this proposal, the breakdown of GFP-Atg8 and accumulation of free GFP was examined in a Western blot. Atg8 is a protein that is selectively enclosed into autophagosomes. It is transported into the vacuole where it is broken down along with other cargo proteins. As more GFP-Atg8 is transported to the vacuole the protease resistant GFP accumulates within the vacuole. In *trs85Δ* cells, though present the accumulation of free GFP was reduced, whereas in a*tg18Δ* cells no free GFP was released (*Figure 4-50*). The autophagic rate was also quantified by the ALP assay. Lacking its membrane domain a truncated version of the alkaline

phosphatase remains cytosolic and is transported to the vacuole via autophagy. After reaching the vacuole it is enzymatically activated and its phosphatase activity can be quantified after different time allotments. The ALP assay indicated that autophagic rate of *trs85Δ* is about half of that of the wild type.

The cargo protein proApe1 is transported to the vacuole within both Cvt and autophagic vesicles where it is properly matured. The Rab GTPase Ypt7 is necessary for the fusion of Cvt vesicles with the vacuole (112). Cells lacking Ypt7 accumulate intact Cvt vesicles in the cytosol; within these vesicles proApe1 is enclosed. Using external proteases the formation of intact Cvt vesicles was tested by examining their ability to artificially mature Ape1. In spheroplasted *trs85Δ ypt7Δ* cells proApe1 was cleaved by proteinase K (*Figure 4-48*), as in *atg1Δ ypt7Δ* cells, which are defective in the biogenesis of Cvt vesicles. In *ypt7Δ* cells proApe1 remained intact. Therefore, because proApe1 is accessible to external proteases in *trs85Δ ypt7Δ* cells we concluded that Trs85 is involved in the intact formation of proApe1-containing Cvt vesicles. Similar results were seen in *trs85Δ* cells (*Figure 4-47*).

The formation of autophagosomes and Cvt vesicles is preceded by the accumulation of several important autophagy proteins at a singular point outside of the vacuole. The PAS is presumably a donor compartment for forming autophagosomes and Cvt vesicles (34,35). The accumulation of the fluorescently marked proteins GFP-Atg9, GFP-Atg19 (*Figure 4-51*) and GFP-Atg8 (*Figure 4-52*) at the PAS was examined in wild type, *atg1Δ* and *trs85Δ* cells. GFP-Atg9 and GFP-Atg19 accumulated normally to the PAS, but interestingly GFP-Atg8 remained cytosolic in growing *trs85Δ* cells. When these cells were shifted to conditions where autophagy was induced GFP-Atg8 was then recruited to the PAS. This is a good indicator that Trs85 influences the recruitment of Atg8 to the PAS during the Cvt pathway. Without Atg8 Cvt vesicles fail to fully form, prohibiting the transport of proApe1 to the vacuole. Unlike Atg21, Trs85 has no effect on the lipidation of Atg8 with phosphatidylethanolamine (*Figure 4-53*). The formation of normal sized autophagosomes in *trs85Δ* cells was also seen using EM (*Figure 4-54*).

Most proteins of the TRAPP complexes are conserved from yeast to mammals (113). Trs85 however has no homologues in higher organisms; it seems to be only present in yeast. The Cvt pathway, unlike autophagy, is also a process that is unique to yeast. This supports the connection of Trs85 involvement in the Cvt pathway. The fact that Trs85 is

not essential for the viability of *S. cerevisiae*, though being a part of an essential complex of membrane trafficking, is also an interesting aspect. Trs85-GFP is located at a point on the vacuole, possibly at the PAS (78). Whereas the other TRAPP proteins are seen as multiple punctae within the cytosol, indicating an association with the Golgi. Perhaps Trs85 uses the TRAPP complexes as a means of transportation to the PAS, or it helps recruit or transport Atg8. Without Atg8 association to the PAS the completion of Cvt vesicles is disrupted and autophagy is impaired. The decline in autophagy hinders the cells ability to sporulate, which is why TRS85/GSG1 was first discovered in a screen for sporulation defects.

5.1.3 ATG23

ATG23/YLR431c was an unknown ORF found during our screen. We performed a basic characterization and identified it as a gene involved in the Cvt pathway (81). When deleted, the strain showed a block in the maturation of aminopeptidase I during stationary conditions but not during conditions where autophagy occurs. In the deletion mutant processing of other proteases such as CPY and PrB was normal. A normal acidic vacuole was also found in these mutants indicating that the defect in the aminopeptidase I processing was not due to a nonfunctioning vacuole. Vesicles were also seen in the vacuole during the "vesicle test", where autophagic body degradation is inhibited by PMSF.

In D. Klionsky's workgroup Atg23 was also linked to the Cvt pathway, efficient autophagy, but not to pexophagy (114). It was identified as a peripheral membrane protein and with a fluorescently marked Atg23 they located it to the PAS and to punctae in the cytosol. This pattern was reminiscent of the pattern seen by Atg9. Because of their similarity, the association of Atg23 with Atg9 was examined. In a pull-down experiment using Atg9-protein A and Atg23-HA, Atg23 was found to eluate with Atg9 thus indicating an association between the two. The study was expanded to examine if this association was necessary for the localization of either one of the proteins. Each fluorescently marked protein was visualized in cells lacking the other protein. The results showed that the localization of Atg23-YFP to the PAS and cytosolic punctae was dependent on the presence of Atg9 in the cell, although cells lacking Atg23 had no effect on the localization of Atg9-YFP. They concluded that Atg23 transiently interacts with Atg9 due to these findings: the distribution of Atg23 is different than that of Atg9

in *atg2Δ*, *atg14Δ* and *atg18Δ* mutants and Atg23 is unaffected by the lack of these proteins whereas Atg9 remains located to the PAS. Atg23's cytosolic pool is not dependent on the physical presence of Atg9 to connect it to the cytosolic punctae (114). When Atg9 is missing not only the Cvt pathway is blocked but also autophagy and pexophagy (107). Both Atg9 and Atg23 remain located at the PAS in *atg1Δ* cells, but the peripheral fraction of Atg23 is dependent on the Atg1 kinase activity whereas Atg9 is not (100).

The Cvt pathway is a biosynthetic pathway in constant need of new membranes and materials. Atg23 is a peripheral membrane protein that seems to cycle between the PAS and many peripheral punctae dependent on the activity of the Atg1 kinase. Perhaps Atg23, along with Atg9, is responsible for the flux of membrane needed to produce Cvt vesicles and some autophagosomes.

5.2   The two remaining genes are involved in vesicle-vacuolar fusion

5.2.1 *CCZ1* and *MON1*

The remaining two genes found in this study, *CCZ1* and *MON1* were both found to be involved in the widely explored mechanism of vesicle-vacuolar fusion needed for vesicular trafficking like in autophagy and the Cvt pathway. The fusion complex comprising of several SNARE components and Class C Vps proteins was found to be larger than first realized.

CCZ1, *YBR131c*, was first characterized by the workgroup of J. Rytka during the collective creation of the *S. cerevisiae* deletion collection (115). Haploid and homozygote diploid deletion mutants of *YBR131c* were found to be increasingly sensitive to <u>C</u>affeine, <u>C</u>alcium and <u>Z</u>inc, hence the name *CCZ1*. *ccz1Δ* cells were unable to grown on plates with higher concentrations of these chemicals. The sporulation of *ccz1Δ* diploid cells was also noticed to be impaired. Furthermore, *ccz1Δ* cells were found to have abnormal vacuolar morphology and impaired vacuolar protein sorting for CPY and ALP. CPY is sorted from the Golgi to the vacuole via the endocytic compartment and ALP bypasses the endosome on route to the vacuole. Both these routes are disturbed in *ccz1Δ* (116). It was noticed here that the fusion of these transport vesicles with the vacuole is blocked in *CCZ1* null mutants. Rytka's group further

identified *YPT7*, a Rab GTPase, in a high copy suppressor screen. *YPT7* completely complemented *ccz1Δ* inability to grown on high calcium, zinc or caffeine media. Ypt7 is a small GTPase that regulates vesicular traffic and homotypic fusion at the vacuolar membrane (117,118). Rab proteins control the correct binding of vesicular and target SNAREs. The deletion of the *YPT7* gene was also seen to have the same phenotypic effects as *ccz1Δ*. Interestingly though, in a reverse high copy suppressor investigation the retrieval of *YPT7* deletion defects was not accomplished by Ccz1 (116). They additionally identified *YPT7* mutants that suppress the *CCZ1* mutant phenotype. All of these mutants were found to be located in the conserved sequence motif of its guanine nucleotide binding protein site, affecting the GDP/GTP exchange (119). GTP binding proteins act as molecular switches; they undergo conformational changes from an active GTP bound state to an inactive GDP bound state (120). There are a number of proteins that enhance this cycle between the active and inactive conformation. Ccz1 is possibly one of these factors regulating GDP/GTP exchange, a guanine nucleotide exchange factor (GEF). Most probably it is Ypt7's guanine nucleotide releasing protein (GNRP); helping it cycle back from GDP to GTP. Ypt7 was also shown to physically interact with Ccz1 by immunoprecipitation (119).

MON1, *YGL124c*, was first identified in a screen for its sensitivity to monensin and brefeldin A. Both drugs affect intracellular transport (121), but no obvious connection to intracellular transport was evident at that time.

At the same time we isolated deletion mutants defective in the maturation of aminopeptidase I (80). Ape1 is a cargo protein of both the Cvt pathway and autophagy *Figure 1-5*. A defect in the maturation of Ape1 in vegetative or starvation conditions is a good indicator that there is a block in the Cvt pathway or autophagy, respectively. As previously described, in *ccz1Δ* cells there is a defect in the sorting of CPY. Our studies also show a sorting defect in both *ccz1Δ* and *mon1Δ* cells, but significant steady state levels of mature CPY and PrB are present, indicated that the lack of Ape1 maturation was not due to lack of vacuolar proteases. Additionally in order to determine if vesicles are formed, the transport of Atg8, tagged with a green fluorescent protein, was observed in cells lacking *CCZ1* or *MON1* under vegetative and starvation conditions. Atg8 is a protein necessary for vesicle formation in both autophagy and the Cvt pathway. It is also one of the only known proteins that is integrated into the membrane of the autophagosomes and Cvt vesicles and it travels into the vacuole with them. A block in

the transport of these vesicles is indicated by the inability of Atg8-GFP to be degraded in the vacuole. In wild type cells GFP is released from Atg8, after degradation. GFP being somewhat protease resistant accumulates in the vacuole and can be seen using fluorescence microscopy or in Western blot analysis. In *Figure 4-39* Atg8-GFP was observed in the wild type, *mon1Δ* and *ccz1Δ* cells under stationary and starved conditions. Under both conditions in both mutants an accumulation of fluorescent punctae was observed outside of the fragmentated vacuoles. Unlike in the wild type where a cytosolic staining was seen in the stationary state and vacuolar staining under starvation conditions this punctated pattern indicated that autophagosomes and Cvt vesicles were being formed but somehow remained outside of the vacuole. In an anti-GFP Western blot of starved wild type, *ccz1Δ*, *mon1Δ* and in *ypt7Δ* cells (*Figure 4-40*), an accumulation of Atg8-GFP was seen after four hours of starvation in the mutants, unlike the increasing accumulation of free GFP in wild type cells over the same amount of time. This validated the assumption that Atg8 was not entering into the vacuole and thus a disruption in the flow of Cvt vesicles and autophagosomes into the vacuole was certain. Though punctated Atg8-GFP structures were seen outside of the vacuole indicating that vesicles were being formed, the presence of Ape1 within these vesicles was yet to be confirmed. To test this, an Ape1 protease protection experiment was performed and it was observed that Ape1 remains in its premature form. But was this due to the lack of vesicular formation and cargo packing or was Ape1 being packed into vesicles but they were not being digested? Ape1, being a vacuolar hydrolase, is transported to the vacuole in an inactive pre-form, upon reaching the vacuole it is cleaved resulting in the mature form. In lysed spheroplasts of *CCZ1*, *MON1*, *YPT7* and *ATG1* deleted cells (*Figure 4-37*) the accessibility of pApe1 to extraneously added proteases was examined. Like in *ypt7Δ*, pApe1 remained uncleaved in *ccz1Δ* and *mon1Δ* cells, indicating that Ape1 is within protective transport vesicles in these strains. In *atg1Δ* spheroplasts Ape1 is pseudo-matured due to its inability to form autophagic vesicles. All in all we concluded that Ccz1 and Mon1 are needed for the fusion of Cvt vesicles and autophagosomes with the vacuole.

In the work group of D.J. Klionsky, Ccz1 and Mon1 were also identified as being involved with the fusion of Cvt vesicles and autophagosomes with the vacuole (58). Ccz1 and Mon1 were shown to be membrane associated and somewhat detergent resistant. In addition, fluorescently tagged Ccz1 and Mon1 were seen to co-localized at

perivacuolar points and co-fractionate in a centrifugation gradient. They concluded that Ccz1 and Mon1 are part of a larger protein complex required for the fusion of several delivery pathways ending in the vacuole (58).

But how does a defect in *CCZ1* or *MON1* prevent the fusion of autophagosomes and Cvt vesicles? It has been shown that vacuolar-vesicle fusion can be interrupted after vesicle docking by keeping the Ca^{2+} concentration very low. Is *CCZ1* regulated by the Ca^{2+} concentration thus allowing fusion to occur? Ca^{2+} sensors have been shown (122) to regulate the fusion of endocytotic vesicles. The elevation of Ca^{2+} along the two joining membrane accelerates the fusion by two powers of magnitude (123). The sensitivity of *CCZ1* deleted cells to increased calcium concentrations could be an indicator that it is part of this calcium sensing/regulating complex and in connection Mon1 would also be a part of this complex.

6   Summary and Outlook

The transport and homeostasis of proteins is an important part of the life cycle of cells. Without such mechanisms life could not be sustained. Autophagy is one of these mechanisms that help provide cells with necessary building blocks. Over the years, the field of autophagy has become increasingly studied. Once thought to be only a mechanism to survive times of nutrient depletion it is now linked to many processes and diseases.

In this study six genes were identified with autophagy. The first four are involved in the completion of Cvt vesicles. (Atg18 is also involved in the completion of autophagosomes.) *ATG18* and *ATG21* are homologues. Atg18 is involved in the recycling of Atg9 from the PAS to the peripderal pool. The removal of Atg9 from the vesicle membrane triggers the completion of the forming vesicle. Atg21 is involved in the lipidation of Atg8 with phosphatidylethanolamine. Possibly the binding of PtdIns(3)P$_2$ triggers Atg21 to relay the 350 kDa complex to the PAS or it enables Atg8 to attach itself to the membrane. *ATG23* cycles between punctae in the cytosol and the PAS; this cycling is dependent on Atg9, which also cycles between cytosolic punctae and the PAS. Atg23 could be a part of the machinery needed for the membrane flux of Cvt vesicles. *TRS85* is a part of the TRAPP complexes, but it was seen to be located at the PAS unlike most TRAPP subunits. Perhaps Trs85 travels with the TRAPP complex through the Golgi and uses the complex to transport Atg8 to the PAS enabling the formation of Cvt vesicles. The remaining two genes *CCZ1* and *MON1* are not involved in vesicle formation. They are both associated with the HOPS complex needed for the fusion of autophagosomes and Cvt vesicles with the vacuole.

Though my study did not intensely characterize all of the new proteins identified in this screen, it succeeded in identifying many new genes involved in either autophagy, the Cvt pathway or both. Six of these genes were characterized in this study. Autophagy is an exciting area of study. Its importance for the maintenance and protection of cells is becoming more and more evident as its machinery and functions are further elucidated. With its links to cancer, myopathic and neurodegenerative diseases and even aging it will be interesting to follow how exactly autophagy plays a role in these diseases.

Erklärung

Hiermit erkläre ich, daß ich die vorliegende Dissertation selbständig angefertigt habe. Es wurden nur die in der Arbeit ausdrücklich benannten Quellen und Hilfsmittel benutzt. Wörtlich oder sinngemäß übernommenes Gedankengut habe ich als solches kenntlich gemacht.

Calw, _____   _____

Ort, Datum   Unterschrift

I declare that I have written this thesis on my own. All external sources and resources used have been named. Quotes or ideas taken from other sources have been referenced as such.

Literature

1.   Clark, S. L., Jr. (1957) *J Biophys Biochem Cytol* **3**, 349-362

2.   Abeliovich, H., and Klionsky, D. J. (2001) *Microbiol Mol Biol Rev* **65**, 463-479

3.   Takeshige, K., Baba, M., Tsuboi, S., Noda, T., and Ohsumi, Y. (1992) *J Cell Biol* **119**, 301-311

4.   Shintani, T., and Klionsky, D. J. (2004) *Science* **306**, 990-995

5.   Aita, V. M., Liang, X. H., Murty, V. V., Pincus, D. L., Yu, W., Cayanis, E., Kalachikov, S., Gilliam, T. C., and Levine, B. (1999) *Genomics* **59**, 59-65

6.   Cuervo, A. M. (2004) *Trends Cell Biol* **14**, 70-77

7.   Paglin, S., Hollister, T., Delohery, T., Hackett, N., McMahill, M., Sphicas, E., Domingo, D., and Yahalom, J. (2001) *Cancer Res* **61**, 439-444

8.   Nixon, R. A., Wegiel, J., Kumar, A., Yu, W. H., Peterhoff, C., Cataldo, A., and Cuervo, A. M. (2005) *J Neuropathol Exp Neurol* **64**, 113-122

9.   Venkatraman, P., Wetzel, R., Tanaka, M., Nukina, N., and Goldberg, A. L. (2004) *Mol Cell* **14**, 95-104

10.   Kegel, K. B., Kim, M., Sapp, E., McIntyre, C., Castano, J. G., Aronin, N., and DiFiglia, M. (2000) *J Neurosci* **20**, 7268-7278

11.   Talloczy, Z., Jiang, W., Virgin, H. W. t., Leib, D. A., Scheuner, D., Kaufman, R. J., Eskelinen, E. L., and Levine, B. (2002) *Proc Natl Acad Sci U S A* **99**, 190-195.

12.   Nakagawa, I., Amano, A., Mizushima, N., Yamamoto, A., Yamaguchi, H., Kamimoto, T., Nara, A., Funao, J., Nakata, M., Tsuda, K., Hamada, S., and Yoshimori, T. (2004) *Science* **306**, 1037-1040

13.   Dorn, B. R., Dunn, W. A., Jr., and Progulske-Fox, A. (2001) *Infect Immun* **69**, 5698-5708

14.   Pizarro-Cerda, J., Moreno, E., Sanguedolce, V., Mege, J. L., and Gorvel, J. P. (1998) *Infect Immun* **66**, 2387-2392.

15.   Wiater, L. A., Dunn, K., Maxfield, F. R., and Shuman, H. A. (1998) *Infect Immun* **66**, 4450-4460

16.   Prentice, E., Jerome, W. G., Yoshimori, T., Mizushima, N., and Denison, M. R. (2004) *J Biol Chem* **279**, 10136-10141

17.   Kuma, A., Hatano, M., Matsui, M., Yamamoto, A., Nakaya, H., Yoshimori, T., Ohsumi, Y., Tokuhisa, T., and Mizushima, N. (2004) *Nature* **432**, 1032-1036

18.   Thumm, M. (2000) *Microsc Res Tech* **51**, 563-572

19.   Klionsky, D. J. (2005) *J Cell Sci* **118**, 7-18

20.   Raught, B., Gingras, A. C., and Sonenberg, N. (2001) *Proc Natl Acad Sci U S A* **98**, 7037-7044

21.   Huang, W. P., and Klionsky, D. J. (2002) *Cell Struct Funct* **27**, 409-420

22.   Noda, T., and Ohsumi, Y. (1998) *J Biol Chem* **273**, 3963-3966

23.   Kamada, Y., Funakoshi, T., Shintani, T., Nagano, K., Ohsumi, M., and Ohsumi, Y. (2000) *J Cell Biol* **150**, 1507-1513.

24.   Abeliovich, H., Zhang, C., Dunn, W. A., Jr., Shokat, K. M., and Klionsky, D. J. (2003) *Mol Biol Cell* **14**, 477-490

25.   Yorimitsu, T., and Klionsky, D. J. (2005) *Mol Biol Cell*

26.   Nice, D. C., Sato, T. K., Stromhaug, P. E., Emr, S. D., and Klionsky, D. J. (2002) *J Biol Chem* **277**, 30198-30207

27.   Kihara, A., Noda, T., Ishihara, N., and Ohsumi, Y. (2001) *J Cell Biol* **152**, 519-530.

28.   Herman, P. K., Stack, J. H., and Emr, S. D. (1991) *Embo J* **10**, 4049-4060

29.   Schu, P. V., Takegawa, K., Fry, M. J., Stack, J. H., Waterfield, M. D., and Emr, S. D. (1993) *Science* **260**, 88-91

30.   Simonsen, A., Wurmser, A. E., Emr, S. D., and Stenmark, H. (2001) *Curr Opin Cell Biol* **13**, 485-492

31.   Wurmser, A. E., and Emr, S. D. (2002) *J Cell Biol* **158**, 761-772

32.   Petiot, A., Ogier-Denis, E., Blommaart, E. F., Meijer, A. J., and Codogno, P. (2000) *J Biol Chem* **275**, 992-998

33.   Dove, S. K., Piper, R. C., McEwen, R. K., Yu, J. W., King, M. C., Hughes, D. C., Thuring, J., Holmes, A. B., Cooke, F. T., Michell, R. H., Parker, P. J., and Lemmon, M. A. (2004) *Embo J* **23**, 1922-1933

34.   Suzuki, K., Kirisako, T., Kamada, Y., Mizushima, N., Noda, T., and Ohsumi, Y. (2001) *Embo J* **20**, 5971-5981.

35.   Kim, J., Huang, W. P., Stromhaug, P. E., and Klionsky, D. J. (2002) *J Biol Chem* **277**, 763-773

36.   Kuma, A., Mizushima, N., Ishihara, N., and Ohsumi, Y. (2002) *J Biol Chem* **277**, 18619-18625.

37.   Kim, J., Huang, W. P., and Klionsky, D. J. (2001) *J Cell Biol* **152**, 51-64.

38.   Khalfan, W. A., and Klionsky, D. J. (2002) *Curr Opin Cell Biol* **14**, 468-475

39.   Lang, T., Schaeffeler, E., Bernreuther, D., Bredschneider, M., Wolf, D. H., and Thumm, M. (1998) *Embo J* **17**, 3597-3607

40.   Kirisako, T., Baba, M., Ishihara, N., Miyazawa, K., Ohsumi, M., Yoshimori, T., Noda, T., and Ohsumi, Y. (1999) *J Cell Biol* **147**, 435-446

41.   Huang, W. P., Scott, S. V., Kim, J., and Klionsky, D. J. (2000) *J Biol Chem* **275**, 5845-5851

42.   Huang, P. H., and Chiang, H. L. (1997) *J Cell Biol* **136**, 803-810

43.   Ichimura, Y., Kirisako, T., Takao, T., Satomi, Y., Shimonishi, Y., Ishihara, N., Mizushima, N., Tanida, I., Kominami, E., Ohsumi, M., Noda, T., and Ohsumi, Y. (2000) *Nature* **408**, 488-492.

44.   Onodera, J., and Ohsumi, Y. (2004) *J Biol Chem* **279**, 16071-16076

45.   Tuttle, D. L., Lewin, A. S., and Dunn, W. J. (1993) *Eur J Cell Biol* **60**, 283-290

46.   Hutchins, M. U., Veenhuis, M., and Klionsky, D. J. (1999) *J Cell Sci* **112**, 4079-4087

47.   Harding, T. M., Morano, K. A., Scott, S. V., and Klionsky, D. J. (1995) *J. Cell Biol.* **131**, 591-602

48.   Harding, T. M., Hefner-Gravink, A., Thumm, M., and Klionsky, D. J. (1996) *J. Biol. Chem.* **271**, 17621-17624

49.   Barth, H., and Thumm, M. (2001) *Gene* **274**, 151-156.

50.   Barth, H., Meiling-Wesse, K., Epple, U. D., and Thumm, M. (2001) *FEBS Lett* **508**, 23-28.

51.   Kiel, J. A., Komduur, J. A., van der Klei, I. J., and Veenhuis, M. (2003) *FEBS Lett* **549**, 1-6

52.   Shintani, T., Huang, W. P., Stromhaug, P. E., and Klionsky, D. J. (2002) *Dev Cell* **3**, 825-837

53.   Thumm, M. (2002) *Mol Cell* **10**, 1257-1258

54.   Kim, J., Scott, S. V., Oda, M. N., and Klionsky, D. J. (1997) *J Cell Biol* **137**, 609-618

55.   Scott, S. V., Guan, J., Hutchins, M. U., Kim, J., and Klionsky, D. J. (2001) *Mol Cell* **7**, 1131-1141.

56.   Hutchins, M. U., and Klionsky, D. J. (2001) *J Biol Chem* **276**, 20491-20498

57.   Sato, T. K., Rehling, P., Peterson, M. R., and Emr, S. D. (2000) *Mol Cell* **6**, 661-671

58.   Wang, C. W., Stromhaug, P. E., Shima, J., and Klionsky, D. J. (2002) *J Biol Chem* **277**, 47917-47927

59.   Wang, C. W., Stromhaug, P. E., Kauffman, E. J., Weisman, L. S., and Klionsky, D. J. (2003) *J Cell Biol* **163**, 973-985

60.   Wurmser, A. E., Sato, T. K., and Emr, S. D. (2000) *J Cell Biol* **151**, 551-562

61.   Thumm, M., and Wolf, D. H. (1998) in *Adv. Mol. Cell Biol.* (Rivett, A. J., ed) Vol. 27, pp. 41-67, JAI Press, Greenwich

62.   Teichert, U., Mechler, B., Muller, H., and Wolf, D. H. (1989) *J. Biol. Chem.* **264**, 16037-16045

63.   Nakamura, N., Matsuura, A., Wada, Y., and Ohsumi, Y. (1997) *J Biochem (Tokyo)* **121**, 338-344

64.   Teter, S. A., Eggerton, K. P., Scott, S. V., Kim, J., Fischer, A. M., and Klionsky, D. J. (2001) *J Biol Chem* **276**, 2083-2087.

65.   Epple, U. D., Suriapranata, I., Eskelinen, E. L., and Thumm, M. (2001) *J Bacteriol* **183**, 5942-5955

66.   Suriapranata, I., Epple, U. D., Bernreuther, D., Bredschneider, M., Sovarasteanu, K., and Thumm, M. (2000) *J Cell Sci* **113 (Pt 22)**, 4025-4033

67.   Stromhaug, P. E., and Klionsky, D. J. (2001) *Traffic* **2**, 524-531

68.   Epple, U. D., Eskelinen, E. L., and Thumm, M. (2003) *J Biol Chem* **278**, 7810-7821

69.   Ausubel, F. M., Brent, R., Kingston, R. E., and Moore, D. D. (1987) *Current Protocols in Molecular Biology, Greene Publishing Associates, New York, N.Y.*

70.   Pan, X., Roberts, P., Chen, Y., Kvam, E., Shulga, N., Huang, K., Lemmon, S., and Goldfarb, D. S. (2000) *Mol Biol Cell* **11**, 2445-2457

71.   Meiling-Wesse, K., Barth, H., Voss, C., Eskelinen, E. L., Epple, U. D., and Thumm, M. (2004) *J Biol Chem*

72.   Lang, T., Reiche, S., Straub, M., Bredschneider, M., and Thumm, M. (2000) *J Bacteriol* **182**, 2125-2133

73.   Leber, R., Silles, E., Sandoval, I. V., and Mazon, M. J. (2001) *J Biol Chem* **276**, 29210-29217.

74.   Güldener, U., Heck, S., Fielder, T., Beinhauer, J., and Hegemann, J. H. (1996) *Nucleic Acids Res.* **24**, 2519-2524

75.   Nothwehr, S. F., Conibear, E., and Stevens, T. H. (1995) *J Cell Biol* **129**, 35-46

76.   Campbell, C. L., and Thorsness, P. E. (1998) *J Cell Sci* **111**, 2455-2464.

77.   Thumm, M., Egner, R., Koch, B., Schlumpberger, M., Straub, M., Veenhuis, M., and Wolf, D. H. (1994) *Febs Lett.* **349**, 275-280

78.   Meiling-Wesse, K., Epple, U. D., Krick, R., Barth, H., Appelles, A., Voss, C., Eskelinen, E. L., and Thumm, M. (2005) *J Biol Chem* **280**, 33669-33678

79.   Meiling-Wesse, K., Barth, H., Voss, C., Barmark, G., Muren, E., Ronne, H., and Thumm, M. (2002) *FEBS Lett* **530**, 174-180

80.   Meiling-Wesse, K., Barth, H., and Thumm, M. (2002) *FEBS Lett.* **526**, 71-76

81.   Meiling-Wesse, K., Bratsika, F., and Thumm, M. (2004) *FEMS Yeast Res* **4**, 459-465

82.   Barth, H., Meiling-Wesse, K., Epple, U. D., and Thumm, M. (2002) *FEBS Lett* **512**, 173-179.

83.   Schlumpberger, M., Schaeffeler, E., Straub, M., Bredschneider, M., Wolf, D. H., and Thumm, M. (1997) *J. Bacteriol.* **179**, 1068-1076

84.   Straub, M., Bredschneider, M., and Thumm, M. (1997) *J. Bacteriol.* **179**, 3875-3883

85.   Robinson, J. S., Klionsky, D. J., Banta, L. M., and Emr, S. D. (1988) *Mol Cell Biol* **8**, 4936-4948

86.   Klionsky, D. J., Cueva, R., and Yaver, D. S. (1992) *J. Cell Biol.* **119**, 287-299

87.   Shimomura, O., Johnson, F. H., and Saiga, Y. (1962) *J Cell Comp Physiol* **59**, 223-239

88.   Kohlwein, S. D. (2000) *Microsc Res Tech* **51**, 511-529

89.   Roberts, C. J., Raymond, C. K., Yamahiro, C. T., and Stevens, T. H. (1991) *Meth. Enzymol.* **194**, 644-661

90.   Mollenhauer, H. H. (1959) *J Biophys Biochem Cytol* **6**, 431-436

91.   Bredschneider, M. (1999), pp. 44-47, Stuttgart

92.   Luft, J. H. (1961) *J Biophys Biochem Cytol* **9**, 409-414

93.   Lämmli, U. K. (1970) *Nature* **227**, 680-685

94.   Noda, T., Matsuura, A., Wada, Y., and Ohsumi, Y. (1995) *Biochem Biophys Res Commun* **210**, 126-132

95.   Higgins, D. G., and Sharp, P. M. (1989) *Comput Appl Biosci* **5**, 151-153.

96.   Klionsky, D. J., Cregg, J. M., Dunn, W. A., Jr., Emr, S. D., Sakai, Y., Sandoval, I. V., Sibirny, A., Subramani, S., Thumm, M., Veenhuis, M., and Ohsumi, Y. (2003) *Dev Cell* **5**, 539-545

97.   Deutschbauer, A. M., Williams, R. M., Chu, A. M., and Davis, R. W. (2002) *Proc Natl Acad Sci U S A* **99**, 15530-15535

98.   Mitchell, A. P. (1994) *Microbiol Rev* **58**, 56-70

99.   Columbia, U. o. B. in *http://www.agsci.ubc.ca/courses/fnh/410/protein/1_54.htm*

100.   Reggiori, F., Tucker, K. A., Stromhaug, P. E., and Klionsky, D. J. (2004) *Dev Cell* **6**, 79-90

101.   Kaytor, M. D., and Livingston, D. M. (1995) *Yeast* **11**, 1147-1155

102.   Sacher, M., Barrowman, J., Wang, W., Horecka, J., Zhang, Y., Pypaert, M., and Ferro-Novick, S. (2001) *Mol Cell* **7**, 433-442

103.   Engebrecht, J., Masse, S., Davis, L., Rose, K., and Kessel, T. (1998) *Genetics* **148**, 581-598

104.   Guan, J., Stromhaug, P. E., George, M. D., Habibzadegah-Tari, P., Bevan, A., Dunn, W. A., Jr., and Klionsky, D. J. (2001) *Mol Biol Cell* **12**, 3821-3838

105.   Shintani, T., Suzuki, K., Kamada, Y., Noda, T., and Ohsumi, Y. (2001) *J Biol Chem* **276**, 30452-30460.

106.   Wang, C. W., Kim, J., Huang, W. P., Abeliovich, H., Stromhaug, P. E., Dunn, W. A., Jr., and Klionsky, D. J. (2001) *J Biol Chem* **276**, 30442-30451

107.   Noda, T., Kim, J., Huang, W. P., Baba, M., Tokunaga, C., Ohsumi, Y., and Klionsky, D. J. (2000) *J Cell Biol* **148**, 465-480

108.   Sacher, M., Jiang, Y., Barrowman, J., Scarpa, A., Burston, J., Zhang, L., Schieltz, D., Yates, J. R., 3rd, Abeliovich, H., and Ferro-Novick, S. (1998) *Embo J* **17**, 2494-2503

109.   Sacher, M., Barrowman, J., Schieltz, D., Yates, J. R., 3rd, and Ferro-Novick, S. (2000) *Eur J Cell Biol* **79**, 71-80

110.   Barrowman, J., Sacher, M., and Ferro-Novick, S. (2000) *Embo J* **19**, 862-869

111.   Morozova, N., Liang, Y., Tokarev, A. A., Chen, S. H., Cox, R., Andrejic, J., Lipatova, Z., Sciorra, V. A., Emr, S. D., and Segev, N. (2006) *Nat Cell Biol* **8**, 1263-1269

112.   Kim, J., and Klionsky, D. J. (2000) *Annu Rev Biochem* **69**, 303-342

113.   Cox, R., Chen, S. H., Yoo, E., and Segev, N. (2007) *BMC Evol Biol* **7**, 12

114.   Tucker, K. A., Reggiori, F., Dunn, W. A., Jr., and Klionsky, D. J. (2003) *J Biol Chem* **278**, 48445-48452

115.   Kucharczyk, R., Gromadka, R., Migdalski, A., Slonimski, P. P., and Rytka, J. (1999) *Yeast* **15**, 987-1000.

116.   Kucharczyk, R., Dupre, S., Avaro, S., Haguenauer-Tsapis, R., Slonimski, P. P., and Rytka, J. (2000) *J Cell Sci* **113 Pt 23**, 4301-4311.

117.   Wichmann, H., Hengst, L., and Gallwitz, D. (1992) *Cell* **71**, 1131-1142.

118.   Schimmoller, F., and Riezman, H. (1993) *J Cell Sci*

119.   Kucharczyk, R., Kierzek, A. M., Slonimski, P. P., and Rytka, J. (2001) *J Cell Sci* **114**, 3137-3145.

120.   Alberts, B., Bray, D., Lewis, J., Raff, M., Roberts, K., Watson, J.D. (1994) *Molecular Biology of the Cell*, Third Ed., Garland Publishing, NY, NY

121.   Muren, E., Oyen, M., Barmark, G., and Ronne, H. (2001) *Yeast* **18**, 163-172.

122.   Burgoyne, R. D., and Morgan, A. (1998) *Cell Calcium* **24**, 367-376

123.   Jeremic, A., Kelly, M., Cho, J. A., Cho, S. J., Horber, J. K., and Jena, B. P. (2004) *Cell Biol Int* **28**, 19-31